MODELLING AND OPTIMIZATION OF A POLYGENERATION HYBRID SOLAR AND BIOMASS SYSTEM FOR POWER, COOLING AND DESALINATION

A Thesis submitted in partial fulfillment of the requirements for the award the degree of

DOCTOR OF PHILOSOPHY

IN

MECHANICAL ENGINEERING

By

UMAKANTA SAHOO

2K13/PhD/ME/11

Under the Supervision of

Prof. RAJESH KUMAR
Professor
Mechanical Engineering Department
Delhi Technological University

Dr. RAJIV CHAUDHARY
Associate Professor
Mechanical Engineering Department
Delhi Technological University

Dr. PRADEEP CHANDRA PANT
Scientist 'F'
Ministry of New and Renewable Energy, Government of India

MECHANICAL ENGINEERING DEPARTMENT
DELHI TECHNOLOGICAL UNIVERSITY
Main Bawana Road, Delhi-42, INDIA

NOVEMBER, 2017

MODELLING AND OPTIMIZATION OF A POLYGENERATION HYBRID SOLAR AND BIOMASS SYSTEM FOR POWER, COOLING AND DESALINATION

A Thesis submitted in partial fulfillment of the requirements for the award the degree of

DOCTOR OF PHILOSOPHY

IN

MECHANICAL ENGINEERING

By

UMAKANTA SAHOO

2K13/PhD/ME/11

Under the Supervision of

Dr. RAJESH KUMAR
Professor
Mechanical Engineering Department
Delhi Technological University

Dr. RAJIV CHAUDHARY
Associate Professor
Mechanical Engineering Department
Delhi Technological University

Dr. PRADEEP CHANDRA PANT
Scientist 'F'
Ministry of New and Renewable Energy, Government of India

MECHANICAL ENGINEERING DEPARTMENT
DELHI TECHNOLOGICAL UNIVERSITY

Main Bawana Road, Delhi-42, INDIA

NOVEMBER, 2017

ACKNOWLEDGEMENTS

I express my deep gratitude to my supervisors Prof. Rajesh Kumar, Dr. Rajiv Chaudhary (Associate Professor), Department of Mechanical Engineering, Delhi Technological University, Delhi and Dr. Pradeep Chandra Pant, Scientist 'F', Ministry of New and Renewable Energy, Government of India, Delhi for assisting me in identifying and formulating the research problem. Despite their busy schedule, Dr. Rajesh Kumar, Dr. Rajiv Chaudhary and Dr. Pradeep Chandra Pant were always available for the advice and discussions. Their valuable comments and advice gave me the confidence to overcome the challenges in formulation of this PhD thesis work.

I express my special thanks to Prof. R.S.Mishra, Head of Mechanical Engineering Department, DTU, Dr. A.K.Tripathi, Director General, Shri S.K.Singh, Scientist 'G' & Adviser, National Institute of Solar Energy (NISE), Prof. H.P.Garg, former Professor and Head of Energy Studies, IIT Delhi and Dr. Ahmar Raza, former Director of Ministry of New and Renewable Energy, Government of India, for their continuous inspiration and support during this research work. I would like to thank all the faculty members of DTU and colleagues of NISE, especially Mr. Birinchi Bora & Mr. Ishan Barbate for helping and guiding me most of the occasion, resulting in successful completion of my PhD thesis work.

I would like to thank my friends, who have supported me through their encouragement, support and friendship during this period of thesis research work. I would like to thank to all those who directly and indirectly supported me in carrying out this thesis work successfully.

Furthermore, I would like to express my deep gratitude to my parents and every member of my family for their endless inspiration, support and guidance throughout my whole life.

DECLARATION

I hereby declare that the thesis entitled **"MODELLING AND OPTIMIZATION OF A POLYGENERATION HYBRID SOLAR AND BIOMASS SYSTEM FOR POWER, COOLING AND DESALINATION"** is an original work carried out by me under the supervision of Prof. Rajesh Kumar, Dr. Rajiv Chaudhary (Associate Professor), Department of Mechanical Engineering, Delhi Technological University, Delhi and Dr. Pradeep Chandra Pant, Scientist 'F', Ministry of New and Renewable Energy, Government of India, Delhi. This thesis has been prepared in conformity with the rules and regulations of the Delhi Technological University, Delhi. The research work reported and results presented in the thesis have not been submitted either in part or full to any other university or institute for the award of any other degree or diploma.

Place: Delhi

Date: 28-11-2017

(Umakanta Sahoo)

(2K13/PhD/ME/11)
Research Scholar
Mechanical Engineering Department
Delhi Technological University,
Delhi-110042

CERTIFICATE

This is to certify that the work embodied in the thesis entitled **"MODELLING AND OPTIMIZATION OF A POLYGENERATION HYBRID SOLAR AND BIOMASS SYSTEM FOR POWER, COOLING AND DESALINATION"** by **Umakanta Sahoo, (Roll No: 2K13/PhD/ME/11)** in partial fulfillment of requirements for the award of Degree of **DOCTOR OF PHILOSOPHY in Mechanical Engineering**, is an authentic record of student's own work carried by him under our supervision.

This is also certified that this work has not been submitted to any other Institute or University for the award of any other diploma or degree.

(Prof. Rajesh Kumar)
Professor
Mechanical Engineering Department
Delhi Technological University
Delhi-42.

(Dr. Rajiv Chaudhary)
Associate Professor
Mechanical Engineering Department
Delhi Technological University
Delhi-42.

(Dr. Pradeep Chandra Pant)
Scientist 'F'
Ministry of New and Renewable Energy
Government of India
Delhi-03.

ABSTRACT

The global warming phenomenon as a significant sustainability issue is gaining worldwide support for development of renewable energy technologies. The term 'polygeneration' is referred to as "an energy supply system, which delivers more than one form of energy to the final user", for example: electricity, cooling and desalination can be delivered from polygeneration process. The polygeneration process in hybrid solar thermal power plant can deliver electricity with lesser impact on environment compared to conventional fossil fuel based power generating system. It is the next generation energy production technique with a potential to overcome intermittence of renewable energy.

In this study, the polygeneration process simultaneous production of power, vapor absorption refrigeration (VAR) cooling and multi-effect humidification and dehumidification (MEHD) desalination system from different heat sources in hybrid solar-biomass (HSB) system with higher energy efficiencies (energy and exergy), primary energy savings (PES) and payback period are investigated.

There are several aspects associated with hybrid solar-biomass power generation installations such as state wise availability of biomass resources, solar direct normal irradiance (DNI) have been analyzed. Month wise solar and biomass heat utilization also has been analyzed for hybrid system in four regions of India (East: Guwahati, Assam; West: Udaipur, Rajasthan; North: Delhi, South: Madurai, Tamil Nadu). The month wise daily average solar radiation is also considered as 20%, 40%, 60% and 80% and remaining heat is taken from biomass resource in northern region (Delhi) in the proposed hybrid plant.

The thermodynamic evaluation (energy and exergy) of HSB power plant has also been investigated. The total input energy of the proposed hybrid system is taken

from the heat transfer fluid through parabolic trough collector (PTC) as per availability of solar resource and remaining from biomass to maintain the steam at superheated state of 500^0C and 60 bar and supplied to turbine at steam mass flow rate of 5 kg/sec. The energy and exergy analyses of 5 MW HSB system with series mode was carried out to identify the effects of various operating parameters like DNI, condenser pressure, turbine inlet temperatures, boiler pressure on net power output energy and exergy efficiencies.

The VAR cooling system operates using the extracted heat taken from turbine and condenser heat of the VAR cooling system is used in MEHD system for production of drinking water as per demand requirement. Though the production of electricity decreases due to extraction of heat from turbine for VAR cooling and MEHD desalination, the complete system meets the energy requirements & increases the PES.

The thermodynamic evaluation (energy and exergy), optimization and payback period of polygeneration process in HSB thermal power plant for combined power, cooling and desalination is investigated to identify the effects of various operating parameters. The system has achieved a maximum energy efficiency of 49.85% and exergy efficiency of 20.94%. The Primary energy savings of polygeneration process (PESPP) in HSB system is achieved at 50.5%. The electricity generation from polygeneration process increased to 78.12% as compared to simple thermal power plant. The payback period of polygeneration process in HSB thermal power plant is 1.5 years, which is less than solar thermal power plant, HSB thermal power plant, Cogeneration in HSB thermal power plant.

Keywords: Polygeneration, hybrid solar-biomass, energy & exergy analysis, optimization, primary energy saving.

CONTENTS

LIST OF FIGURES

LIST OF TABLES

NOMENCLATURE

a	Solar altitude angle (degrees)
a_1	First order heat loss coefficient $(W/m^2 - {}^oC)$
a_2	Second order heat loss coefficient $(W/m^2 - {}^oC^2)$
A_{ap}	Aperture area of the parabolic trough collector field (m^2)
C	Cost of the system (Rs)
C_{fg}	Specific heat of flue gas $(kJ/kg - {}^oC)$
C_p	Specific heat $(kJ/kg - {}^oC)$
$DNI(G)$	Monthly mean value of DNI based on ground measured data (kWh/m^2)
$DNI(S)$	Monthly mean value of DNI based on satellite data (kWh/m^2)
$\overline{d}$	Monthly and range wise mean DNI of each year (kWh/m^2)
E	Energy (kW)
$E_{x,b}$	Exergy of biomass
E_{xi}	Inlet exergy of the flowing stream
E_{xe}	Exit exergy of the flowing stream
$E_{xD,b}$	Exergy destruction of boiler
$E_{xD,C}$	Exergy destruction of condenser
$E_{xD,FWH}$	Exergy destruction of feed water heater
$E_{xD,HE}$	Exergy destruction of heat exchanger
$E_{xD,P}$	Exergy destruction of pump
$E_{xD,T}$	Exergy destruction of turbine
g	Specific gravitational force $(m/\sec^2)$

h	Specific enthalpy (kJ/kg)
L	Local latitude (degrees)
L_{boiler}	Percentage heat losses in boiler (%)
LiBr	Lithium bromide
L_C	Heat losses in condenser (kW)
L_p	Heat losses in pump (kW)
L_{PTC}	Heat losses in PTC (kW)
L_T	Heat losses in turbine (kW)
m_{fg}	Mass of flue gas (kg/kg of fuel)
m_b	Mass of biomass (kg/sec)
m_{oil}	Mass of oil (kg/sec)
m_w	Mass of water (kg/sec)
n	Total number of range wise DNI data
P_v	Vapor pressure (kPa)
P_{vs}	Saturated vapor pressure (kPa)
Q_1	Hourly useful heat gain (kW)
Q_b	Heat produced from biomass (kW)
Q_C	Condenser heat (kW)
Q_g	Generator heat (kW)
Q_{HE}	Heat exchanger heat (kW)
Q_{solar}	Solar energy falling on PTC field (kW)

R_{air}	Gas constant of air (kg/mol)
R_v	Gas constant of vapor (kg/mol)
T	Temperature (^{0}C or K)
T_a	Ambient temperature (^oC)
T_{fg}	Flue gas temperature (^oC)
T_m	Mean temperature (^oC)
T_x	Outlet temperature of PTC field (^oC)
T_y	Inlet temperature of PTC field (^oC)
s	Specific entropy (kJ/kg K)
W_{net}	Network output of the plant (kW)
W_p	Pump work (kW)
W_{SPP}	Simple power plant work (kW)
W_T	Turbine work (kW)
Z	Azimuth angle (degrees)

Greek

α	Fraction of steam bleed from turbine
ΔT	Temperature difference (^oC)
δ	Declination (degrees)
$\eta_{E,boiler}$	Energy efficiency of boiler (%)
$\eta_{E,HE}$	Energy efficiency of heat exchanger (%)
$\eta_{electrical}$	Electrical efficiency of polygeneration system (%)

$\eta_{E,HSB}$	Energy efficiency of hybrid solar and biomass power plant $(\%)$
$\eta_{Ex,HSB}$	Exergy efficiency of hybrid solar and biomass power plant $(\%)$
$\eta_{E,PTC}$	Energy efficiency of PTC $(\%)$
$\eta_{Ex,PTC}$	Exergy efficiency of PTC $(\%)$
η_{heat}	Heat efficiency of polygeneration process $(\%)$
$\eta_{ref,electrical}$	Efficiency reference value for separate electricity production in polygeneration process $(\%)$
$\eta_{ref,heat}$	Efficiency reference value for separate heat production $(\%)$
η_{opt}	Optical efficiency $(\%)$
θ	Angle of Incident (degrees)
ϕ	Multiplication factor (degrees)
ω	Hour angle (degrees)

Subscripts

a	Absorber
b	Biomass
Bt	Beam radiation on tilted surfaces
Bw	Brackish water of MEHD system
c	Condenser
DH	Dehumidification
Dw	Distilled water of MEHD system
e	Evaporator
FWH	Feed Water Heater

fw	Feed water of MEHD system
g	Generator
HE	Heat Exchanger
HSB	Hybrid solar-biomass
i,e	Exergy flowing stream at inlet and outlet
j	Heat source of each state points of the system
opt	Optical
$P1$ & $P2$	Pump 1 and 2.
PTC	Parabolic trough collector
s	Solar
SPP	Simple power plant
T	Turbine
w	Water
v	Vapor
0	Surrounding (or reference environment) condition
1-29 , c, a, x & y	State points of the system

Acronyms

AAS	Actual mass of air supplied
AST	Apparent solar time
COP	Coefficient of performance
CSIRO	Commonwealth scientific and industrial research organization
CSP	Concentrated solar power
CST	Concentrated solar thermal
CLFR	Compact linear fresnel reflector

DNI	Direct normal irradiance
ET	Equation of time
EV	Expansion valve
GA	Genetic algorithm
GHG	Greenhouse gas
JNNSM	Jawaharlal Nehru national solar mission
HHV	High heating value
HSB	Hybrid solar and biomass
LFR	Linear fresnel reflector
LHV	Lower heating value
L_{local}	Local longitude
L_{st}	Standard longitude
MAPE	Mean absolute percentage error
MEHD	Multi effect humidification and dehumidification
MJ	Mega Joules
MNRE	Ministry of new and renewable energy
MT	Metric tons
MW	Mega watt
NISE	National institute of solar energy
NIWE	National institute of wind energy
NREL	National renewable energy laboratory
PES	Primary energy savings
PESPP	Primary energy savings of polygeneration process
P&M	Plant and machinery
PTC	Parabolic trough collector

RH	Relative humidity
ST	Standard time
VAR	Vapor absorption refrigeration
VP	Vapor phase

CHAPTER 1: INTRODUCTION

The energy scene in the world is a complex picture of variety of energy sources being used to meet the growing energy needs. However there is a gap in the demand and supply position. It is recognized that decentralize generation based on the various renewable energy technologies can, to some extent, help in meeting the growing energy needs. Renewable energy landscape in India, during the last few years, has witnessed tremendous changes in the policy framework with accelerated and ambitious plans to increase the contribution of renewable energy such as solar, wind, bio-power etc. Concentrated solar thermal & biomass power have good potential for power generation and/or process heat in the industrial sector from renewable energy.

The launching of the Jawaharlal Nehru National Solar Mission (JNNSM) symbolizes both and indeed encapsulates the vision and ambition for the future of solar energy in India. The cost of power produced from Concentrated Solar Power (CSP) is becoming competitive with conventional energy sources with the development of technologies [1].

As capacity of CSP with heat energy storage is growing rapidly but hybridization with CSP is receiving more attention due to low level of insolation in this country. The demand for biomass is increasing for use as solid fuels including wood pellets. It is the power generation potential of biomass, however, which has recently been attracting greater attention. On the other hand, biomass power plants should have a secured supply of required quality and quantity of biomass resources at a competitive price for sustainable operation of the plant. The cost of biomass resources has been slowly increasing due to non-availability of feed stock at right price in recent years.

So, biomass and solar resources are important and supplement/ complement each other for hybridization for continuous power generation.

Solar-biomass hybrid system could be viable reliable option for meeting energy demand in industrial sector. In the hybrid systems, solar energy can be optimally utilized in the regions of high direct normal solar irradiance and where the biomass is available in abundance for supplementing and complementing each other in a cost effective manner. Solar thermal technology drives the thermal power system in peak sunshine hours and biomass heat drives in short transient periods during the day and at night time to generate constant power.

The energy demand for cooling, process heat and desalination applications is increasing continuously in industry, office complexes, institutions, hospitals, residential areas, shopping complexes etc. This is at present being met by the conventional electricity, thus increasing the load on the grid and causing environmental pollution. Globally, in industrial sector about two-thirds of total consumption of energy is used for process heat applications.

World's huge and growing population is putting a severe strain on all the natural sources of the countries. Most of the water resources are contaminated by sewage and agricultural runoff. India has made progress in supply of drinking water to people but gross disparity in coverage exists across the country. In India access to drinking water to different communities and States has increased in the recent past, but as per estimation of World Bank about 21% of communicable diseases are related to unsafe water supply. Ground water is the major source of drinking water in our country with 85% of the population dependent on it [2-3]**.** It is true that providing drinking water to such a large population is an enormous challenge.

Presently, most of the industries either buy power from the state electricity boards, or generate their own power largely for end use applications like industrial, production of materials and goods, office works, communication, cooling and desalination. In India, the increase in huge electricity demand for industry, institutions, office complexes, commercial establishments, etc. has resulted in higher consumption of conventional energy, as well as increasing the greenhouse gas (GHG) emissions and responsible for negative impact on climate change. Process heat requirement is more than 67% of total energy consumption at global level and about 50% of this heat requirement is for temperature lower than 400^0C. At present level, about 40% of primary energy consumption of the industry is contributed by natural gas and contribution that of petroleum is about 41% [4]. Some of industries through cogeneration produce power as well as process heat for their end use applications to reduce their net power consumption. Cogeneration system can reduces the grid electricity demand of the residential sector for lighting, space heating and cooling & hot water, thus reducing the greenhouse gas emissions.

Cogeneration is considered as the advanced technology for generation of both electricity & process heat, but it is not possible to provide energy for more than two such outputs like space cooling, water desalination and/or process heat for their requirements. However, polygeneration process can meet their full energy demand such as power, space cooling & heating, process heat including desalination. Polygeneration process in hybrid solar thermal power plant can improve the overall efficiencies (energy, exergy), reliability.

1.1 GLOBAL SCENARIO ON RENEWABLE ENERGY

Renewable energy is one of the options to transform the energy system to make it less carbon intensive, sustainable, climate change goals and bring energy security

benefits. Renewable energy encompasses a broad range of energy resources and technologies that have differing attributes and applications. Renewable energy resources include solar, bioenergy, geothermal, wind and hydropower. These sources are abundant and widely distributed; but they are not equally easy to harness. Solar, biomass and geothermal resources are for generation of electricity & water pumping, and process heat applications. Hydropower and wind resources are for only generation of electricity and water lifting and bioenergy resources are utilized for electricity generation and in transport sector. Renewables energy are the world's second largest source of electricity generation after coal based power generation plants. These sources have huge potential in meeting energy requirements for process heat in industry and transport sectors. For the first time the renewables industry has achieved a major milestone in 2015, with capacity additions exceeding as compared to fossil fuels and nuclear [5]. The total renewable power capacity has reached 1849,000 MW (including hydro power) at the end-2015 [6]. Of this renewable power capacity, wind energy contribution to 23.41 % of installed capacity (433,000 MW), Solar photovoltaic power (SPV) 12.33 % (228,000 MW), Bio-power capacity 5.73 % (106,000 MW), Geothermal power capacity 0.713 % (13,200 MW) and Concentrated solar thermal power capacity 0.259 % (4,800 MW) and hydro power capacity 57.54% amounting to 1064,000 MW as shown in Figure 1.1.

- **Wind Power**

Globally total wind power generation capacity is 433,000 MW at the end of 2015. China has the world's highest generation capacity of 29.87% (129,340 MW) followed distantly by the United States 16.76% (72,578 MW), Germany 10.39% (45,000 MW), India 5.79% (25,088 MW), Spain 5.31% (23,008 MW), United Kingdom 3.27% (14,191 MW), Canada 2.58% (11,205 MW), France 2.39% (10,358

MW), Italy 2.1% (9,126 MW), Brazil 2.01% (8,715 MW) and rest of World 19.48% (84,391 MW).

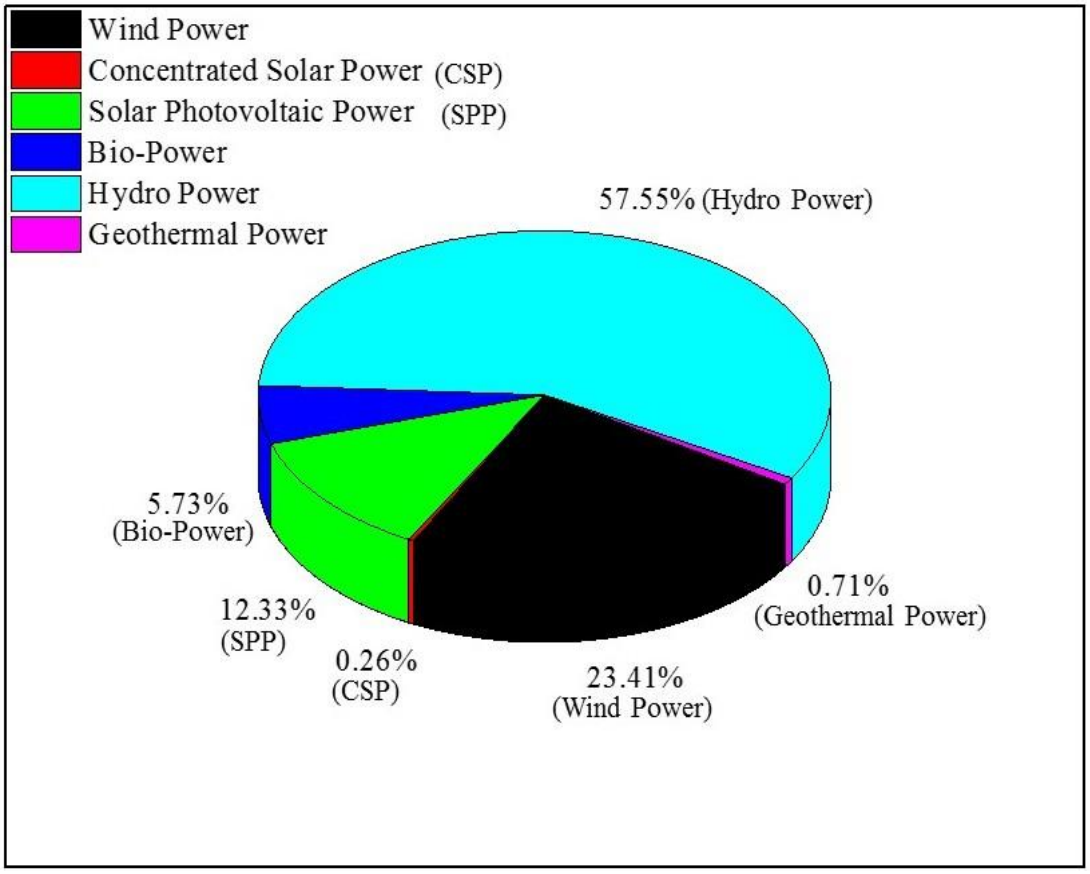

Figure 1.1 World's renewable energy scenario at the end-2015

- **SPV Power**

Globally, the present installed capacity of SPV power is 228,000 MW. China, Germany, Japan, the USA and Italy are the top five countries on the SPV power generation. Out of 228,000 MW, China achieved 18.93% (43,180 MW) of SPV power installed capacity followed by Germany 17.38% (39,634 MW), Japan 14.60 % (33,300 MW), the United States 9.7% (22,178 MW), Italy 8.29% (18,910 MW), the United Kingdom 3.91% (8,915 MW), India 3.8% (8,727 MW), France 2.87% (6,549 MW), Australia 2.20% (5,031 MW), Spain 2.12% (4,832 MW) and other countries 16.11 % (36,744 MW).

- **Bio-power**

Bio-power is increasing with rapid growth for power generation in the major countries i.e. Brazil, the United States, China, Germany, India, Sweden, the United Kingdom and Japan. The total installed capacity of bio power is 106,000 MW. Brazil is the largest producer of bio-power electricity 14.98% (15,887 MW), followed by the United States China 11.76% (12,474 MW), China 9.73% (10,320 MW), Germany 8.61% (9,132 MW), India 5.28% (5,605 MW), Sweden 4.58% (4,864 MW), the United Kingdom 4.21% (4,463 MW), Japan 3.84% (4,076 MW) and other countries 36.96% (39,179 MW).

- **Geothermal power**

The total installed capacity of geothermal power is 13,200 MW. The major countries with the largest geothermal power capacity are the United States 27.27% (3,600 MW), the Philippines 14.39% (1,900 MW), Indonesia 10.6% (1,400 MW), Mexico 8.33% (1,100 MW), New Zealand 7.57% (1000 MW), Italy 6.81% (900 MW), Iceland 5.3% (700 MW), Turkey and Kenya 4.54% (600 MW), Japan 3.78% (500 MW) and other countries 11.36 % (1500 MW).

- **Concentrated solar thermal power**

Globally the concentrated solar thermal power generation capacity increased by 420 MW to reach nearly 4800 MW at the end of year 2015. Spain is the highest producer of solar thermal electricity 47.91% (2300 MW) followed by the United States 37% (1776 MW), India 4.24% (203.5 MW) & South Africa 3.12% (150 MW), United Arab Emirates 2.08% (100 MW) and rest of world 5.63% (270.5 MW). Apart from thermal power generation, the total installed capacity of solar thermal heating,

cooling other industrial process heat applications in the World is 37200 MWth (collector installed capacity of solar thermal technologies 53.1 million m^2).

- **Hydro power**

The total installed capacity of small, medium, large and pump storage& mixed hydro power plant is 1064,000 MW. The major seven countries for hydropower capacity are China, the United States, Brazil, Canada, the Russian Federation, Japan and India at the end 2015. China has the highest hydro power generation of 30.16% (320,910 MW) followed by the United States 9.63% (102,543 MW), Brazil 8.65% (92,062 MW), Canada 7.42% (79,043 MW), Russian Federation 4.84% (51,523 MW), Japan 4.61% (49,145 MW), India 4.4% (46,816 MW) and rest of World 30.25% (321,949 MW).

1.2 INDIAN SCENARIO ON RENEWABLE ENERGY

The total installed capacity of renewable energy system in India is 45,743 MW (including small hydro power only) as on November 2016. This includes, 61.39% (28,082 MW) from wind power, 17.79% (8,138 MW) from SPV power, 10.92% (4,997 MW) from bio-power, 9.45% (4,323 MW) from small hydro power & 0.44% (203 MW) from concentrated solar thermal power as shown in Figure 1.2 [7].

- **Wind Power**

Wind energy is most successful renewable energy option in India for generating grid connected power. The present installed capacity of wind power generation is 28,028 MW. Tamil Nadu state is the largest wind power producer (7,700 MW) followed by Maharashtra (4,660 MW), Gujarat (3,950 MW) and Rajasthan (4,000 MW) and rest of India (7,772 MW). The on-shore wind power generation potential is estimated is 49,130 MW and 102,788 MW at 50 meters & 80 meters of height respectively [7].

On a conservative consideration, a fraction of 2% land availability for all states except Himalayan states, Northeastern states and Andaman & Nicobar Islands which has taken as 0.5% of land availability.

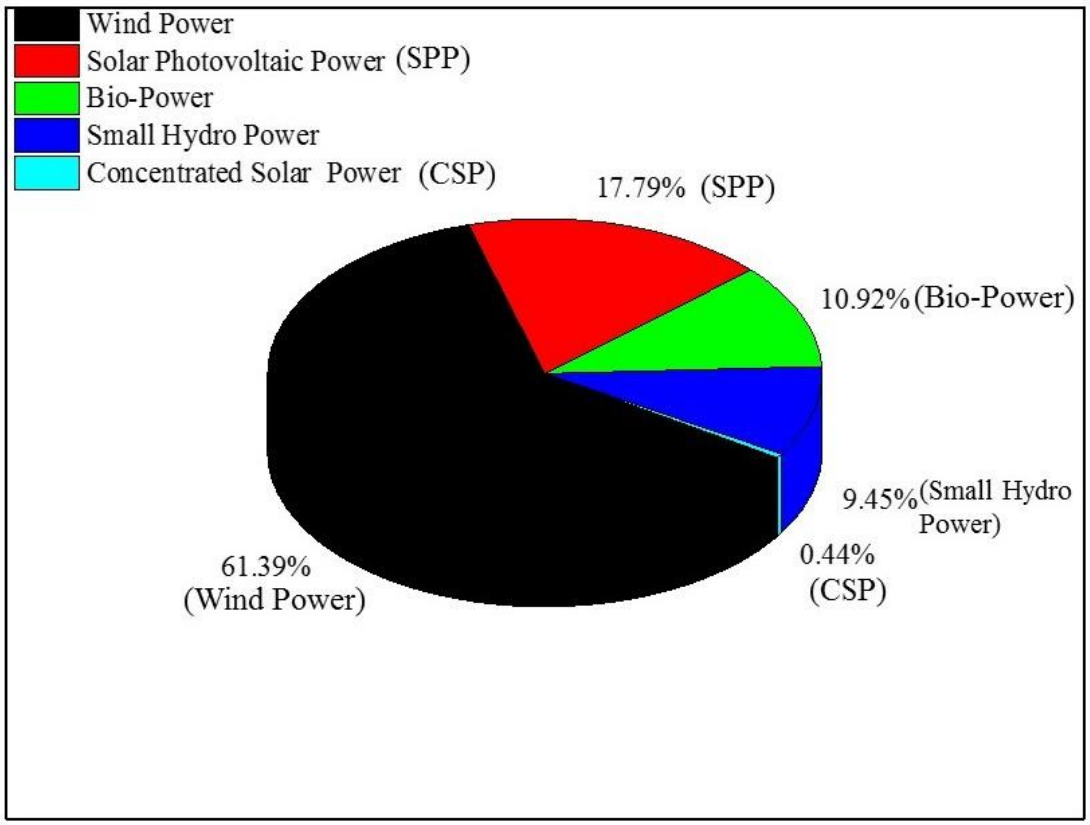

Figure 1.2 Indian renewable energy scenario as on November 2016

- **SPV Power**

The cumulative installed capacity of SPV power achieved at 8,138 MW as on 31.12.2015. Tamil Nadu is the largest SPV power producer with capacity of 1,550 MW, followed by Rajasthan (1,300 MW), Gujarat (1,138 MW), Andhra Pradesh (968 MW), Telangana (963 MW), Madhya Pradesh (811 MW), Punjab (571 MW) and Maharashtra (386 MW) and rest of India 451 MW [9]. The Government of India has set an ambitious target of generating 100,000 MW of Solar Power by the year 2021-22. This includes 60,000 MW of grid-connected solar power and 40,000 MW through roof-top grid interactive solar power to fulfill the target of 100,000 MW.

- **Bio-power**

Presently the total installed capacity of bio-power for feeding power to the grid is 4,760 MW (i.e. 300 biomass power and cogeneration projects) as on December 2015 and other 30 numbers of biomass power projects i.e. 350 MW are under various stages of completion. The potential for power generation from agricultural and agro-industrial residues is estimated at about 18,000 MW. With progressive higher steam temperature and pressure and efficient project configuration in new sugar mills and modernization of existing ones, the potential of surplus power generation through bagasse cogeneration in sugar mills is estimated at 7,000 MW [8]. The potential for bagasse cogeneration lies mainly in the nine sugar producing States, with the maximum potential of about 1,250 MW each in the States of Maharashtra and Uttar Pradesh. Thus, the total estimated biomass power potential is about 25,000 MW.

- **Concentrated solar thermal power**

In the country concentrated solar power plants of total 203.5 MW capacity have been installed using different solar thermal technologies. 101 MW parabolic trough collectors based CSP have been commissioned in various states of this country. 100 MW compact linear fresnel reflector based CSP has been built by M/s. AREVA [10]. A 1 MW solar thermal power plant based on Scheffler dish solar concentrators has also been installed at Mount Abu, Rajasthan, India.

- **Hydropower**

Present installed capacity of small and mini hydro power generation is 4,323 MW which is 9.45% of total installed capacity of renewable energy in India. The total estimated potential of small and mini hydro power for power generation is 19,749 MW [8]. Out of this potential, about 50% lies in the States of Himachal Pradesh,

Uttarakhand, Jammu & Kashmir and Arunachal Pradesh as river based projects as per run off river scheme. Some of the plain regions of various states have sizeable potential (i.e. Maharashtra, Chhattisgarh, Karnataka and Kerala) in this country. Presently, there are total 1048 numbers of small hydropower projects as capacity of 4,170 MW have been initiated in various regions of India.

1.3 RESEARCH GAP AND OBJECTIVE

The efficient use of heat energy sources is a key solution by considering the useful outputs like cooling, desalination. Polygeneration process in hybrid solar-biomass thermal power plant for combined power, cooling & desalination draw interest in this regard. Polygeneration provides opportunity to increase further efficiency through proper thermodynamic arrangement of different process or end products. In this section, research gap and objectives of this study are discussed in a specific forms.

1.3.1 Research Gap

Research gaps on proposed work has been identified after survey of the literatures in various publications (i.e. literature surveys are studied in the Chapter-2) and are given below;

- Many researcher have studied the solar thermal power plant technologies, but very little research work has been done on the hybridization of solar thermal power generation with other resources like coal, biogas and biomass. In India the resource assessment potential for solar and biomass hybrid system has not been attempted.
- Most of the research work has been carried out on cooling, heating and power in co-generation and tri-regeneration process which are able to provide more than one product commodity but no research work has been attempted in

polygeneration hybrid solar and biomass system for power, cooling and desalination.

- Research work has not been carried out in economics analysis and primary energy savings on polygeneration hybrid solar and biomass system for power, cooling and desalination.

1.3.2 Research Objective

The specific objectives of this study are summarized as follows:

- Solar and biomass resources assessments for modelling a hybrid solar and biomass power plant
    - State wise solar and biomass resource assessments
    - State wise solar and biomass power potential in India
- To modelling, optimization, energy and exergy of polygeneration hybrid solar and biomass system for power, cooling and desalination
    - Solar PTC system and biomass with a steam rankine cycle
    - To identify the effects of various operating parameters of the proposed system using Engineer Equation Solver (EES) software.
    - To determine the energy efficiency, exergy efficiency of each cycle. (Cycle-I: Hybrid solar-biomass power plant, Cycle-II: Vapor absorption refrigeration system, Cycle-III: Multi effect humidification and dehumidification desalination system).
    - To optimize the polygeneration hybrid solar & biomass system using genetic algorithm.
    - To analyze primary energy savings of the system.
- Cost analysis of polygeneration hybrid solar and biomass system for power, cooling and desalination and comparing with hybrid system that produce

equivalent output separately. The objective is to show the improvement potential by employing polygeneration process in hybrid solar and biomass system for power, cooling and desalination instead of a solar thermal power plant.

CHAPTER 2: LITERATURE REVIEW

Various literature reviews of studies conducted on system modelling performance have been undertaken. State of art of solar thermal technologies for power generation, hybrid solar thermal systems, refrigeration cooling systems, desalination systems and polygeneration systems are covered under this study. This chapter mainly focusses on the literature review to validate the originality of the proposed system in this research work.

2.1 STATE-OF-THE-ART OF CONCENTRATED SOLAR THERMAL TECHNOLOGIES FOR POWER GENERATION

The concentrated solar thermal technologies (CST) capture the direct normal irradiance and reflect to the receiver. This makes the technologies best suited to areas with a high percentage of clear sunny days. These CST have combinations of mirrors to concentrate direct normal irradiance to produce useful thermal energy for generation of electricity and process heat for end use applications. The following major technologies are currently used commercially for power generation and other process heat applications.

2.1.1 Parabolic Trough Collector

2.1.2 Linear Fresnel Reflector

2.1.3 Central Solar Tower

2.1.4 Parabolic Dish

2.1.1 Parabolic Trough Collector

Parabolic Trough Collector (PTC) basically focuses the sunlight at a receiver (line focusing) to achieve higher temperature up to 400^0C. PTC focuses the direct radiation coming from the sun and need to be tracked [1-axis for E-W & 2-axis for both E-W and N-S] along with the sun as shown in Figure 2.1. The solar radiation

received on the collector surface on the double axis tracking is slightly greater [11-12] due to the smaller incident angle. However the most of the PTC are single axis solar tracking, due to the lower cost and ease of installation & maintenance. When the PTC orientation axis is N-S, the annual incident energy received on the collector surface is greater, which results in a higher annual collector efficiency [13]. Depending on their tracking arrangement; these can be put in the category of high temperature applications. The receiver is normally an evacuated tube series which contains heat transfer fluid. Parabolic troughs using thermal oil are the most advanced among all CST and considered to be the most economical and high temperature solar thermal technology available today. In these tubes heat transfer fluid, such as synthetic thermal oil is circulated. It is heated up to 400^0C by the concentrated sun's rays, and pumped through a series of heat exchangers to produce superheated steam. The steam is used to produce electrical energy in a conventional steam turbine power plant. A 354 MW PTC based solar thermal power plant has been in operation in the United States since 1980s and two projects with each having a capacity of 70 MW have been installed. Forty-five PTC based solar thermal power plants with each of 50 MW capacity have been installed in Spain. These power plants are using synthetic oil as heat transfer fluid and molten salt for thermal storage for a period of 7.5 hours. In Italy, a 5 MW power plant with eight hours of thermal storage was installed in 2010. A large PTC power plant of capacity 250 MW in California and another of 280 MW in Arizona, the United Sates were commissioned in 2013 [14]. A 50 MW PTC based Solar Thermal Power Plant has been commissioned in Rajasthan [15]. The pressure and temperature of the superheated steam is at 40 bar and 300^0C. In, India there are total 101 MW capacity of solar thermal power plant has been installed based on PTC.

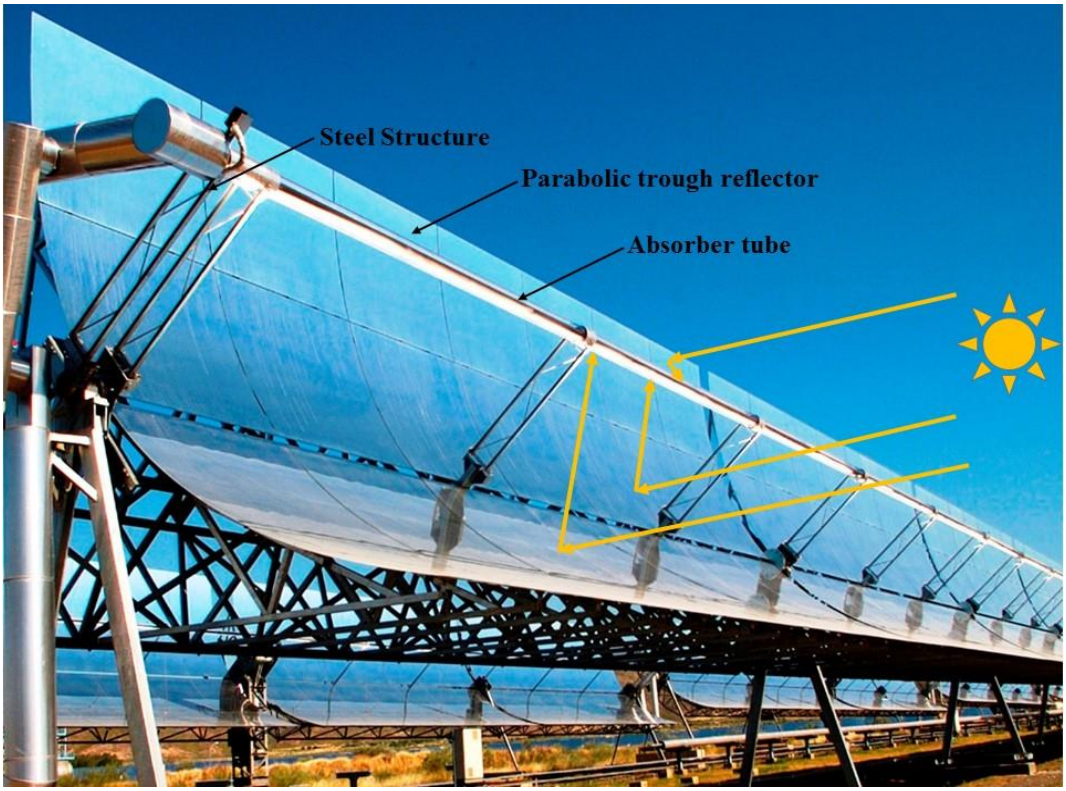

Figure 2.1 A typical parabolic trough collector installed at NISE

A grid-connected solar thermal power plant, with a capacity of 1 MWe at direct normal irradiance (DNI) of 600 W/m^2, has been designed and commissioned at National Institute of Solar Energy (NISE) as shown in Figure 2.2. The unique feature of the plant is the integration of two different solar fields (parabolic trough collectors and linear fresnel reflectors) without fossil fuel backup. The plant intends to combine the advantages of synthetic oil based PTC field and direct steam generation of linear fresnel reflector (LFR) field. The hot oil from PTC field and saturated steam from LFR field are integrated to produce superheated steam at 350°C and 42 bar to run a turbine-generator to produce electricity. It has also been designed for generating power for the period of 8 hours in a clear sunny day and having heating storage of the thermic oil for 30 minutes [16].

Figure 2.2 1 MW solar thermal power plant installed at NISE

Another three PTC based solar thermal power plants 280 MW capacity each have been installed in the United States in 2014 [17]. For other applications like process heat, a few companies have undertaken specific efforts in the development of modular, small, lightweight and low cost PTC as shown in Table 2.1. PTC technology is the best proven and easy in operation, high pressure and temperature capability, lowest cost large scale solar power technology available in many countries.

Table 2.1 Development of modular, small, lightweight and low cost PTC by various manufacturers

Manufacturer	Model	Aperture Width (meters)	Weight (Kg/m^2)	Concentration Ratio	References
Abengoa	PT-1	2.3	n/a	14	[18,19,20]
	RMT	1.1	7.7	14	[18,21]
Thermax	Solpac -P60	n/a	n/a	n/a	[22,23]
Smirro	Smirro -300	1.1	14.6	10	[24,25]
Koluacik	SPT-	1.2	47.2	8	[26]

Research & Development	0312				
	SPT-0324	2.4	33.8	15	[26]
	SPT-0536	3.6	27.1	23	[26]

2.1.2 Linear Fresnel Reflector

Linear fresnel reflector (LFR) is a single-axis tracking technology that focuses sunlight reflected by long heliostats onto a linear receiver to convert solar energy to heat. The classical LFR uses an array of mirror strips close to the ground to DNI onto a single, linear, elevated, fixed receiver as shown in Figure 2.3. The technology is seen as a low cost alternative to trough technology for the production of solar steam for power generation. The main advantages of the LFR as compared to PTC, are its low cost [27], no need for flexible high pressure joints or thermal expansion bellows due to fixed absorber tube, no vacuum technology and no metal-to-glass sealing. The other advantages are the substantially reduced wind loads on the reflector strips, increasing its width to three times the width of PTC reflector for one absorber tube and no heat exchanger is required as direct steam generation takes place. In 2012, two LFR based power plants of 30 MW capacity each began operating in Spain.

Figure 2.3 A typical linear fresnel reflector installed at NISE

A 9 MW and 12 MW LFR based power plant were constructed SOLAR EUROMED in France. In Australia, two power plants (i.e. 6 MW and 9.3 MW) are currently operating using this technology [28]. A 30 MW LFR based solar thermal power plant was installed and commissioned in Calasparra, Spain [17] and Areva has installed 100 MW CSP plants using its LFR technology at turbine temperature and pressure of 390^0C and 90 bar in Rajasthan, India [29-30].

2.1.3 Central Solar Tower

A central tower system consists of an array of tracking heliostats mirrors, which are spaced in a field and reflect the DNI into an elevated receiver [31] as shown in Figure 2.4. By concentrating the sunlight 300 to 1500 times, they achieve temperature from 800-1000^0C. The receiver is designed to effectively intercept the concentrated incoming beam radiation on tilted surface and absorb in the form of thermal energy at a specific temperature. This thermal energy is collected by heat transfer fluid used for power generation. The average solar flux impinging on the receiver has value between 200 to 1000 kW/m^2. This high flux allows working at high temperatures with high efficient power cycle.

In the United States, a 392 MW solar power plant using this technology has been installed. The temperature of superheated steam is 565°C with 29% plant efficiency [28]. Two commercial tower concentrating solar power plants (i.e. PS-10; PS-20) of total capacity of 31 MW have been installed in Spain. Both power plants are equipped with one hour steam based thermal storage for continuous operation in intermittency of the radiation during the day time [14]. The saturated steam temperature is 250°C with receiver efficiency of 92% and plant generates 24.3 GWh a year with plant efficiency of 17%. Two small high flux solar towers of capacities of 0.6 MW and 1.2 MW have been developed for high temperature air, steam, CO_2

bryaton cycle in Commonwealth Scientific and Industrial Research Organization, Australia. 450 numbers of good precision heliostat mirrors (each 2.5 m^2) have been used in the power plants. The Chinese Academy of Science has developed and demonstrated a 7.5 MW solar thermal power plants using this technology. The cavity receiver generates steam for power generation. The area of each heliostat mirrors is 100 m^2 [32]. Solar thermal power tower system with solid packed bed thermal storage (1 MW_{th}) in collaboration with M/s Sun borne Energy Technologies Private Limited is being developed at NISE as shown in Figure 2.5. The unique feature of this plant is the world's largest heliostat with an area of 150 m^2. The system uses the atmospheric air as working fluid with an output temperature from the volumetric receiver of 600 ^{0}C. Prototype 50 kW_{th} receiver has been tested and second round of the receiver is under developed [33].

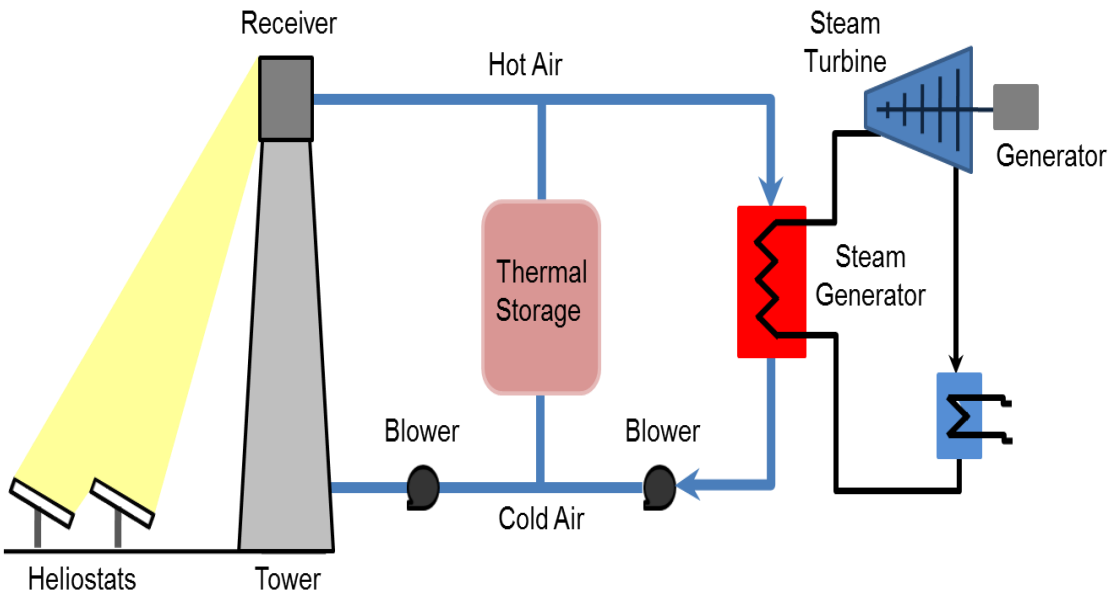

Figure 2.4 Schematic of solar power tower

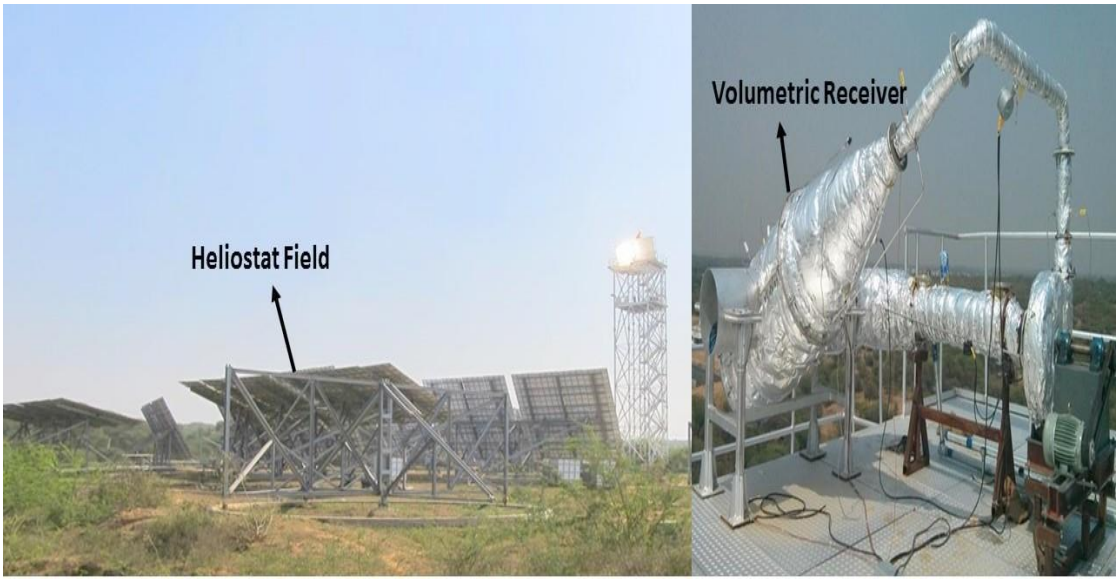

Figure 2.5 Solar power tower installed at NISE

2.1.4 Parabolic Dish

Parabolic dish technology consists of paraboloid mirrors which track as per sun direction (2-axis tracking) and reflect the solar energy (beam radiation on tilted surface) onto the receiver. The receiver absorb the radiation, increases the temperature of heat transfer fluid for electricity generation and process heat applications. The receiver can also be integrated with Stirling engine for direct electricity generation. This technology has the highest concentration ratio, overall conversion efficiency and optical efficiency of all the concentrated solar thermal technologies. The parabolic dishes have wide range of applications. Electricity generation is the main application of the parabolic dishes from kW to MW [34-37].

A β-type Striling engine with rhombic-drive mechanism and cam drive mechanism has been developed. The numerical modelling was also developed to predict the transient response of the engine at the starting moment and obtain the effect of various geometric & operating parameters [38]. Coupling of parabolic dish with air micro gas turbine was investigated (32.5 kW) to increase the conversion efficiency. The yearly prediction efficiency analysis is also carried out and the sun to electricity

has achieved efficiency of 26.48 % at DNI of 1000 W/m^2 and ambient temperature of 35 ^{0}C [39]. At present, 1.5 MW parabolic dish power plant was installed by Maricopa Solar in Arizona, the United State. The system consists of 60 numbers of dishes with each having Striling engine coupled with electrical generator (25 kW each). The glass mirrors are silver plated with solar reflectance of 94%. The working fluid of the engine is hydrogen, which is heated up to 750 ^{0}C through concentrated DNI [40].

A parabolic dish based concentrating solar thermal system integrated with fossil fuel based heat transfer fluid heating system was installed at NISE. The area of the dish is of 95 m^2, of peak thermal rating 46 kWh, into an existing thermic fluid heating system at 400 ^{0}C. The parabolic dish tracks the sun in two axes and maximizes the solar input at all times to yield high efficiency & output energy delivered to the industrial process. This dish tracks the sun with an accuracy within 0.2 degree and concentrates the incoming solar energy up to 1000 times at the focal point. The land footprint of a 95 m^2 dish is less than 0.5 m^2 on ground. The average solar radiation to thermal efficiencies of megawatt solution (MWS) dish system has been tested in the actual climatic condition and found to be more than 60% [41]. A parabolic dish technology with aperture area of 500 m^2 was developed and installed in Australia National University (ANU) in collaboration with Wizard power limited. The aim of the project was to commercialize the technology for large scale power generation. This technology is mounted on a turntable running on wheel on steel track [42]. A proto-type Stirling engine for net 1.5 kWe electrical output has been designed and fabricated at Indian Institute of Technology, Bombay. The conversion efficiency of the system achieved is in between 30-35%. The parabolic dish technology is still under demonstration and investment costs are high. Several parabolic dish

technology based prototypes systems have been successfully operated over the last ten years with capacities ranging from 10-100 kW in Australian National University [43]. Multi-megawatt projects up to 100 MW using this technologies are recently proposed in Australia and the United States.

Another solar Stirling engine capacity of 3kWp has been developed by ONGC in collaboration with INFINIA company limited, USA and installed at NISE for performance evaluation test under Indian climatic conditions as shown in Figure 2.6. This system has 2-axis tracking, i.e. it tracks the sun according to the time of the day and also according to the time of the year. As a result, it always faces towards the sun and concentrates all the direct solar radiation falling on the aperture. The system is having maximum conversion efficiency of 37% due to zero cosine losses. The concentration ratio of this system is about 800-8000 and can achieve a temperature of about 500^{o}-1200^{o}C. The Stirling engine at the receiver point of the dish concentrator is a helium gas engine with 'free piston'. When high radiation is concentrated on to the bottom part of the engine, the helium gas present in the compartment expands and pushes the piston upwards.

During this motion, another valve opens and helium gas flows through it on to the top of the piston and it pushes it down. This completes a cycle and the process is repeated to generate direct electric power with the arrangement made in it. This system is the solar power generator which produces alternate current at the frequency of 50Hz. Due to this advantage, this system can be directly connected to the grid and the requirement of inverter is eliminated. 1 MW solar thermal power plant based on parabolic dish solar concentrators with 16 hours thermal storage for continuous operation has been developed and is being built at Mount Abu, India as shown in Figure 2.7.

Figure 2.6 Paraboloid dish concentrators with stirling engine installed at NISE.

Figure 2.7 1 MW solar thermal power plant at Mount Abu, Rajasthan [44-45].

The estimated solar to electric efficiency is about 12%. The configuration of power plant consists of 750 numbers of solar dishes having a provision of thermal storage and each having 60 m^2 of aperture area. The estimated output of the power plant is electrical power of 1 MW for 8 hrs in day time and electrical power of 800 kW for 16 hrs with storage.

2.2 HYBRID SOLAR THERMAL POWER PLANT

Hybridisation of solar thermal is the best combination with other source of heat like biomass and fossil fuel. The major advantages of the hybrid solar thermal power plant are;

- Overcoming the variation of solar DNI
- Continuous generation of power with higher efficiency
- Minimizing the cost of power generation

The steam produced from solar field as per availability of sunshine hours and remaining heat can take from biomass and other resources to fulfill the heat requirement for running the hybrid power plant. Popov modelled a hybrid solar LFR and fossil fuel power plant using Thermoflow software [46]. The LFR technology is

used for preheating the working fluid and fossil fuel is used for superheating the working fluid to run the turbine of the power plant. A case study on 30 MW solar and biomass hybrid power plant has been carried out in Griffith, New South Wales, Australia. The boiler provides working fluid (steam) at temperature of 525°C and pressure of 120 bar to steam turbine of the hybrid system. It is seen that, the hybrid system decreases the investment cost (43%) as compared to stand alone solar thermal system with 15 hours thermal storage [47] and 69% lesser as compared to stand alone solar thermal power without thermal storage [48].

Hybrid biomass-solar power generation has been studied and investigated for several capacities (2-25 MW) and mainly focus on the integration of biomass combustion boiler with CSP [49-52]. PTC heats the heat transfer fluid (oil) as per availability of DNI and supplied to the boiler for making saturated steam and then supplied to biomass combustion boiler for superheating the steam to run the turbine. A hybrid power plant was investigated to provide electricity as well as process heat for running a cold storage [53]. Very little literature is available on energy and exergy analysis of solar-biomass hybrid system. An article informs about the thermal efficiency of 22.5 % at turbine inlet temperature and pressure of 500 ^{0}C and 60 bar and mass flow rate of steam at 5 kg/sec [54]. Another thermodynamic study recently reported a thermal efficiency of 36.5% when solar was hybridized with biomass integrated gasification [55]. A grid interactive hybrid solar power plant built by Thermosolar Borges having a capacity of 22.5 MW in Spain is using heat from solar DNI of 18 MJ/m^2/day and remaining from biomass residue to supplement each other [56]. The operational experience obtained from this grid interactive hybrid system will be more valuable in further development of solar-biomass hybridization strategies.

Several authors investigated on hybrid solar biomass for power generation where water gets heated to saturated state through solar thermal technologies and superheated state through biomass boiler [57-59]. Electricity production cost from hybrid solar thermal power plant is lower than that of stand-alone system [60, 61] and reduction in the amount of CO_2 emitted to the atmosphere is also observed [62]. The literature survey shows the limited focus in the area of solar and biomass for hybridization.

2.3 COOLING SYSTEM

Demand for human comfort as well as industrial application for air-conditioning, especially in India is increasing rapidly. Recently most of the industrial office complexes, educational institutions and commercial establishments are using VAR cooling system. Solar energy driven commercial VAR systems are costly and technologically difficult to operate due to variation of DNI in most places of this country. In polygeneration process VAR cooling system can be operated by using extracted steam from turbine, which is the second cycle (VAR cooling system) of this proposed power plant.

The performance data of a water cooled VAR machine has been presented for 16 kW cooling capacity, generator temperature 90^{o}C, cooling water temperature 32^{o}C, chilled water temperature 15^{o}C with COP of 0.75 [63]. An experimental analysis of Solar FPC based single effect VAR cooling system of 35 kW cooling capacity has been done in Madrid. This system is operated by using heat from storage tank at the temperature of 80^{o}C through heat exchanger [64]. A study on industrial solar refrigeration & air conditioning system has been conducted to analyze the techno-economical feasibility of solar driven VAR cooling system. It is shown that there is a possibility to replace the existing system according to the requirement of

heating/cooling of the Industry [65]. Performance of Yazaki single effect solar absorption cooling (LiBr-H_2O) system is analyzed for cooling capacity of 70 kW. FPC & vacuum tubular collector is used for heating refrigerant up to 95^oC in the generator. The area of FPC & vacuum tubular collector is 124 m^2 & 108 m^2 respectively. An absorption cooling system is simulated by using transient system simulation tool. Results showed that such systems are economically competitive in comparison to conventional cooling systems [66, 67]. A 10 kW prototype solar operated VAR cooling system has been developed for office building in Berlin, Germany. This system is driven by hot water at 85^oC, cooling tower temperature of 27 ^oC, chilled water temperature at 15^oC with COP of 0.74 [68]. The single effect system gives best result up to a heat source temperature of 105 ^oC. Above that temperature, it is worthwhile to switch over to double effect system. A 15 kW double effect air cooled absorption cooling system with evaporator temperature of 12^oC and generator temperature of 140^oC with the COP of 1.16 is installed in NISE, India [69]. A Solar operated (double effect) cooling system of cooling capacity 70 kW has been installed in a commercial building in California. The achieved COP of this system is 1.1 at a given heat source temperature of 170^oC from integrated compound parabolic collector [70]. A 16 kW double effect (LiBr-H_2O) absorption cooling system has been developed with heat source of 160^oC from linear parabolic trough collectors. This system can be used for space heating/cooling in summer & winter with COP of 1.0-1.1 [71]. A 100 kW double-effect (LiBr-H_2O) absorption cooling system has been developed with heat source temperature of 144^oC and pressure of 4bar from PTC. The cooling water temperature and evaporator temperature are 27^oC & 7^oC respectively [72].

2.4 DESALINATION SYSTEM

Literature survey of desalination system based on multi effect humidification and dehumidification, multi stage flash type and solar still was carried out. The maximum pure water (120 m^3/day) was found from desalination system based on flat plat solar collector with hot water temperature of 60-80^oC for a duration of eight months (February to October) in a year at daily insolation of 5.8-7.9 kWh/m^2day & ambient temperature of 20-33^oC [73]. Numerical solution and experimental data of multi stage flash type desalination system with a heat recovery system was studied. The desalination system consists of solar collectors and six stages of desalination tower. It was observed that the production of pure water was up to 25 liters/m^2 /day [74]. On an average, fresh water production was approximately 6,000 liters per month by using heat from solar with a maximum of 10,500 liters in the month of May and a minimum 1,700 liters in the month of January. It was found that generation of fresh water per month depends on the radiation (heat) [75]. The multi effect desalination system could be coupled with membrane distillation to minimize the production cost of desalination water in coastal areas because of the problem of land cost and low DNI. The Solar collector is used to provide heat and photovoltaic system is used for electricity to operate membrane distillation system [76].

A multi-effect distiller has been developed with water capacity of 3m^3/day. The temperature of hot water is 75^oC with volume flow rate of 4.8 m^3/hour and sea water inlet temperature of 18^oC with flow rate of 6m^3/hour. The mechanical efficiency is increased by using the shell and the tube type heat exchanger [77]. Approximately 6800 liters/hour of fresh water could be generated through multi effect humidification & dehumidification (MEHD) at heat source of 80^oC through condenser-2 and heat exchanger-2 of VAR cooling system [181].

2.5 POLYGENERATION SYSTEM

The term “polygeneration system” provides a generalized idea on the integration of heat management of energy system which simultaneously generates several outputs like electricity, cooling & water desalination and in some cases process heat. Polygeneration system effectively reduces the installation cost of each system and improves the overall efficiency, reliability and economical aspects for energy conversion applications. The development of the polygeneration system with internal combustion engine is the simultaneous production of electricity, cooling & domestic hot water to meet a complete set of demands of tourism sector [78].

Polygeneration process with Organic Rankine Cycle (ORC) has been analyzed for MEHD water desalination from renewable energy which generates both electricity and water desalination [79]. Theoretical and experimental investigations have been conducted on microtrigeneration system. The system is saving the energy up to 28% and reduction of CO_2 emission up to 36% as compared to conventional system [80]. The comparative study of energetic performance of three systems i.e. solid oxide fuel cell (SOFC) trigeneration, solar trigeneration, biomass trigeneration has been carried out on different output parameters like electrical power, heating to cooling & reduction of greenhouse gasses emission. From this comparative study, it is shown that SOFC trigeneration system has highest electrical conversion efficiency on electrical power among them. Whereas biomass trigeneration and solar-storage trigeneration systems have highest overall efficiency as compared to SOFC-trigeneration system. The maximum efficiency achieved in Solar-storage trigeneration system was 90% in standalone mode, 45% on short period storage due to variation of DNI & only 41% on storage mode [81]. The Biomass based polygeneration systems are investigated theoretically and experimentally. The

electricity is generated from biomass and methanol is produced as a byproduct. It shows that about 10% of the energy consumption is reduced through this system [82]. A new cogeneration process through renewable sources has been developed using Stirling engine and fluidized bed combustor separately. The Stirling engine is operated by solar energy and biomass combustion is operated by fluidized bed combustor. The drawback of the system was the high investment cost & small size [83]. The combination of vegetable oil-fed reciprocating engine with concentrated PTC has been developed in polygeneration process. Dynamic simulation showed that the polygeneration system provides electricity, space cooling (LiBr-H_2O) and hot water [84].

An energetic analysis has been done on micro combine heat power system for residential sector. From this study, it is observed that combined production of power & heat is one of the solutions for saving the energy and environmental conservation for residential sector [85]. Although the investment cost of the combined system is slightly higher than individual cooling, heating & power production systems but in long term it will be more economical [86]. Renewable energy plays a vital role in polygeneration process. Performance analysis of polygeneration system has been developed by using natural gas, solar energy & biomass gasification, applied to Spanish tourist resort. The system gives maximum primary energy savings (PES), reduction of greenhouse gasses & high economic feasibility [87]. The polygeneration or multi-generation process produces different energy vectors such as power, cooling and process heat, which is termed as highest efficient than co-generation and trigeneration [88]. Polygeneration has good potential in renewable energy sector as it reduces the energy consumption and increases the energy efficiency. The three applications of polygeneration system are electricity generation, process heat and

desalination for agro food industry, residential sector and other end uses. These systems have good future as help in CO_2 emission reduction [89]. The Polygeneration process is reliable in supply of energy, decrease the greenhouse gasses and economically viable [90, 91]. Solid waste of bioethanol used as feed stock of biomass based polygeneration process which provides electricity and heating for drying process. The overall efficiency of the system is increased to 3.1% by utilizing the flue gas as drying process [92]. Polygeneration system has its applications in chemical Industry as well. The electricity is produced from power plant by using the steam from unreacted syngas [93]. Weekly data for the duration of one year has been analyzed on evacuated solar collector and proton exchange membrane (PEM) fuel cell for polygeneration system. The system produces cooling (single effect VAR) and domestic hot water. PEM fuel cell produces electrical power and supplementary heat energy for cooling & heating through heat exchanger [94]. The plant efficiency increases up to 90% by a coal based polygeneration systems with reduced CO_2 emission in energy sector [95]. Hybrid polygeneration system has been designed with PTC and solid oxide fuel cell. The solid oxide fuel cell is producing electricity and heat for space heating and cooling from fuel directly by electrochemical reaction [96]. Waste heat from ORC is utilized for heating through heat exchanger and remaining part of heat is utilized in generator of single effect absorption chiller. Three case studies have been considered on solar power generation, cooling-cogeneration & heating-cogeneration. The output of these case studies is the increase in the efficiency of the combined system [97].

Polygeneration process is more efficient and cost effective than co-generation and multi generation process because waste heat from one system is utilized for the other applications as per load demand. Wood chips were used as feed stock in Biomass

gasification polygeneration system and converted into three phase products such as gas, charcoal & liquid. The overall efficiency of the polygeneration by using these three products was increased up to 95.84% [98]. The development of an investment planning and polygeneration infrastructure design has been done through mixed-integer programming. It showed that the polygeneration process is more efficient than conventional standalone system. Biomass based polygeneration system is more profitable, if the price of biomass resource is less than coal [99]. A Mixed-Integer Nonlinear Program (MINLP) modelling framework has been developed and optimized for coal-based polygeneration plant. By producing electricity & methanol together, the overall efficiency gets increased. In this frame work, a polygeneration process is consisting of four functional blocks: gasification, chemical synthesis, gas turbine, steam turbine and heat recovery steam generator. For each block, all alternative technologies are considered and mathematical representation has been carried out by using first-principal sub-models. And all sub-model are linked into substructure based MINLP program. This frame work provides design variables of technologies, equipment, capacity, size of each functional block, power generation for polygeneration process [100]. Annual energy yield has been calculated on heliostat based small hybrid solar power plant in trigeneration process. The hybrid solar tower consists of heliostat fields, receiver tower, micro turbine and cooling chiller. The cooling system is operated by using the heat from recuperator & a heat exchanger is used for heating the water [101].

Most of the research work has been done on cogeneration and trigeneration systems but the studies on polygeneration processes based on hybrid solar-biomass power plant are missing in the literatures. Under this an attempt has been made to investigate a novel polygeneration process based on hybrid solar-biomass power

plant which continuously produces electricity, cooling and desalination [102]. A schematic of polygeneration process based on hybrid solar-biomass power plant is shown in Figure 2.8.

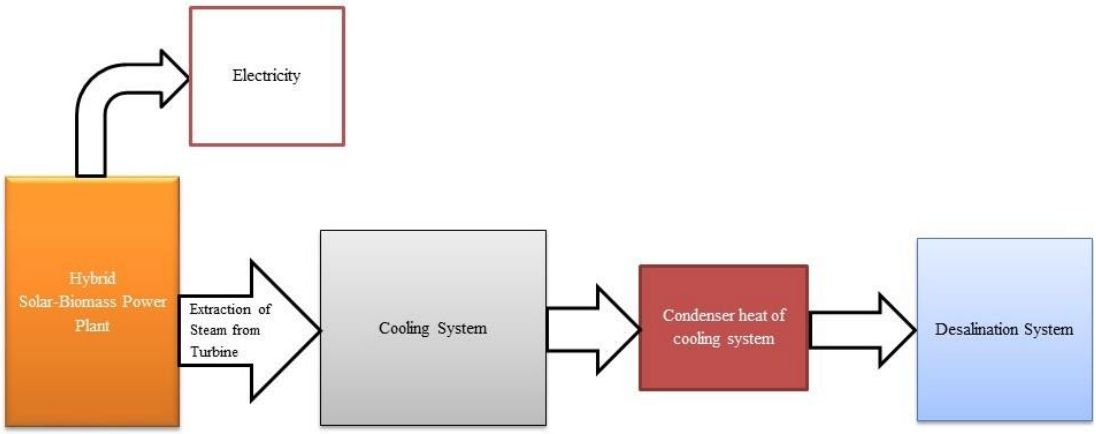

Figure 2.8 Flow diagram of polygeneration process in HSB power plant [104]

2.6 SUMMARY OF THE RESEARCH WORK DONE

So far the research work has been done on cogeneration and trigeneration systems but the study on the polygeneration process in hybrid Solar Thermal power plant has not been attempted. From the study of polygeneration process in hybrid Solar Thermal power plant has been analyzed and optimized. The simulation is performed in EES Software. Availability of both Solar Resources (DNI, Ambient Temperature & Wind Speed) and biomass at a same regions/places is highly desirable to design and simulation for hybrid solar thermal power plant. Therefore consequent upon the discussion on introduction is in the **First Chapter** and literature review discussed in the **Second Chapter**. Resource assessment of solar and biomass for hybrid thermal power plant in India is discussed in the **Third Chapter** of the thesis. In this chapter, several aspects associated with hybrid solar and biomass power generation installations such as state wise availability of biomass resources, DNI has been discussed. The DNI is based on daily average of DNI mapping resulted from the data available with National Renewable Energy Laboratory (NREL)-National Institute of

Solar Energy (NISE). This DNI resources analysis results are reliable indication of the solar potential. For assessing the solar energy potential, only 10% of the total waste land area available has been considered in the major biomass energy contributing states like Punjab, Uttar Pradesh, Haryana, Maharashtra, Madhya Pradesh, Karnataka, Tamil Nadu, Gujarat, Rajasthan, Kerala, Bihar, Andhra Pradesh, West Bengal, Odisha and Assam. For biomass resources, the assessment of scale up potential on biomass has been carried out separately for biomass crop residues and energy plantations. The major agricultural based biomass crop wise potential for different states of India are mapped by analyze the energy potential of biomass. Simulation study of biomass consumption in the power plant at different radiation conditions to meet heat requirement for operation of solar hybrid power plant is also carried out. The modelling, simulation of hybrid solar and biomass thermal power plant is discussed in **Fourth** chapter. For the hybrid system, biomass boiler arrangement is taken to operate on the biomass, whenever it needed at different load conditions. Solar field is utilized to heat the heat transfer fluid as per availability of DNI. Hot water from feed water heater gets heated through heat transfer fluid using heat exchanger. The total input energy of the proposed hybrid system is taken from the heat transfer fluid through PTC as per availability of solar resource and remaining from biomass to maintain the steam at superheated state and supplied to turbine. The detailed performance analysis (energy and exergy) of solar and biomass hybrid thermal power plant are carried out to identify the effects of various operating parameters like DNI, condenser pressure, turbine inlet temperatures, boiler pressure on net power output energy and exergy efficiencies. A 5 MW hybrid solar and biomass power plant has been designed. The hybrid solar and biomass power plant is an extremely promising energy system and is likely to provide a major share of

renewable bulk electricity production. Taking in view, government of India is making biomass policy to minimize the biomass feed stock in the hybrid power plant for establishing the market. The energy demand for cooling and process heat applications are increasing continuously due to increasing industries, office campuses, institutions demand resulting in requirement of huge amount of electricity. Globally, in industrial sector about two-thirds of total consumption of energy is used for process heat applications. This increasing huge amount of electricity demand is resulting in higher consumption of conventional energy e.g. coal, fossil fuel, which results in increasing the greenhouse gas (GHG) emissions and negative impact of climate change in this country. Presently these industries either buy power from the state electricity boards or generate their own power largely. Finally to reduce their net power consumption, some of industries produce power as well as process heat for their use through cogeneration. Although cogeneration is playing as advanced technology for generation of both electricity & process heat application, but it is not possible to provide more than two such outputs like space cooling, water desalination for their requirement. To reduce energy demand and provides more than two such outputs like cooling, water desalination using different reject heat source, a new concept of polygeneration process is developed in hybrid solar-biomass power plant. The modelling and optimization of polygeneration hybrid solar and biomass system for power, cooling and desalination and for the economic aspect, the cost analysis are discussed in the **Fifth Chapter** of the thesis. In the polygeneration process simultaneous production of power, cooling and desalination from different heat sources in hybrid solar-biomass system with higher energy efficiency take place. It is one of the solutions to fulfill energy requirements from renewable sources and also helps in the reduction of carbon dioxide emissions. The turbine is designed in such

that, condensation heat of power plant can be input for the vapor absorption refrigeration (VAR) and condensation heat of VAR cooling system is used as heat input sources of desalination system. The VAR cooling system operates using the extracted heat taken from turbine and condenser heat of the VAR cooling system is used in desalination system for production of drinking water as per demand requirement. Though the production of electricity decreases due to extraction of heat from turbine for VAR cooling system and evaporator load decreases due to heat taken from condenser of VAR cooling system for desalination, the complete system meets the energy requirements, increases the overall performance & PES. The technical modelling and thermodynamic analysis (energy and exergy) of polygeneration process in HSB thermal power plant for combined power, cooling and desalination has been analyzed. Specifically, the energy and exergy analysis are taken to better understand the performance of polygeneration process in solar-biomass hybrid system. The optimization of polygeneration process in hybrid solar thermal power plant has been done in this chapter of the thesis. Various scenarios are examined parametrically in order to present the system performance for various operation condition. In this section, optimization using EES software, (genetic method) is conducted with respect to these aforementioned analyses and is utilized to compensate for the shortcomings of traditional objective approaches by allowing a larger perspective and determining a more complete spectrum of solutions. The results and discussions of the system is discussed in **Sixth Chapter** of the thesis. It is observed that the heat input sources from solar and biomass is very important for improving the overall efficiency of system and these supplement with each other. From this study it becomes apparent that the heat utilization from solar and biomass is considered as 37% and 63% respectively for modelling of HSB system in

polygeneration process. The evaporator load, output of distilled water continuously increases at a faster rate up to a generator temperature of 150^0C, thereafter the rate of increase in the evaporator load and output distillation declines with increase in generator temperature while keeping other parameters of the system as constant. For better understanding the effect of generator temperature on cooling load and desalination water output, we should concentrate on the effect of temperature on work output, VAR cooling and distilled water output. The optimization of the proposed system has also been carried out for increase the energy efficiency, VAR cooling load, output of desalination system and total output. Though the production of electricity decreases due to extraction of pressure from turbine, the complete system (combined power, cooling and desalination) meets the energy requirements and its overall efficiency increases.

In the last chapter (**Seventh Chapter)** of the thesis the overall conclusions of the result which is obtained in the above study and some recommendations are made for future studies to guide researchers who want to perform further works.

CHAPTER 3: RESOURCE ASSESSMENT OF SOLAR AND BIOMASS FOR HYBRID THERMAL POWER PLANT

Biomass energy has provided sustenance to mankind through the ages and also attracting greater attention for power generation in India. Government of India recognized the potential role of biomass power generation in the Indian economy quite early and since then has been the vanguard of its promotion. If it is used as much as it is produced its benefits will include its wide availability, carbon neutrality and the potential to provide large productive employment in rural areas. As a further outcome of the carefully planned mix of policy and financial incentives introduced by the Government of India, capacity has been built up in the country for biomass power technologies, their operation and maintenance. The availability of crop residues like bagasse, rice husk, coconut shells and the wood processing wastes inherently limit the growth of the capacity of biomass power generation [102]. One of the major barriers confronted by the biomass power plants is a secured supply of required quality and quantity at a competitive price for sustainable operation of the plant. The price of biomass resources has slowly increased due to non-availability of biomass at right price in recent years [103].

On the other hand, CSP do not continuously generate power due to daily & seasonal variations and low level of direct normal irradiance in most places in the country. Although CSP with storage is one of the solution to maintain required amount of heat [104,105] due to DNI variations or short transients but difficult to store for long duration of time for night cycle [106,107]. Hybridization with CSP is most important for continuous generation of power for fulfilling the energy requirements. So, the choice of biomass resources is a judicious selection with solar resource (DNI) for hybridization with CSP for continuous power generation, which supplement with

each other. The solar (DNI) and biomass resource analysis has been studied in this chapter.

3.1 APPARENT SOLAR TIME

In solar energy calculation it is always desirable to convert clock time into apparent solar time (AST). AST measured with respect to solar noon, which is the time when the sun is crossing the observer's meridian [148, 150 & 152]**.**

3.2 SOLAR ANGLES

For designing of solar field for various applications, the solar angle is most important. For calculating the solar angles many researcher have been developed different algorithms [108-114]. The following important solar angles analysis are taken in this thesis research work.

Declination (δ) in degree for any day of the year (N) can be calculated as [115]:

$$\delta=23.45\sin\left[\frac{360}{365}(284+N)\right] \quad (3.1)$$

Solar hour angle (ω) increases by 15° every hour and is expressed as:

$$\omega=\pm 0.25\times(\text{Number of minutes from local solar noon}) \quad (3.2)$$

Where the positive sign for afternoon hours and the negative sign for morning hours. From AST, the solar hour angle (ω) can also calculated as:

$$\omega=(\text{AST}-12)\times 15 \quad (3.3)$$

Solar altitude angle is expressed as:

$$\sin(a)=\sin(L)\sin(\delta)+\cos(L)\cos(\delta)\cos(\omega) \quad (3.4)$$

Where L is local latitude, which is the center of the earth to the site of interest and equatorial plane. This is positive for north of equator and negative for south of equator.

Mathematical expression of solar azimuth angle is written as [116]:

$$\sin(z) = \frac{\cos(\delta)\sin(\omega)}{\cos(a)} \qquad (3.5)$$

The angle of incidence can be obtained for horizontal N-S axis with E-W tracking [117, 148].

$$\cos(\theta) = \sqrt{\sin^2(a) + \cos^2(\delta)\sin^2(\omega)} \qquad (3.6)$$

3.3 SOLAR RESOURCES (DNI) IN INDIA

DNI is the key resource for operation of concentrating solar power plant. The DNI has a significantly higher variability in space and time in comparison to global horizontal irradiance and its measurement needs high attention & accuracy. In order to find authenticated long term data, ground measurement (NISE) and satellite (NREL-NISE) derived values are taken for this analysis.

3.3.1 Solar DNI from Satellite and Ground Measured Data

Different radiation parameters like global radiation, diffuse radiation and DNI are required for performance evaluation and research of solar system. DNI resource is used in concentrating solar thermal power technologies like PTC, LFR, Parabolic dish and heliostat. From the Earth surface, satellite measure the reflected DNI in several wavelength bands. There are various complex model and algorithms can be used to determine DNI at various locations. Raw data are available from various satellite operators and processed by various organizations providing solar satellite data services. One of the best known satellite data is provided by NREL, the United States of America. Under a collaborative project between NREL and NISE solar radiation map covering India at $10\ \text{km} \times 10\ \text{km}$ resolution has been developed using weather satellite (METEOSAT) observations incorporated into a site-time specific solar modelling approach developed at the State University of New York at Albany [118].

Solar mapping of the entire country based on satellite imagery and ground measured data provide information of DNI on a continuum basis with an approximate accuracy of $\pm 15\%$ [119]. It is possible to identify the areas with higher solar radiation and set up ground stations for more accurate measurement of solar DNI at those locations. The maximum deviation of DNI average falls below $\pm 5\%$ from the long term average [120]. Thus the site selection for installation of solar thermal power plant is highly desirable to have reliable 10 years long term DNI data. However, in this study the solar resource availability as per NREL-NISE satellite data (ideally for at least 14 years) and recent ground measurement data at NISE have been taken into account.

NREL has developed solar maps and data for India to provide 15 years of hourly satellite data spanning between 2002 and 2014 as shown in Figure 3.1 [121]. It is seen that, most of the places in the country are having good sunshine, about 5,000 trillion of kWh per year incident over India's land area with most of the parts receiving DNI of 4-5.5 kWh/m^2/day [122]. About 200-250 sunny days are available in a year in most parts of the country. Solar thermal for the generation of heat and electricity can be deployed during these sunny days. This map and data help identify locations for high-quality solar thermal projects, which can help accelerate the deployment of solar thermal power generation in India.

Government of India has launched a flagship program on Solar Radiation Resource Assessment (SRRA) to aim world's largest network of ground measurement SRRA stations. The program was implemented by Ministry of New and Renewable Energy (MNRE), Government of India in Phase-I & Phase-II. Presently, there are total 111 numbers of SRRA stations and 4 numbers of advance measuring stations have been installed. This programs aims to overcome the deficiencies in the availability of

investor grade ground measurement data crucial for planning and implementation of CST power projects.

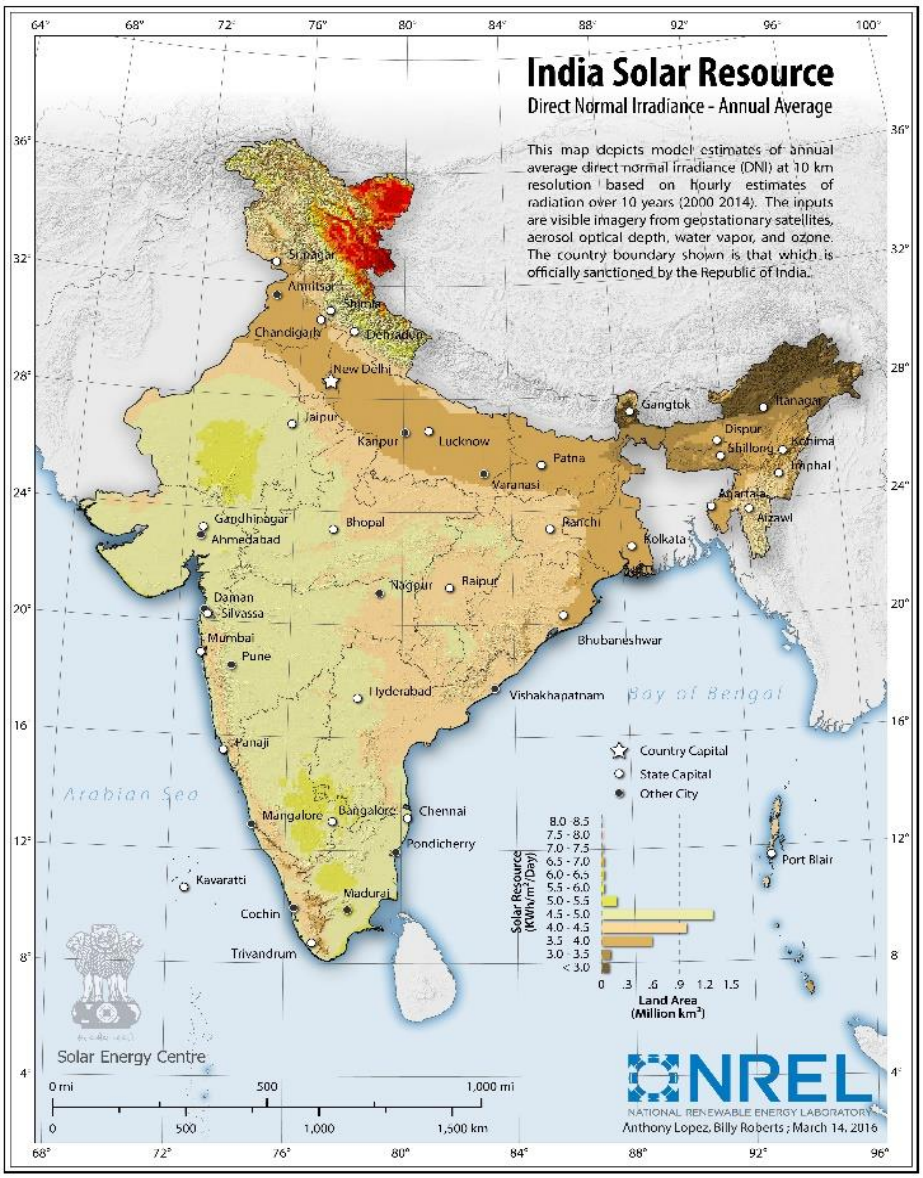

Figure 3.1 State wise annual average DNI available in India based on satellite modelling [124]

3.3.2 DNI Assessment at NISE

A SRRA Station has been set up at NISE campus under phase-I program of SRRA and is in operation since 20th October, 2011 as shown in Figure 3.2. This station is providing data of all solar radiation parameters along with meteorological parameters with an aim of mapping of various solar thermal technologies installed at NISE

campus. The geographical parameters of this site are given in Table 3.1. The data pertaining to all these parameters is measured at every one minute interval and is transmitted to central data receiving server at National Institute of Wind Energy using GPRS. The data thus logged is uploaded to web server through which data can be assessed and monitored in real time mode as shown in Figure 3.3.

Solar radiation parameters are measured by World Meteorological Organization (WMO) specified high quality sensors with their traceability to World Radiometric Reference (WRR) scale. Global horizontal irradiation & diffuse horizontal irradiation are measured by world meteorological organization (WMO) secondary standard pyranometer sensors while DNI is measured by WMO first class pyrheliometer sensor. Also the meteorological parameters are measured by highly precise instruments traceable to National Institute of Standards and Technology (NIST), USA.

In the designing of the CSP systems, along with DNI, the other parameters like wind speed, ambient temperature and relative humidity (RH) also have very crucial role. Ambient temperature have an effect on the thermal losses from receiver and measurement of wind speed is required for safety of the solar field. The efficiency of the wet cooling system decreases with increasing of RH and finally reduces the plant efficiency. Therefore, RH parameters are required for assessing the operational conditions. DNI and other parameters like wind speed, ambient temperature and RH data have been collected from ground stations and satellite data (NREL) for evaluation of hybrid solar thermal system. As per availability of DNI the biomass resources are taken into account for designing the hybrid power plant.

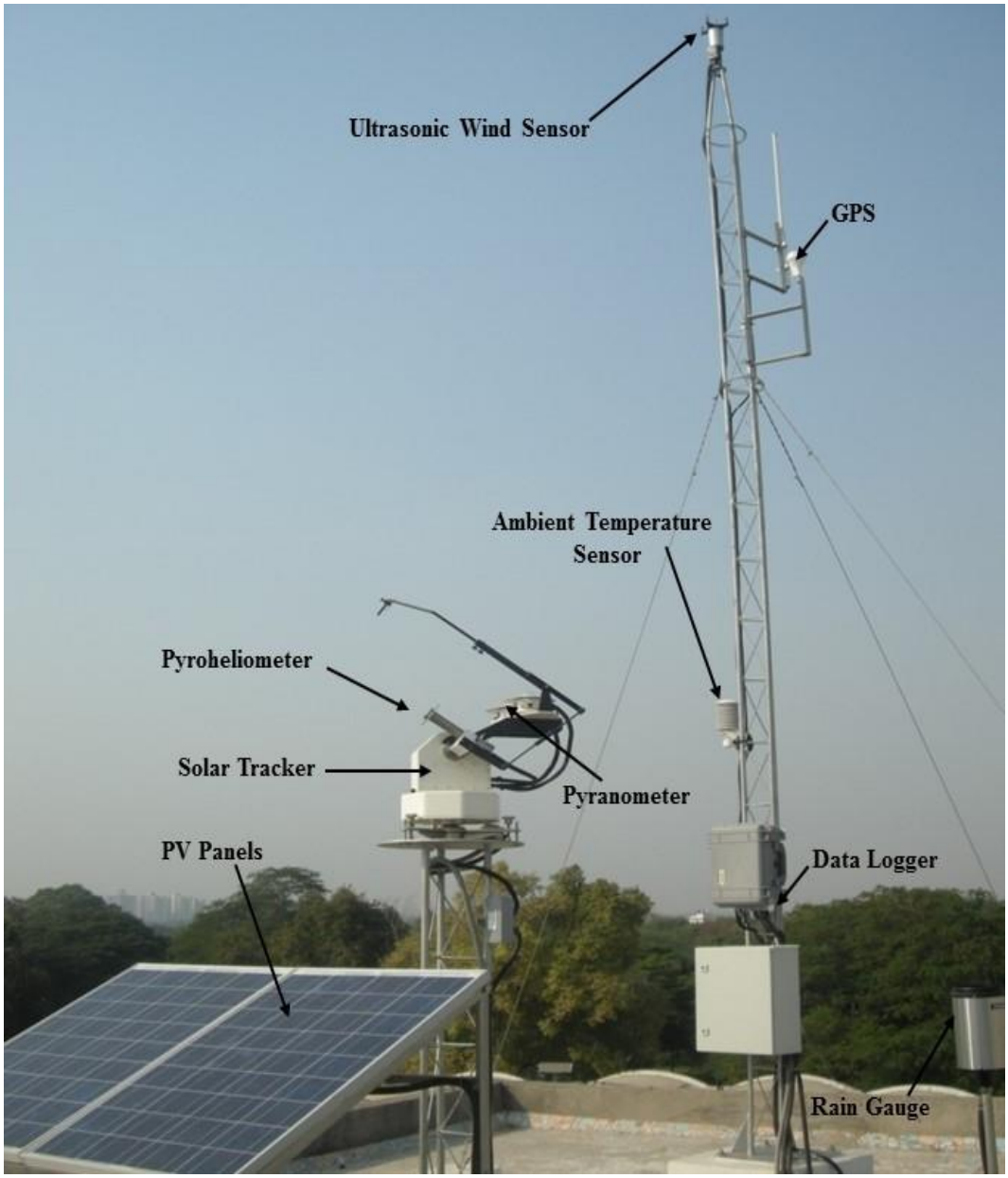

Figure 3.2 SRRA station at NISE

Table 3.1 The geographical parameters for the Gurugram region of Haryana, India.

DNI	3.5-4.0 kWh/m^2/day
Ambient Temperature	35 ^{0}C
Latitude	28.425^0
Longitude	77.155^0
Elevation	259 m

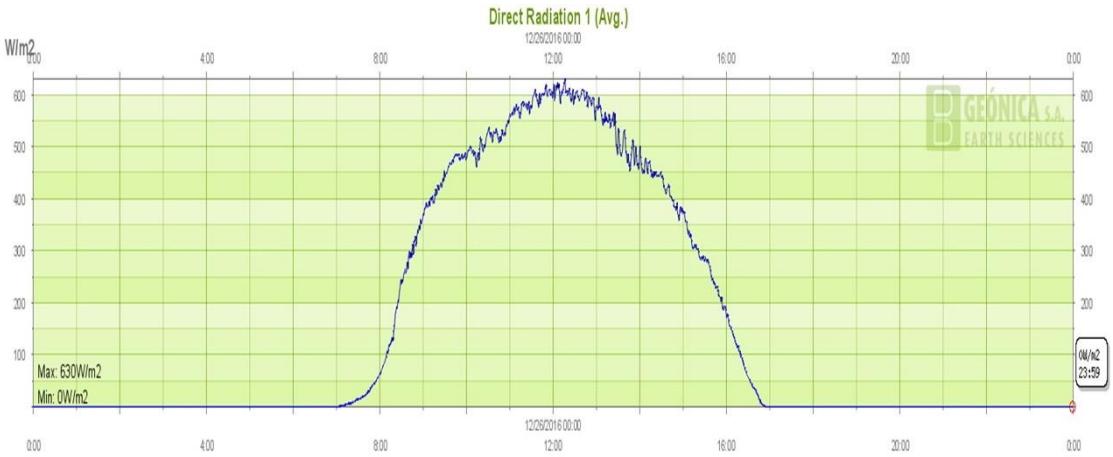

Figure 3.3 Online accessed monitored real data at NISE on dated 26.12.2016

The monthly (January to December) and range wise standard deviation of DNI is expressed as:

$$s = \frac{\sum_{i=1}^{n}\left(d_i - \bar{d}\right)^2}{n-1} \tag{3.7}$$

The monthly and range wise mean DNI of each year can be written as:

$$\bar{d} = \frac{d_1 + d_2 + d_3 ... + d_n}{n} \tag{3.8}$$

Where, $d_1 + d_2 + d_3 ... + d_n$ are the total range wise DNI for each month of the year.

The mean absolute percentage error (MAPE) between NISE and NREL data for each month can be expressed as:

$$\text{MAPE} = \frac{1}{n}\sum_{t=1}^{n}\left(\frac{DNI(G) - DNI(S)}{DNI(G)}\right) \times 100 \tag{3.9}$$

3.4 BIOMASS RESOURCES IN INDIA

In India over 500 million tons (MT) of biomass is produced every year in different states like; Uttar Pradesh, Andhra Pradesh, Bihar, Odisha, Chhattisgarh, Gujarat, Punjab, Haryana, Karnataka, Kerala, West Bengal, Maharashtra and Madhya Pradesh [123,124]. The biomass resides are collected from the report of states of agriculture of India 2012-13.

The state wise biomass energy potential from residue surplus is analyzed using the following equation [54];

$$E(j)=\sum_{i=1}^{n} CRs(i,j)\times H.V(i,j) \qquad (3.10)$$

Where, $E(j)$ is biomass energy potential of 'n' crops at j^{th} state(MJ), $CRs(i,j)$ is surplus residue potential of i^{th} crop at j^{th} state (kg) and $H.V(i,j)$ is heat value of i^{th} crop at j^{th} state, MJ/kg, as given in Table 3.2.

The Surplus residue potential of i^{th} crop at j^{th} state are as per following equation;

$$CRs(j)=\sum_{i=1}^{n} CRg(i,j)\times SF(i,j) \qquad (3.11)$$

Where, $CRs(j)$ is the residue surplus at j^{th} states, $CRg(i,j)$ is the potential of residue on i^{th} crop at j^{th} states (kg) and $SF(i,j)$ is the fraction residue of i^{th} crop at j^{th} states [125].

Table 3.2 High heating value (MJ/kg) of various biomass residue [126-134].

Crop	Types of Residue	High Heating Value(MJ/kg)	References
Rice	Straw	15.54	Ref.[126]
	Husk	15.54	Ref.[127]
Wheat	Stalk	17.15	Ref.[127]
Coarse Cereal	Straw and husk	18.16	Ref.[128]
Sugarcane	Bagasse	20	Ref.[127]
	Tops	20	
	Trash	20	Ref.[127]

Coconut	Shell	10	Ref.[129]
	Fibre	19.4	Ref.[130]
	Pith	19.4	Ref.[130]
Cotton	Stalks	17.4	Ref.[131]
	Gin Waste	16.7	Ref.[132]
Oilseeds	Straws and husks	14.35	Ref.[133]
Pulse	Straw	14.65	Ref.[132]
Jute/Mesta	Stalks	19.7	Ref.[134]

CHAPTER 4: MODELLING AND SIMULATION OF HYBRID SOLAR AND BIOMASS THERMAL POWER PLANT

This chapter mainly focuses on the solar and biomass hybridization where, the biomass boiler could be operated continuously and solar field is supplying heat to preheated water using heat transfer fluid THERMINOL VP-1 (eutectic mixture of 73.5% of diphenyl oxide and 26.5% of diphenyl) during sunshine hours and depending upon the season. Besides the hybridization, attention is also paid on the state-wise availability of biomass resources and DNI at selected places in India. Solar thermal technologies selection and site selections are most important factors for different locations of the country for hybrid solar-biomass thermal power generation to supplement with each other. In India about 380 MW of PTC based power plants have been planned for installation as part of the JNNSM (Phase-II) [135] as shown Figure 4.1.

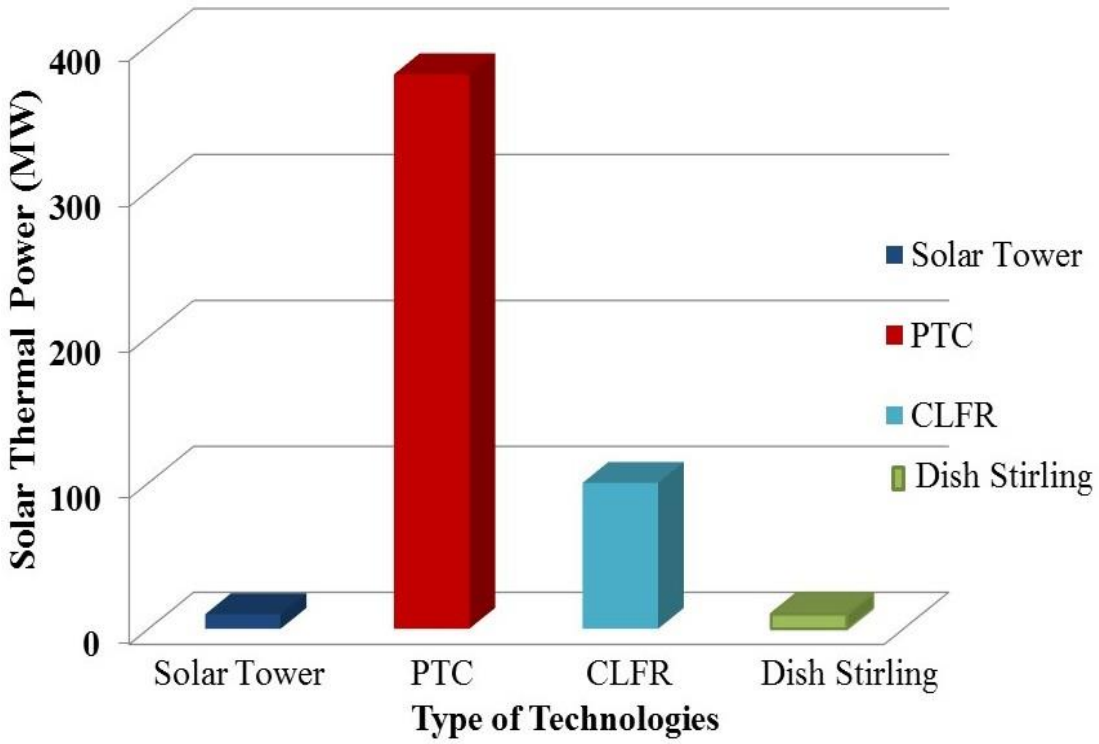

Figure 4.1 Installation of solar thermal technologies for power generation in India

Temperature up to 391^0C is achieved by using single-axis parabolic trough reflectors on East–West tracking [136]. As per 12^{th} five year plan, the proposed power generation installation capacity is 1000 MW. The state wise biomass power plant target and installed capacity are shown in Figure 4.2.

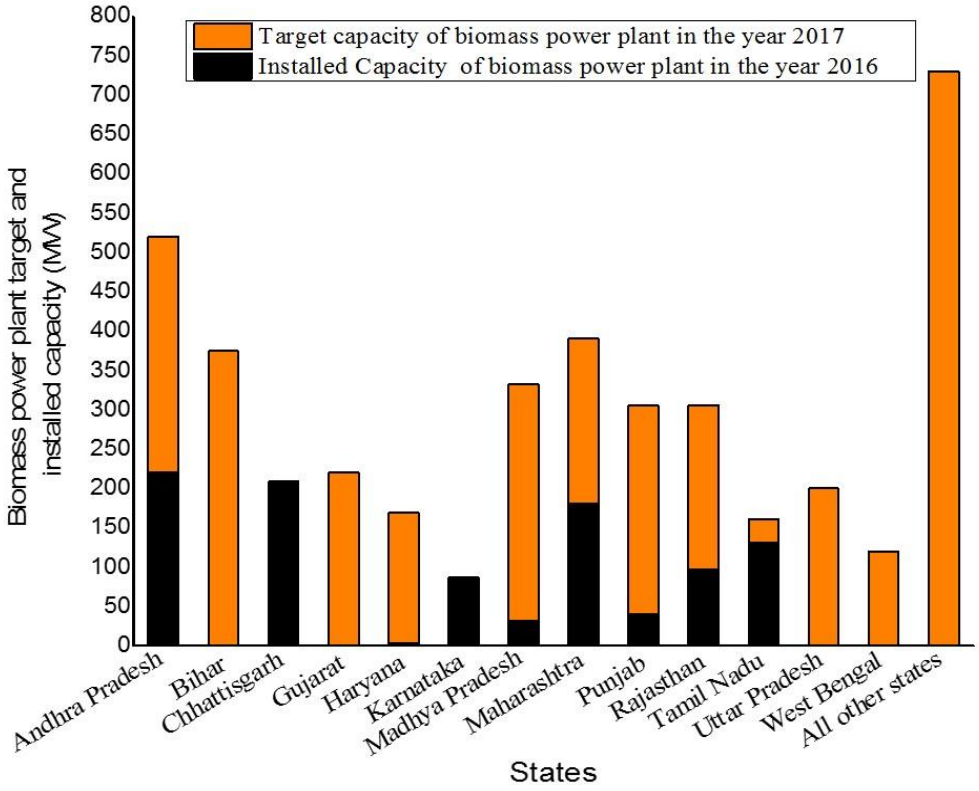

Figure 4.2 Biomass power plant target and installed capacity in India

The targeted biomass power plant capacity addition for 13^{th} five year plan is estimated as 5730 MW [137]. Biomass based power generation capacity of 10×10^3 MW by the year of 2022 has been proposed for India [138].

In the off-season the feed stock biomass residue will be used as boiler fuel to generate power from solar-biomass hybrid power system for continuous power supply. Biomass fuels are saved and are utilized in off-season due to integration of solar with biomass thermal power plant. The month wise harvesting period of major biomass production are considered to minimize the savings of biomass fuels as

shown in Figure 4.3 [139,140]. It is seen that, the harvesting period of rice husk is maximum among major available biomass types. The harvesting period of rice husk is from December to April of every year and cotton stalks harvesting period is from January to March. Therefore, biomass fuels utilization is comparatively high during the low solar DNI period, i.e. January, July, August, September, and December.

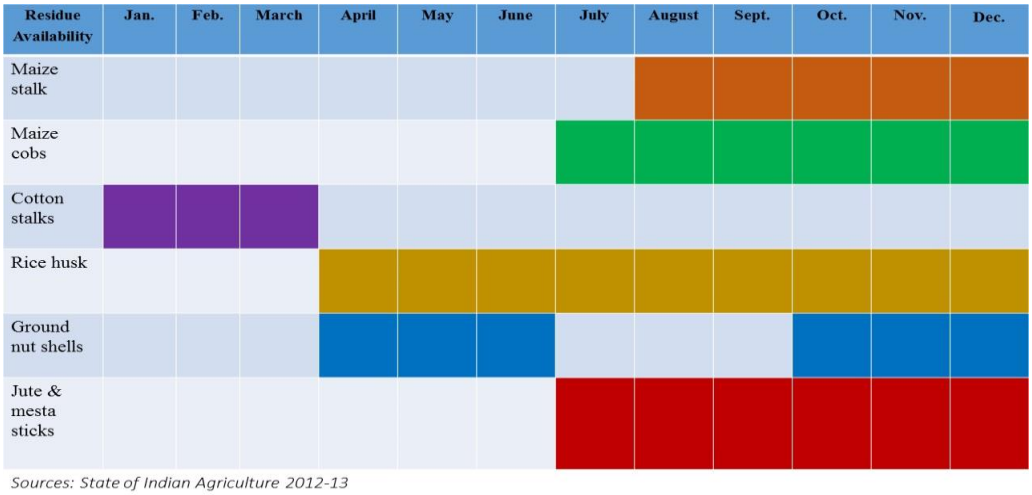

Figure 4.3 Month-wise harvesting period of biomass resources

Government of India is planning to encourage installation of hybrid biomass with solar thermal back up for sustainable power supply through various incentives [141]. The main objective of the plan is to assess the techno economic and commercial viability of solar and biomass thermal hybrid technologies for power generation in India.

4.1 MODELLING APPROACH OF HYBRID SOLAR-BIOMASS THERMAL POWER PLANT

The technical modelling of 5 MW hybrid solar-biomass power plant has been carried out in this study, using EES software. In this hybrid power plant, biomass boiler arrangement is taken to operate on the biomass, whenever it is needed at different load conditions. Solar field is utilized to heat the heat transfer fluid as per availability of DNI. Hot water from feed water heater gets heated through heat transfer fluid

using heat exchanger (H.E) as shown in Figure 4.4. Biomass boiler will run at lower capacity depending upon the condition of water at state point 'a' through PTC field (4-8-9-a) and biomass boiler will operate at full load capacity in intermittency of day & night cycle (4-c-a). Steam gets superheated at pressure of 60 bar and temperature of 500 °C through biomass boiler and is supplied to turbine at mass flow rate of 5 kg/sec steam. In this cases, steam is bled at point '6' and remaining steam is expanded at low pressure and medium temperature.

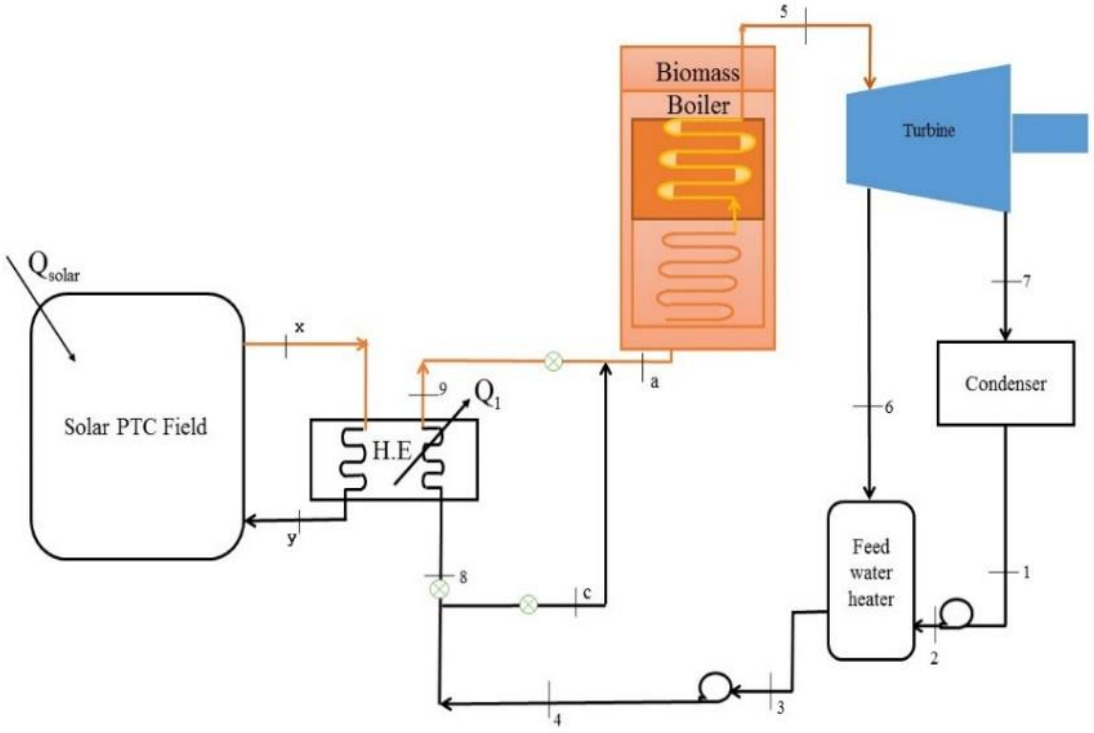

Figure 4.4 Schematic diagram of the hybrid solar and biomass power plant

The bled steam is mixed with condensed water to be preheated in feed water heater. At state point 1, condensed water is pumped to the feed water heater at pressure of 5 bar and mixed with bled steam in feed water heater. Hot water from feed water heater is pumped to the heat exchanger, 4-8 and/or directly pumped to the biomass boiler in intermittency of day / night time, (4-c-a).

4.2 THERMODYNAMIC EVALUATION

The thermodynamic (energy and exergy) equation is mainly defined for the major components and better understanding of the hybrid solar and biomass thermal power plant. PTC field transfers solar DNI into useful heat (Q_1) at specific mass flow rate of heat transfer fluid (m_{oil}) which circulates through absorber tube. Specifications of major components of the hybrid system used in this analysis, are shown in Table 4.1. The following assumptions are made for the thermodynamics analyses:

- Steady-state, steady-flow operating conditions are considered.
- The Pressure drops in pipes and heat losses are negligible.
- All components are well insulated and are considered adiabatic.
- Kinetic and potential energy changes are negligible.

Table 4.1 System specifications of major components of the hybrid system that are used in this study.

Equipment	Input Parameters	Value	Units
Parabolic Trough Collector Field	Aperture Area, A_{ap}	18000	m^2
	Optical Efficiency, η_{opt}	65	%
	a_1	0.1	W/m^2-^{o}C
	a_2	0.001	W/m^2-^{o}C
	Mirror reflectance	94	%
	Mass flow rate of heat transfer fluid	25	kg / sec
Biomass Boiler	Moisture of rice husk	8	%
	Ash in rice husk	15	%
	LHV of bottom ash	3.762	MJ / kg

	LHV of fly ash	2.7	MJ / kg
	Ratio of bottom ash to fly ash	80:20	
	Percentage of oxygen in flue gas	7	%
	Flue gas temperature	200	^0C
	Atmospheric temperature	35	^0C
	Humidity of air	0.018	Kg/kg of dry air
Turbine	Efficiency	96	%
Pump		88	%

4.2.1 Energy Evaluation

First law of thermodynamic is used to analyze the performance of hybrid power plant by several authors [142-148]. The performance analysis of the parabolic trough collector are investigated by several authors [149-153].

The hourly useful heat gain (Q_1) is defined as: $Q_1 = Q_{solar} \times \eta_{E,PTC}$ (4.1)

Where Q_{solar} is the solar energy falling on PTC field may be expressed as

$$Q_{solar} = A_{ap} \times G_{Bt} \quad (4.2)$$

Where, G_{Bt} is beam radiation on titled surface and expressed as

$$G_{Bt} = DNI \times \cos(\theta) \quad (4.3)$$

The energy efficiency $(\eta_{E,PTC})$ of the parabolic trough collector is expressed as

$$\eta_{E,PTC} = \eta_{opt} - a_1 \frac{(T_m - T_o)}{G_{Bt}} - a_2 \left[\frac{(T_m - T_o)^2}{G_{Bt}} \right] \quad (4.4)$$

Where η_{opt} is optical efficiency of the parabolic trough reflector, a_1 is the first order coefficient of the collector efficiency $\left(W/m^2\text{-}^0C\right)$, a_2 is the second order coefficient of the collector efficiency $\left(W/m^2\text{-}^0C^2\right)$, T_m is the mean temperature of the heat transfer fluid (oil) is defined as

$$T_m = \frac{T_y + T_x}{2} \tag{4.5}$$

The mass flow rate of heat transfer fluid $\left(m_{oil}\right)$ is calculated as

$$m_{oil} = \frac{\eta_{E,PTC} \times A_{ap} \times DNI \times \cos(\theta)}{\Delta T \times C_p} \tag{4.6}$$

Where, C_p is the specific heat of heat transfer fluid, ΔT is the temperature difference of heat transfer fluid across the PTC field is expresses as

$$\Delta T = \left(T_x - T_y\right) \tag{4.7}$$

The energy balance equations of the major components of hybrid solar and biomass power plant are expressed as [148,154]

Turbine: $W_T = m_w\left[\left(h_5 - h_6\right) + \left(1-\alpha\right)\left(h_6 - h_7\right)\right]$ (4.8)

Where, 'α' is fraction of steam bled from turbine, m_w is the flow rate of water $\left(kg/\sec\right)$

Condenser: $Q_C = m_w(1-\alpha)\left(h_7 - h_1\right)$ (4.9)

Pump: $W_p = m_w\left[\left(h_3 - h_4\right) + \left(1-\alpha\right)\left(h_2 - h_1\right)\right]$ (4.10)

The energy efficiency of the hybrid solar and biomass $\left(\eta_{E,HSB}\right)$ power plant is expressed as the ratio of output energy to input energy.

$$\eta_{E,HSB} = \frac{W_{net}}{Q_{solar} + Q_b} \tag{4.11}$$

Where W_{net} is the net-work output of the plant and Q_b is the heat produced from biomass and formulated as

$$Q_b = m_b \times LHV_b \quad (4.12)$$

$$LHV_b = HHV_b - (226.04 \times H) - 25.82 \times \textit{moisture content of biomass} \quad (4.13)$$

$$HHV_b = 338.3 \times C + 1443 \times (H - O/8) - 94.2S \quad (4.14)$$

Where m_b the flow rate of biomass residue, LHV_b is the lower heating value and HHV_b the higher heating values of biomass or can be calculated using Dulong's and Perit formula [155]. The ultimate analysis of the dry biomass weight (%) of carbon (C), hydrogen (H), oxygen (O) and Sulphur (S) are given in Table 4.2.

Table 4.2 Ultimate analysis of biomass [156].

Crops	Carbon (%)	Hydrogen (%)	Nitrogen (%)	Oxygen (%)	Sulphur (%)
Rice Husk	37	5.5	0.5	37	0.09
Wood	44-52	5-7	0.5-0.9	40-48	2.78
Bagasse	47	6.5	0.0	42.5	0.001
Groundnut Shell	34-45	2-4.6	1.1-1.4	43-60	0.01
Maize Stalk	48.23	8.18	0.81	31.08	0.18
Maize Cobs	46.2	4.9	0.6	36.18	0.25
Cotton Stalks	48.7	5.9	0.8	44.7	0.0
Jute Stalks	49.79	6.02	0.19	0.05	41.37

On an average biomass consists of 40-50% Carbon, 4-7% Hydrogen and 30-45% Oxygen on moisture and ash free basis. Biomass contains negligible amounts of Nitrogen and Sulphur. The moisture content of rice husk has been taken as 10%. The net-work output (W_{net}) of the plant is defined as the difference of turbine work output and pump work input.

$$W_{net} = W_T - W_P \tag{4.15}$$

Heat transfer rate (Q_2) in the heat exchanger is expressed as

$$Q_2 = m_w\left(h_9 - h_4\right) = m_{oil}\left(h_x - h_y\right) \times \eta_{E,HE} \tag{4.16}$$

Where $\eta_{E,HE}$ is energy efficiency of heat exchanger. The heat is taken from biomass boiler (Q_{boiler}) to maintain the quality of the steam at superheated condition may be expressed as

$$Q_{boiler} = m_w\left(h_5 - h_a\right) = Q_b \times \eta_{E,boiler} \tag{4.17}$$

Where $\eta_{E,boiler}$ is the energy efficiency of the boiler.

The mathematical analysis of the energy losses of the major components of the hybrid power plant are as follows;

(a) Heat losses in PTC (L_{PTC}) : $L_{PTC} = A_{ap} \times G_{Bt} \times (1 - \eta_{E,PTC})$ (4.18)

(b) Percentage heat losses of the biomass boiler [157-163].

1. Percentage heat loss due to dry flue gas (L_{b1})

$$L_{b1} = \frac{m_{fg} \times C_{fg} \times (T_{fg} - T_o) \times 100}{LHV_b} \tag{4.19}$$

$$m_{fg} = \left[1 + \frac{\mathrm{EA}}{100}\right] \times \mathrm{Th}_{\mathrm{Air}} \tag{4.20}$$

$$\text{Excess Air (EA)} = \frac{\%\mathrm{O}_{\text{flue gass}}}{(21 - \%\mathrm{O}_{\text{flue gass}})} \times 100 \tag{4.21}$$

Theoretical air (Th_{Air}) required for complete combustion in kg per kg of biomass.

$$Th_{Air} = \frac{\left[\left(11.43\times C\right)+\left\{34.5\times(H-\frac{O}{8})+(4.32\times S)\right\}\right]}{1000 \text{ kg/ kg of biomass}} \quad (4.22)$$

Where m_{fg} is the mass of dry flue gas in kg per kg of fuel, T_{fg} is the flue gas temperature in K, and C_{fg} is the specific heat of flue gas, and $\%\,O_{\text{flue gass}}$ is the percentage of oxygen in flue gas.

2. Percentage heat loss due to hydrogen in biomass (L_{b2})

$$L_{b2} = \frac{9H_2\left[584+C_{p2}(T_{fg}-T_o)\right]}{LHV_b}\times 100 \quad (4.23)$$

Where C_{p2} is the specific heat of super-heated steam (1.881 kJ/kgK), H_2 is kg of hydrogen present in biomass in 1 kg basis.

3. Percentage heat loss due to moisture in biomass (L_{b3})

$$L_{b3} = \frac{m_{moistutre}\left[584+C_{p2}(T_{fg}-T_o)\right]}{LHV_b}\times 100 \quad (4.24)$$

Where $m_{moistutre}$ is mass of moisture in kg per kg of biomass.

4. Percentage heat loss due to moisture in air (L_{b4})

$$L_{b4} = \frac{AAS\times humidity\ factor\times C_{P2}\times(T_{fg}-T_o)\times 100}{LHV_b} \quad (4.25)$$

Where AAS is actual mass of air supplied in kg per kg of biomass. Air humidity factor is 0.019 kg of water per kg of dry air.

5. Percentage heat loss due to unburnt biomass in bottom ash (L_{b5})

$$L_{b5} = \frac{\left(\begin{array}{l}\text{Total bottom ash collected in}\\ \text{kg per kg of biomass burnt}\end{array}\right)\times\text{LHV of bottom ash}\times 100}{\text{LHV}_\text{b}} \quad (4.26)$$

6. Percentage heat loss due to unburnt in fly ash (L_{b6})

$$L_{b6} = \frac{\text{Total ash collected in kg per kg of fuel burnt} \times \text{LHV of fly ash} \times 100}{\text{LHV}_b} \quad (4.27)$$

7. Percentage heat loss due to surface radiation, convection and other unaccounted (L_{b7})

Normally the actual radiation, convection, surface loss and other unaccounted losses were considered as 2.3 %.

The total percentage heat losses in boiler is expressed as (L_{boiler})

$$L_{boiler} = L_{b1} + L_{b2} + L_{b3} + L_{b4} + L_{b5} + L_{b6} + L_{b7} \quad (4.28)$$

Boiler efficiency will be also calculated $\eta_{boiler} = 1 - \frac{L_{boiler}}{100}$ (4.29)

(c) Heat losses in turbine (L_T): $L_T = W_T - (W_T \times 0.96) = 0.04 \times W_T$ (4.30)

(d)Heat loss in condenser (L_c): $L_c = m_w \times (1-\alpha) \times (h_7 - h_1)$ (4.31)

(e)Heat losses in pump (L_p): $L_P = W_p - (W_p \times 0.88) = W_p \times 0.12$ (4.32)

4.2.2 Exergy Evaluation

Exergy analysis is a useful tool of the thermodynamic analysis to provide a detailed breakdown of the losses in terms of waste exergy emissions and exergy destruction for the overall system. However, limited researchers have analyzed on the exergy analysis of the thermal power plant [164-171]. The exergy analysis for the major components of hybrid solar-biomass power plant is analyzed in this study.

The steady-state process, respective balances for exergy can be written as [172]

$$\sum_i E_{xi} + \sum_j \left[1 - \frac{T_o}{T_j}\right] Q_j = \sum_e E_{xe} + W + E_{xD} \quad (4.33)$$

Exergy of the flowing stream at each state point (E_x) may be expressed as

$$E_x = \left[\left(h - h_o \right) - T_o \left(s - s_o \right) \right] \tag{4.34}$$

Exergy of solar radiation may be expressed as (E_{xSolar}) is expressed as [173]

$$E_{xSolar} = Q_{solar} \times \left(1 - \left(\frac{4}{3} \right) \times \left(\frac{T_o}{T_{sun}} \right) + \left(\frac{1}{3} \right) \times \left(\frac{T_o}{T_{sun}} \right)^2 \right) \tag{4.35}$$

Where, Q_{solar} is the useful heat gain from solar DNI and T_{sun} is apparent sun temperature.

Exergy heat gain of fluid (E_{x1}) from the Parabolic Trough Collector (PTC) field is expressed as

$$E_{x1} = \frac{Q_1}{T_x - T_y} \times \left(\left(T_x - T_y \right) - T_o \cdot ln \frac{T_x}{T_y} \right) \tag{4.36}$$

The exergy efficiency $(\eta_{Ex,PTC})$ of the parabolic trough collector is expressed as

$$\eta_{Ex,PTC} = \frac{E_{x1}}{E_{xsolar}} \tag{4.37}$$

The chemical exergy of biomass $(E_{x,b})$ is expressed as

$$E_{x,b} = m_b \times \phi \times LHV_b \tag{4.38}$$

Where ϕ is the multiplication factor and calculated as [174]

$$\phi = 1.0401 + 0.1728 \frac{H}{C} + 0.0432 \frac{N}{C} + 0.2169 \frac{O}{C} \times \left(1 - 0.2062 \frac{H}{C} \right) \tag{4.39}$$

The exergy efficiency of the HSB power $(\eta_{Ex,HSB})$ is formulated as:

$$\eta_{Ex,HSB} = \frac{W_{net}}{E_{xSolar} + E_{xb}} \tag{4.40}$$

Exergy destruction equations in major components of the hybrid system are given as:

Boiler: $E_{xD,Boiler} = E_{xb} - m_w \left[\left(h_5 - h_a \right) - T_o \left(s_5 - s_a \right) \right]$ (4.41)

Turbine: $E_{xD,T} = m_w\left[\left\{h_5 - \alpha h_6 - (1-\alpha)h_7\right\} - T_o\left\{s_5 - \alpha s_6 - (1-\alpha)s_7\right\}\right] - W_T$ (4.42)

Condenser: $E_{xD,C} = (1-\alpha)m_w\left[\left(h_7 - h_1\right) - T_o\left(s_7 - s_1\right)\right]$ (4.43)

Pump-1: $E_{xD,P1} = W_{p_1} - (1-\alpha)m_w\left[\left(h_2 - h_1\right) - T_o\left(s_2 - s_1\right)\right]$ (4.44)

Pump-2: $E_{xD,P2} = W_{p_2} - \alpha m_w\left[\left(h_4 - h_3\right) - T_o\left(s_4 - s_3\right)\right]$ (4.45)

Feed water heater: $E_{xD,FWH} = m_w\left[\alpha h_6 + (1-\alpha)h_2 - h_3 - T_o\left\{\alpha s_6 + (1-\alpha)s_2 - s_3\right\}\right]$ (4.46)

Heat exchanger: $E_{xD,HE} = \dfrac{Q_1}{\left(T_x - T_y\right)\times\left\{\left(T_x - T_y\right) - T_o \times ln\dfrac{T_x}{T_y}\right\}} - m_w\left\{\left(h_a - h_8\right) - T_o\left(s_a - s_8\right)\right\}$ (4.47)

CHAPTER 5: MODELLING, OPTIMIZATION AND COST ANALYSIS OF POLYGENERATION PROCESS IN HSB THERMAL POWER PLANT

The term “polygeneration process” provides a generalized idea on the integration of heat management of energy system which simultaneously generates several outputs like electricity generation, cooling & water desalination and in some cases process heat. Many researchers explained about the performance evaluation of VAR systems in their required temperature ranges and most of the research work has been done on combined cooling, heating and power which are able to provide more than one product commodity [175-180] but very little research work has been carried out for polygeneration process. The proposed system in HSB power plant in polygeneration process will produce continuous power, cooling and desalination as shown in Figure 5.1 and the detailed study has been carried out in this chapter.

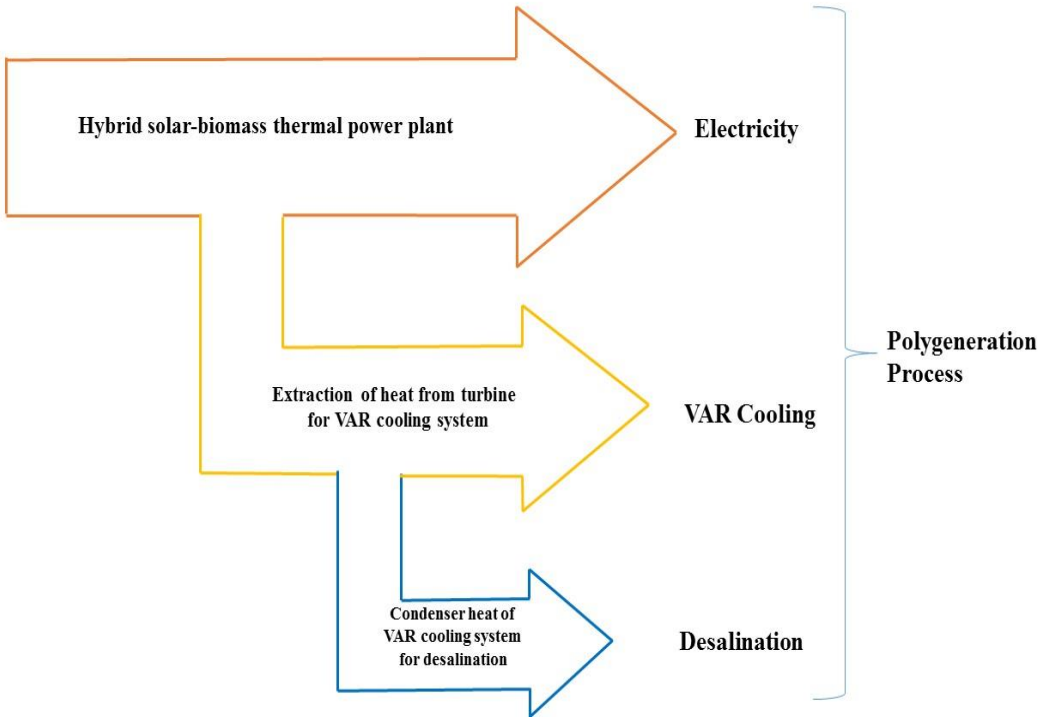

Figure 5.1 Flow diagram of proposed polygeneration system.

The extraction steam from turbine of HSB can be utilized for VAR cooling system and limited amount of heat taken from condenser-2 and HE-2 of VAR cooling system is utilized for MEHD water desalination system. Simultaneous generation of above affects by different components (i.e. steam extracted from Pass-Out turbine → VAR cooling & heat rejected from HE-2 & condenser-2 of VAR cooling → water desalination) is termed as *Polygeneration* Process [181].

5.1 MODELLING APPROACH OF POLYGENERATION PROCESS IN HSB THERMAL POWER PLANT

The HSB thermal power plant produces steam at pressure of 60 bar and temperature of 500 ^{0}C and supplies it to turbine at mass flow rate of 5 kg/sec (state point 5). The selection of solar thermal technology is a real challenge to meet the heat requirement for power generation due to variation of DNI in most places of the country. The cost of solar thermal collector field is determined primarily by its size and technology, which will affect the cost of the energy generation from the system. The implementation of the technology depends on the cost effective conversion of the solar energy into useful thermal energy. From the literature survey, PTC & paraboloid dish technology are recognized as the most efficient systems and best suited technologies for generation of power in India [182]. PTC technology has been deployed in this HSB system to supply primary heat, however, biomass boiler is considered to supply secondary heat in intermittency of the day and full load capacity at night cycle (4-c-a) as shown in Figure 5.2. In this case, steam is bled and expanded at specific steam flow rate to an intermediate stage and supplied to generator of VAR cooling system (State point 6-6'). And remaining steam is expanded at low pressure and medium temperature at state point 7. The bled steam at point 6' is sent to feed water heater. Condensed water is pumped to the feed water

heater at pressure of 5 bar (State point 2) and mixed with bled steam in feed water heater. The VAR cooling system has been designed such that the heat of condenser-2 and HE-2 can be used to heat the preheated water of condenser chamber of MED system (State points 16-17-18). The condensate from the HE-2 is supplied (State point 18) to the evaporator through throttle valve (State point 19). Water vapor formed from the evaporator is absorbed (State point 20) by the strong LiBr salt sprayed in the absorber maintaining low pressure in the evaporator. As LiBr salt solution absorbs water vapor, it becomes weak solution (LiBr-water) and then pumped to the generator through HE-1 (State points 10-11-12). In generator the solution (LiBr-water) splits into LiBr and water vapors and the heated water vapor at super-heated condition is supplied to the condenser (State point 16) whereas LiBr salt returns back to the absorber through HE-1 and EV-1 (State points 13-14-15). In MEHD system, the feed water is pumped (State points 21-22) to condenser chamber (State point 22-23) of distillation chamber for preheating and supplied to the HE-2 (State point 23). The preheated water is getting further heated and supplied to the condenser of VAR cooling system through storage tank (State point 24-24') and then the hot water is sprayed on to the top of the evaporator chamber at a desired mass flow rate (State point 25). The humidified hot air from evaporator chamber is drifted toward the condenser chamber by natural convection. Then the air gets partially dehumidified in the condenser chamber and brought back to the evaporator chamber. The water vapor gets condensed in condenser chamber and collected the water droplet in desalination water collection tank.

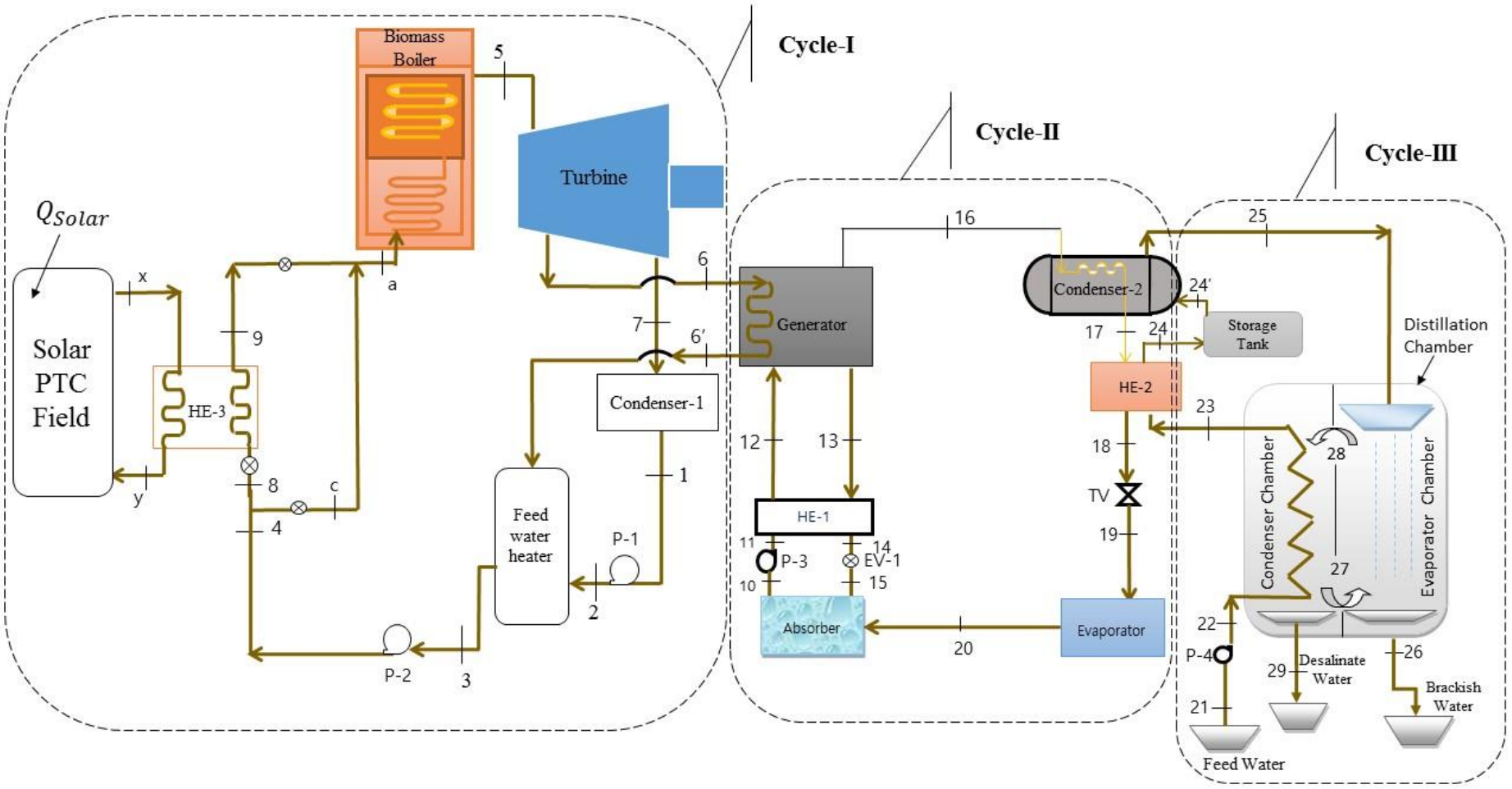

Figure 5.2 Schematic diagram of polygeneration process in HSB thermal power plant for power, cooling & desalination

5.2 THERMODYNAMIC EVALUATION

The technical modelling and thermodynamic analysis (i.e. energy and exergy) of polygeneration process in HSB thermal power plant for combined power, cooling and desalination has been analyzed and optimized. Specifically, the energy and exergy analysis are taken to better understand the performance of polygeneration process in HSB system.

5.2.1 Energy Evaluation

- **HSB power plant (Cycle-I)**

The mass and energy balance equations has been applied on each components of the hybrid system [183].

$$\sum_i m_i = \sum_e m_e \qquad (5.1)$$

$$Q_{solar} + Q_b + m(h_i + \frac{V_i^2}{2} + gZ_i) = m(h_e + \frac{V_e^2}{2} + gZ_e) + W_{net} \qquad (5.2)$$

Where W_{net} is the net-work output of the HSB plant, Q_b is the total heat produced from biomass and Q_{solar} is the solar energy falling on PTC field. V is the bulk velocity of the working fluid, Z is the altitude of the stream above the sea level and g is the specific gravitational force. The energy balance equations of parabolic trough collector and major components of HSB power plant (cycle-I) are expressed in the previous chapter-4.

- **VAR Cooling System (Cycle-II)**

The following energy balance equation of major components of cooling system are expressed as:

Generator: $Q_g = m_{13} \cdot h_{13} + m_{16} \cdot h_{16} - m_{12} \cdot h_{12}$ (5.3)

Condenser-2: $Q_{c2} = m_{16} \cdot h_{16} + m_{24'} \cdot h_{24'} - m_{17} \cdot h_{17} - m_{25} \cdot h_{25}$ (5.4)

Evaporator: $Q_e = m_{20} \cdot h_{20} - m_{19} \cdot h_{19}$ (5.5)

Pump 3: $W_{p_3} = m_{11} \cdot h_{11} - m_{10} \cdot h_{10}$ (5.6)

HE-2: $Q_{HE-2} = m_{17} \cdot h_{17} + m_{23} \cdot h_{23} - m_{18} \cdot h_{18} - m_{24} \cdot h_{24}$ (5.7)

The coefficient of performance of the single effect VAR cooling system is expressed as

$$COP = \frac{Q_e}{\left(Q_g + W_{P3}\right)} \quad (5.8)$$

- **MEHD desalination system (Cycle-III)**

The energy balance equations for distillation chamber can be written as

$$m_{fw}(h_{22} + h_{25}) = m_{fw}\, h_{23} + m_{Bw}\, h_{26} + m_{Dw}\, h_{29} \quad (5.9)$$

$$m_{Dw} = 0.001 \times (w_{28} - w_{27}) \times m_{air} \quad (5.10)$$

$$m_{Bw} = m_{fw} - [0.001 \times (w_{28} - w_{27}) \times m_{air}] \quad (5.11)$$

Amount of heat transfer required (Q_d) for heating the preheating water at state point '23' is

$$Q_d = m_{fw} \cdot c_{p,fw} \cdot (T_{25} - T_{23}) \quad (5.12)$$

The heat transfer of feed water in the humidification process is defined as

$$Q_{25-26} = m_{fw} h_{25} - m_{Bw} h_{26} \quad (5.13)$$

The heat transfer of saturated air in the humidification process is defined as

$$Q_{28-27} = m_{air}(h_{28} - h_{27}) \quad (5.14)$$

The energy efficiency of humidification process is expressed as

$$\eta_{energy,humidification} = \frac{Q_{28-27}}{Q_{25-26}} \quad (5.15)$$

By using pinch technology, T_{26} and T_{28} can be determined.

The heat transfer of feed water in the dehumidification process is expressed as

$$Q_{DH,22-23} = m_{fw}(h_{23} - h_{22}) \quad (5.16)$$

The heat transfer of saturated air in the dehumidification process can be calculated as

$$Q_{DH,28-27} = m_{air}(h_{28} - h_{27}) \quad (5.17)$$

The energy efficiency of dehumidification process is expressed as

$$\eta_{energy,dehumidification} = \frac{Q_{DH,22-23}}{Q_{DH,28-27}} \quad (5.18)$$

By using pinch technology [184] T_{23} and T_{27} can be determined.

The energy efficiency of MEHD distillation system is expressed as

$$\eta_{energy,distillation} = \frac{m_{Dw} \times h_{fg}}{Q_d} \quad (5.19)$$

Where h_{fg} is latent heat of vaporization of feed water (kJ/kg).

- **Energy Efficiency of Polygeneration process in HSB system**

The energy efficiency of polyegeneration process in HSB power plant $\left(\eta_{E,polygeneration}\right)$ is expressed as:

$$\eta_{E,polygeneration} = \frac{W_{net} + Q_e + (m_{Dw} \times h_{fg})}{Q_{solar} + Q_b} \quad (5.20)$$

5.2.2 Exergy Evaluation

- **HSB power plant (Cycle-I)**

The steady-state process, respective balances for exergy can be written as [173]

$$\sum_i E_{xi} + \sum_j \left[1 - \frac{T_o}{T_j}\right] Q_j = \sum_e E_{xe} + W_{net} + E_{xD} \quad (5.21)$$

Exergy of the flowing stream at each state point of hybrid system (E_x) can be expressed as

$$E_x = \left[\left(h - h_o \right) - T_o \left(s - s_o \right) \right] \tag{5.22}$$

The exergy analysis for balance equations of parabolic trough collector and major components of HSB power plant (cycle-I) are expressed in the previous Chapter-4.

- **VAR Cooling System (Cycle-II)**

Generator: $E_{x,g} = Q_g \left(1 - \frac{T_o}{T_g} \right)$ (5.23)

Condenser-2: $E_{x,c2} = Q_{c2} \left(1 - \frac{T_o}{T_{c2}} \right)$ (5.24)

Evaporator: $E_{x,e} = m_{20} \left[\left(h_{19} - h_{20} \right) - T_o \left(s_{19} - s_{20} \right) \right]$ (5.25)

Absorber: $E_{x,ab} = m_{15} \left(h_{15} - T_o s_{15} \right) + m_{20} \left(h_{20} - T_o s_{20} \right) - m_{10} \left(h_{10} - T_o s_{10} \right)$ (5.26)

The exergy coefficient of performance of the single effect VAR cooling system is expressed as

$$E_{x,COP} = \frac{E_{x,e}}{\left(E_{x,g} + W_{P3} \right)} \tag{5.27}$$

- **MEHD Distillation System (Cycle-III)**

The exergy balance equations of the system is expressed as;

$$m_{fw}(Ex_{22} + Ex_{25}) = m_{fw} Ex_{23} + m_{Bw} Ex_{26} + m_{Dw} Ex_{29} \tag{5.28}$$

The exergy of feed water in humidification process:

$$Ex_{25-26} = m_{fw} Ex_{25} - m_{Bw} Ex_{26} \tag{5.29}$$

The exergy on water vapor at state points 27 & 28 in humidification is defined as:

$$Ex_{28-27} = m_{air} \left(Ex_{28} - Ex_{27} \right) \tag{5.30}$$

The exergy at point n (i.e. point 27 and 28) is also calculated by [185]

$$Ex_{27,28} = \left[(C_p)_{air} + d_n(C_p)_v\right](T_n - T_0) - T_0\left\{\left[(C_p)_{air} + d_n(C_p)_v\right]\ln\left(\frac{T_n}{T_0}\right) - (R_{air} + d_n R_v)\ln\left(\frac{P_n}{P_0}\right)\right\} + T_o\left[\left(R_{air} + d_n R_v\right)\ln\left(\frac{1+1.6078d^o}{1+1.6078d_n}\right) + 1.6078 d_n R_{air}\ln\left(\frac{d_n}{d^o}\right)\right] \quad (5.31)$$

Where d is calculated as;

$$d = 622\left(\frac{RH \times P_v}{P - RH \times P_v}\right) \quad (5.32)$$

Where relative humidity (RH) is defined as;

$$RH = \frac{P_v}{P_{vs}} \quad (5.33)$$

The exergy efficiency of humidification process is defined as;

$$\eta_{ex,humidification} = \frac{Ex_{28-27}}{Ex_{25-26}} \quad (5.34)$$

The exergy on the sprayed water in dehumidification process;

$$Ex_{DH,22-23} = m_{fw}\left(Ex_{23} - Ex_{22}\right) \quad (5.35)$$

The exergy on saturated air in the dehumidification process;

$$Ex_{DH,28-27} = m_{air}(h_{28} - h_{27}) \quad (5.36)$$

The exergy efficiency of the system by dehumidification process is written as;

$$\eta_{ex,dehumidification} = \frac{Ex_{DH,22-23}}{Ex_{DH,28-27}} \quad (5.37)$$

The exergy efficiency of MEHD distillation system is expressed as

$$\eta_{exergy,distillation} = \frac{m_{Dw} \times (h_{fg} - T_o \times s_{fg})}{Q_{ex,d}} \quad (5.38)$$

Where $Q_{ex,d}$ is exergy on heat transfer required for heating the preheating water.

- **Exergy Efficiency of Polygeneration process in HSB system**

The exergy efficiency of polyegenration process in HSB power plant is expressed as:

$$\eta_{Ex,polygeneration} = \frac{W_{net} + E_{x,e} + E_{x,Dw}}{E_{xSolar} + E_{xb}} \quad (5.39)$$

Where E_{xSolar} and E_{xb} are the exergy of solar and biomass respectively [183].

Generally in thermal power plants, electricity is used for cooling and water desalination. But in polygeneration process heat is directly used to operate VAR cooling and desalination system. The total output in polygeneration process is expressed as

$$W_{Polygeneration} = W_{net} + Q_e + Q_{Dw} \quad (5.40)$$

5.3 PRIMARY ENERGY SAVINGS ON POLYGENERATION PROCESS IN HSB THERMAL POWER PLANT

Directive 2004/8/EC of the European parliament and of the council of 11th February 2004 established a common rule for the promotion of cogeneration regarding primary energy savings (PES) [186]. The PES on polygeneration process in HSB thermal power plant can be calculated on the basis of following formula:

$$PES = 1 - \left(\frac{1}{\frac{\eta_{heat}}{\eta_{ref.,heat}} + \frac{\eta_{electrical}}{\eta_{ref.,electrical}}} \right) \times 100 \quad (5.41)$$

$$\eta_{heat} = \text{Heat efficieicency in Polygeneration process} = \frac{Q_e + Q_{Dw}}{Q_{solar} + Q_b} = \frac{\text{Useful heat output}}{\text{Heat Input to the polygeneration process}} \quad (5.42)$$

$$\eta_{ref,heat} = \text{Efficiency reference value for separate heat production} = 0.9$$

$$\eta_{electrical} = \text{Electrical efficieicency of Polygeneration system} = \frac{W_{net}}{Q_{solar} + Q_b} = \frac{\text{Useful Electrical Output}}{\text{Heat Input to the polygeneration system}} \quad (5.43)$$

$\eta_{ref,electrical}$ = Efficiency reference value for separate electricity production through solar-biomass=0.35

and

$$\eta_{electrical} = \frac{W_{net}}{Q_{solar} + Q_b} \quad (5.44)$$

The percentage (%) increase of equivalent electricity production in polygeneration process as compared to simple power plant is expressed as;

$$(\%) \text{ increased} = \frac{W_{Polygeneration} - W_{SPP}}{W_{SPP}} \quad (5.45)$$

5.4 OPTIMIZATION

In this section the thermodynamic parameters of the polygeneration process in HSB thermal power plant for combined power, cooling and desalination are optimized with energy efficiency, VAR cooling output, desalination output and the total output in polygeneration process in HSB thermal power plant as an objective functions using genetic algorithm.

5.4.1 Objective Functions

In this study, an objective functions are taken for maximized energy efficiency, VAR cooling output, desalination output and the total output in polygeneration process in HSB thermal power plant. The heat inputs are taken as solar and biomass heat and the total output in polygeneration process are output of turbine, output of evaporator and output of desalination water.

$$\eta_{E,polygeneration} = \frac{W_{net} + Q_e + Q_{Dw}}{Q_{solar} + Q_b} \quad (5.46)$$

5.4.2 Decision Variable and Constraints

In this study, various inequality constraint are taken to define the feasibility regions for the engineering optimization problem and feasible operating conditions for an

optimal performance. The following relevant parameter were selected as decision variables for the analysis:

- Extraction pressure from turbine (P_6)
- Fraction of steam extraction from turbine (f)
- Desalination inlet heated water temperature (T_{25})

The limitations of minimum and maximum ranges of the above selected decision variables are given in Table 5.1.

Table 5.1 Ranges of constraints defined for the decision variable

Decision Variable	Range of Variation
Extraction pressure from turbine (P_6)	$390 \le P_6 \le 600$
Fraction of steam extraction from turbine (f)	$0.1 \le P_6 \le 0.89$
Desalination inlet heated water temperature (T_{25})	$80 \le T_{25} \le 90$

5.4.3 Genetic Algorithm (GA)

Presently, some of the optimization methods that are conceptually different from the traditional mathematical programming techniques have been developed. These methods include GA, simulated annealing, ant colony, particle swarm, fuzzy programing optimization, neural-network-based methods.

In this study, genetic algorithm is employed to optimize the thermodynamic parameters of the proposed system. The GA is used since it needs no initial conditions, works with multi design variables, finds global optima, uses objective function formation and utilizes population i.e. opposed to individuals and are well suited for solving such problems. The GA, which was first presented systematically

by Holland in 1970s [187] is a stochastic global search method that simulates the natural biological evolution and can be found in the work of Rechenberg [188]. Basically, GA is based on Darwin's theory of survival of the fittest principle that operates on a population of potential solutions to produce better approximations to the optimal solution. This is based on the principles of natural genetics and natural selection. The basic elements of natural genetics-reproduction, crossover, and mutation-are used in the genetic search procedure.

In this research analysis, GA technique adopted by [189 & 190] is used for optimization. The GA encodes a simple potential solution to a specific domain problem on a chromosome and consists of discrete units called genes. Further, the set of coded chromosome are called the population, with the following three basis genetic operators i.e. selection, cross over and mutation and are used to generate new solution from the existing ones. Cross over operators called parent (i.e. two chromosomes) and combined together to new chromosomes called offspring. The parent is chosen with a probability based on its fitness. In this optimization for the polygeneration process in HSB thermal power plant, the exergy efficiency is selected as fitness functions. Although fitness is a preferred feature, these offspring borrowed some good genes from parent through iterative process. These genes are expected to be present more frequently in the population. On the other side, the mutation operator randomly applied with low probability to modify chromosomes values at the gene level and adopted to optimize the parameter of the proposed system. This is important that the crossover leads the population to converge and mutation reintroduce natural genetic.

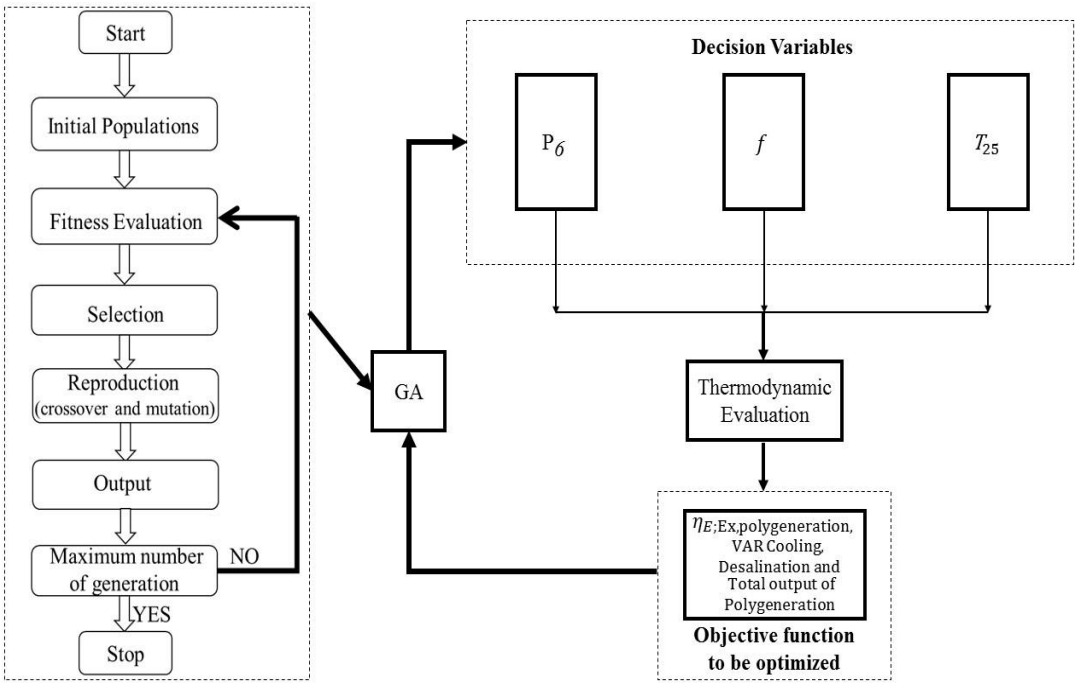

Figure 5.3 Work flow of the optimization process in polygeneration in HSB thermal power plant

Reproduction involves selection of chromosome for the next generation, where the fitness of an individual determines the probability of its survival. Basically the selection procedure can vary depending on fitness values. The new generation are obtained by the mean of the three operators i.e. selection, cross over and mutation to increase the average fitness through the evaluation of the objective functions values. The work flow of the optimization process is shown in Figure 5.3.

5.5 COST ANALYSIS

Even though the energy and exergy analysis of the polygeneration process in HSB thermal power plant for combined power, cooling and desalination can be used to improve the efficiency, the feasibility of applying these improvements is generally constrained by the limitations of the financial resources. The cost analysis is to find the actual size that gives the cheapest combination of solar and biomass energy system for various applications.

The complete cost analysis of the system is examined below thoroughly:

The total capital cost of the system (CC_{total}) is expressed as

$$CC_{total} = C_s + C_B + C_{VAR} + C_{desalination} \quad (5.47)$$

Where C_{VAR} , $C_{desalination}$ is cost of VAR cooling system and desalination system respectively.

The total cost of solar (C_s) can be calculated as:

$$C_s = C_a \times A_{ap} \quad (5.48)$$

Where (C_a) is the area dependent cost of components (PTC collectors, piping with fitting and heat pump).

The total cost of biomass (C_B) is expressed as:

$$C_{B(n)} = P\&M_{(n)} \times [1 + F_1 + F_2 + F_3] \quad (5.49)$$

$P\&M_{(n)}$ is the plant and machinery cost for the nth year (2016-17) and calculated as

$$P\&M_{(n)} = P\&M_{(0)} \times (1 + d(n)) \quad (5.50)$$

Where the value of $P\&M_{(0)}$ (i.e base year plant & machineries) is considered as Rs. 443.61 lakhs and $d(n)$ is the capital cost escalation factor of 3.52 %. The values of each factors used in the formulae are given in Table 5.2 [191]. The capital costs of VAR cooling system and desalination system have been considered approximately as Rs. 560 lakhs and Rs. 25 lakhs respectively as per their actual capacity. The cost of VAR cooling system and desalination system as per proposed capacity are taken from various Indian manufacturers such as M/s Thermax and M/s Amba Engineers & Project [192 & 193].

Table 5.2 Value of each factor used for calculation of capital cost of biomass power system [191].

Variables	Description	Value
a	Steel index	0.7
b	Machinery index	0.3
F_1	Factor for civil works	0.1
F_2	Factor for commissioning	0.09
F_3	Factor for inancing	0.14

In addition, the costs of fitting piping and electronics are considered as 5 % of the total cost of each system. For calculation of overall cost per kWh of the system the following assumptions are considered in Table 5.3:

Table 5.3 Assumption value for polygeneration process in HSB thermal power plant

Assumption Head	Units	Value
Overall System:		
Auxiliary consumption during the stability	%	13
Auxiliary consumption after stability	%	12
Plant load factor (stabilization for six month)	%	60
Plant load factor (during first year after stabilization)	%	70
Plant load factor (second year onwards)	%	80
Useful Life	Years	20
Financial Assumption:		
Debt	%	70

Equity	%	30
Moratorium period	Years	0
Interest rate	%	12.76
Repayment period	Years	12
Return on equity for first 10 years	%	20
Return on equity after 10 years	%	24
Weighted average of rate of Return on	%	22
Discount rate	%	10.74
Income tax	%	33.99
Depreciation rate	%	5.83
Depreciation rate 13th year onwards	%	2.505
Working capital:		
Operation and maintenance spares	%	15
Interest on working capital	%	13.26
Fuel: Biomass price escalation factor	%	5
Operation and maintenance:		
Operation and maintenance expenses	Rs. Lakhs	50
Operation and maintenance expenses escalation	%	5.72

The payback period of the system is expressed as:

$$\text{Pay back period} = \frac{\text{Energy consumed by the system (MWh)}}{\text{Energy produce by the system per year (MWh)}} \quad (5.51)$$

CHAPTER 6: RESULTS & DISCUSSION

In this chapter, various output key parameters are investigated to identify the effects of various operating parameters. Solar DNI results the numbers of hours availability on different ranges and biomass resources results state wise major agricultural based biomass residue potential. State wise solar DNI and biomass resources available in MJ/year in India and percentage of heat contribution for HSB thermal power plant have been carried out in this chapter. The 5 MW HSB system results to identify the effects of various operating parameters like beam radiation on tilted surface, condenser pressure, turbine inlet temperatures, boiler pressure on net power output, energy & exergy efficiencies and exergy destruction. The polygeneration process in HSB system for combined power, cooling and desalination is also investigated to identify the effects of various operating parameters, PESPP, optimization and cost analysis.

6.1 SOLAR DNI AND BIOMASS

A detailed analysis of hourly availability of DNI is carried out to hybridize solar thermal power plant using biomass for NISE, Gurugram, India. Four years of ground measured solar DNI data has been collected and analyzed for designing of HSB system as shown in Table 6.1, 6.2, 6.3 & 6.4. It is seen that, the maximum number of hours available in the DNI ranges in 400-600 W/m^2 in the year of 2010, 2011, 2012 and 2013, which account for approximately 35% of total DNI for these years. It can be seen that in March, April, May & October months maximum amount of DNI is received as compared to other months of the year. It is also observed that, DNI of 400-600 W/m^2 is available for approximately 1019 hours while DNI of more than 600 W/m^2 is available for approximate 535 hours out of 8760 hours a year, which is nearly half of availability hours of DNI in 400-600 W/m^2.

Table 6.1 Month wise hourly available of various ranges of DNI in the year 2010 at NISE

DNI (W/m^2)	Numbers of Hours												Total hours	Hours (%)
	JAN 2010	FEB 2010	MAR 2010	APR 2010	MAY 2010	JUNE 2010	JULY 2010	AUG 2010	SEP 2010	OCT 2010	NOV 2010	DEC 2010		
100-200	29.77	27.95	26.38	31.75	42.85	38.37	30.22	28.20	18.62	45.37	37.51	34.66	391.65	15.25
200-300	36.32	25	26.68	47.20	45.58	42.63	30.17	29.10	16.57	42.95	44.30	35.88	422.38	16.44
300-400	30.32	28.20	34.73	43.78	52.88	42.25	28.08	27.20	16.55	55.38	34.68	47.11	441.16	17.17
400-500	28.33	34.30	48.42	54.22	52.73	42.87	26.68	22.60	17.05	45.72	21.73	40.78	435.43	16.95
500-600	17.03	42.10	62.10	61.30	46.20	46.90	23.13	17	23.90	48.32	15.11	34.81	437.9	17.05
600-700	5.17	40.15	64.92	37.88	30.62	20.30	13.10	8.32	22.83	27.18	13.46	22.61	306.54	11.93
700-800	2.17	20.30	39.15	13.13	7.73	2.15	3.58	1.25	19.25	8.70	5.25	3.38	126.04	4.91
800-900	0	0.98	2.75	2.17	0.50	0	0.70	0	0.47	0	0	0	7.57	0.29
Total hours	149.11	218.98	305.13	291.43	279.09	235.47	155.66	133.67	135.24	273.62	172.04	219.23	2568.67	
Hours (%)	5.80	8.53	11.88	11.35	10.87	9.17	6.06	5.20	5.26	10.65	6.70	8.53		
Energy (kWh)	53.37	102.75	153.82	127.87	114.24	93.29	60.46	49.10	64.85	110.64	61.44	86.61		

Table 6.2 Month wise hourly available of various ranges of DNI in the year 2011 at NISE

DNI (W/m^2)	Numbers of Hours												Total hours	Hours (%)
	JAN 2011	FEB 2011	MAR 2011	APR 2011	MAY 2011	JUN 2011	JULY 2011	AUG 2011	SEP 2011	OCT 2011	NOV 2011	DEC 2011		
100-200	29.05	21.98	23.45	26.78	30.9	38.57	34.1	29.35	21.07	32.85	36.85	32.72	357.67	12.93
200-300	30.06	19.21	22.76	29.72	39.78	49.65	32.53	19.65	19.97	44.3	46.36	41.82	395.81	14.31
300-400	36.81	20.9	28.33	36.48	57.9	62.03	30.28	18.78	22.57	50.38	53.56	52.26	470.28	17.00
400-500	37.05	20.27	32.733	54.15	61.82	43.8	20.87	26.5	27.17	52.8	52.81	46.26	476.233	17.22
500-600	39.31	43.6	50.06	63.08	82.07	28	8.37	27.72	42.68	48.82	39.67	35.55	508.93	18.40
600-700	30.7	51.4	51.2	51.57	16.38	10.55	4.65	21.13	58.03	49.87	15	25.7	386.18	13.96
700-800	4.81	20.75	52.42	16.77	0.73	0.05	1.02	5.27	27.95	15.93	5.72	1.16	152.58	5.52
800-900	0	3.7	9.37	0.23	0	0	0.07	0.55	3.58	0.183	0.21	0	17.893	0.65
Total Hours	207.79	201.81	270.32	278.78	289.58	232.65	131.89	148.95	223.02	295.13	250.18	235.47	2765.576	
Hours (%)	7.51	7.30	9.77	10.08	10.47	8.41	4.77	5.39	8.06	10.67	9.05	8.51		
Energy (kWh)	89.76	105.07	143.25	130.90	120.62	83.83	44.50	63.26	114.80	118.57	75.10	92.79		

Table 6.3 Month wise hourly available of various ranges of DNI in the year 2012 at NISE

DNI (W/m^2)	Numbers of Hours												Total hours	Hours (%)
	JAN 2012	FEB 2012	MAR 2012	APR 2012	MAY 2012	JUNE 2012	JULY 2012	AUG 2012	SEPT 2012	OCT 2012	NOV 2012	DEC 2012		
100-200	35.33	29.83	34.5	32.5	36.17	47	46.83	82	31.95	38	56.72	21.13	491.96	16.36
200-300	27	25.67	31.67	30	35	51.83	43.17	54.33	28.55	43.98	48.92	26.07	446.19	14.84
300-400	30.67	35.83	47.67	36.3	44.17	67.17	41.67	63.5	33.28	50.85	34.1	29.18	514.39	17.10
400-500	26.5	41.17	49.33	49.67	59.67	72.5	24.33	38	34.12	55.3	32.88	32.77	516.24	17.17
500-600	34.67	47	70.17	53	75.67	37.5	16.33	20	35.37	58.5	30.03	24.92	503.16	16.73
600-700	28.5	37.5	45.33	56.17	47	0.67	2.67	12.33	46.9	39.08	19.18	31.93	367.26	12.21
700-800	9	22.67	14.33	18.83	7	0	0.67	7.5	19.55	7.35	7.92	37.68	152.5	5.07
800-900	0	3.17	2.33	0.83	0	0	0	0	1.53	0	0.15	6.73	14.74	0.490
Total hours	191.67	242.84	295.33	277.3	304.68	276.67	175.67	277.66	231.25	293.06	229.9	210.41	3006.44	
Hours (%)	6.37	8.07	9.82	9.22	10.13	9.20	5.84	9.23	7.69	9.74	7.64	6.99		
Energy (kWh)	81.865	115.33	134.43	131.04	137.46	100.42	58.441	101.00	107.80	125.04	86.172	105.87		

Table 6.4 Month wise hourly available of various ranges of DNI in the year 2013 at NISE

DNI (W/m^2)	Numbers of Hours												Total hours	Hours (%)
	JAN 2013	FEB 2013	MAR 2013	APR 2013	MAY 2013	JUNE 2013	JULY 2013	AUG 2013	SEPT 2013	OCT 2013	NOV 2013	DEC 2013		
100-200	23.68	19.42	22.67	29.03	36.77	42.97	22.33	30.92	27.08	25.12	19.9	32.17	332.06	13.76
200-300	27.51	16.98	23.15	31.9	37.55	39.75	15.22	25.06	27.77	24.12	21.7	31.97	322.68	13.37
300-400	23.18	23.6	32	38.03	52.28	47.53	15.43	24.37	34.38	13.97	30.23	48.02	383.02	15.87
400-500	22.78	24.4	43.3	51.38	67.4	49.65	16.55	26.5	41.7	8.97	43.95	47.02	443.6	18.38
500-600	24.5	33.68	46.98	55.62	68.07	28.95	8.7	22.53	54.58	8.9	41.65	37.67	431.83	17.89
600-700	30.8	40.3	56.4	53.42	37.05	6.32	5.95	15.52	17.93	4.45	22.43	9.15	299.72	12.42
700-800	12.33	26.72	44.83	31.05	20.4	1.42	0.7	2.86	1.05	2.92	0.72	0.067	145.067	6.01
800-900	0.2	10.52	28.95	4.73	1.48	0	0	0	0	0	0	0	45.88	1.9
Total Hours	164.98	195.67	307.38	295.16	321	216.59	84.88	147.76	204.49	88.45	180.58	206.06	2413.007	
Hours (%)	6.84	8.12	12.74	12.23	13.30	8.98	3.51	6.12	8.47	3.66	7.48	8.54		
Energy (kWh)	74.30	102.49	172.60	144.59	145.39	80.44	32.15	59.11	87.278	31.32	79.02	79.96		

Table 6.5 Monthly and range wise standard deviation of DNI

Monthly Deviation:

Months	JAN	FEB	MAR	APR	MAY	JUNE	JULY	AUG	SEPT	OCT	NOV	DEC
Mean $\left(kWh/m^2\right)$	74.82	106.4	151.03	133.60	129.43	89.50	54.47	68.12	93.68	110.70	75.43	91.31
Standard Deviation $\left(kWh/m^2\right)$	15.63	6.06	16.42	7.47	14.46	9.09	7.10	22.71	22.49	15.89	10.39	11.03

Range-wise Deviation:

DNI (W/m^2)	100-200	201-300	301-400	401-500	501-600	601-700	701-800	801-900
Mean(hours)	14.58	14.74	16.79	17.43	17.52	12.63	5.38	0.83
Standard Deviation (hours)	1.53	1.29	0.61	0.64	0.77	0.91	0.49	0.73

The monthly deviation and range wise deviation of DNI have also been considered as shown in Table 6.5. It is seen that, mean and standard deviation on monthly deviation (kWh/m^2) is maximum in the month of March and August. The mean and standard deviation on range wise deviation (hours) is maximum at DNI of 400-600 W/m^2 and 100-200 W/m^2 respectively. The beam radiation on tilted surface of 450 W/m^2 is considered for the modelling of HSB thermal power plant at NISE, Gurugram, India and biomass is taken to fulfill the heat energy requirement for continuous operation during non-availability of sunshine hours. The month wise four years (2010-2013) ground measured data of DNI of this site is validated with NREL satellite data as shown in Table 6.6. It is observed that, the maximum mean percentage errors are in the month of January, July, November & December. The month of November is showing maximum mean error due to smoke in the atmosphere, because of paddy stalk burning in Punjab and Haryana states & in the months of December and January due to smog effect and in July due to cloud cover over Gurugram and Delhi & pollution effect in the atmosphere on the image based satellite data. The satellite data doesn't consider the aerosol effect, so that the image based satellite data shows the maximum percentage error on these months.

Table 6.6 Validation of site data (NISE) with satellite data (NREL)

Months	**MAPE (%)**
January	38.92
February	16.52
March	8.93
April	17.30
May	19.08

June	31.93
July	34.52
August	21.71
September	17.74
October	20.03
November	36.48
December	38.91

The State wise biomass resources availability has been analyzed for designing of HSB power plant. It is seen that Uttar Pradesh is one of the states, which produces the highest quantity of major crop residue (56 MT) followed by Maharashtra (40 MT) and Punjab (37 MT) as shown in Figure 6.1. The major agricultural based biomass crop wise potential for different states of India are presented in Figure 6.2. Uttar Pradesh has highest potential of crop residue in sugarcane, rice husk, wheat straw and pearls millet.

The state wise biomass energy potential from major seven surplus residue is maximum in Uttar Pradesh (1044×10^3 MJ). The other major surplus residue states are Punjab (434.75×10^3), Maharashtra (258.82×10^3), Haryana (198.50×10^3), Madhya Pradesh (180.75×10^3), Gujarat (159×10^3), Karnataka (157.9×10^3), Tamil Nadu (155.75×10^3), Rajasthan (151.30×10^3) and Andhra Pradesh (121.73×10^3) as shown in Figure 6.3. State-wise solar energy per square meter and biomass energy potential are shown in the Figure 6.4. For assessing the solar energy potential only 10% of the total waste land area available has been considered in the major biomass energy contributing states like Punjab, Uttar Pradesh, Haryana, Maharashtra, Madhya Pradesh, Karnataka, Tamil Nadu, Gujarat, Rajasthan, Kerala, Bihar, Andhra

Pradesh, West Bengal, Odisha & Assam. All these States can contribute about 96% of biomass power generation of the total national biomass power generation in the country.

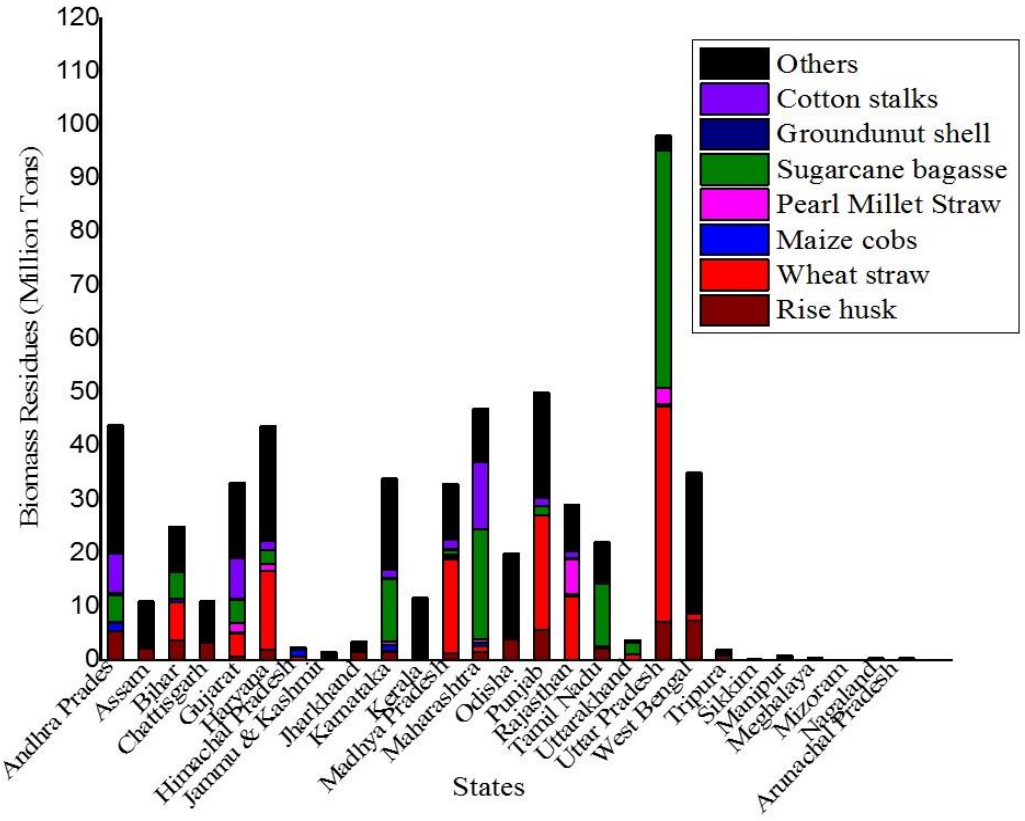

Figure 6.1 State wise major agricultural based biomass residues

Figure 6.5 represents monthly average utilization of heat gain from solar and biomass. A 5 MW capacity of HSB thermal power have been designed. The heat input have been taken as per the percentage heat utilization of solar and biomass. The PTC field will heat the heat transfer fluid and pump to the receiver depending upon the availability of beam radiation on tilted surface (i.e. 20%, 40%, 60% & 80%) and remaining heat will come from biomass boiler (i.e. 80%, 60% ,40% & 20%) for making steam at superheated condition.

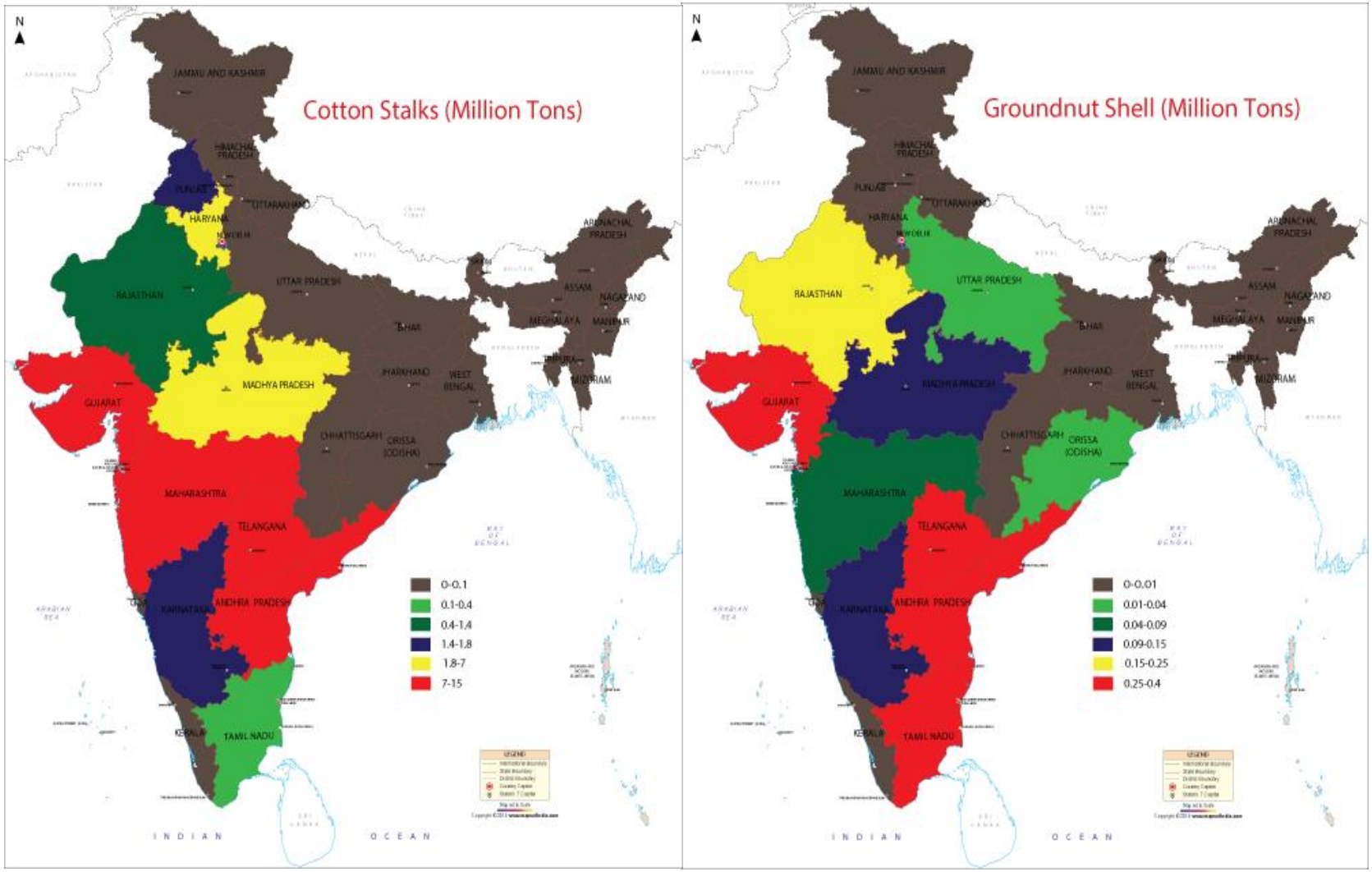
Cotton Stalks (Million Tons)
N
JAMMU AND KASHMIR
HIMACHAL PRADESH
PUNJAB
UTTARAKHAND
HARYANA
NEW DELHI
RAJASTHAN
UTTAR PRADESH
BIHAR
ARUNACHAL PRADESH
ASSAM
NAGALAND
MEGHALAYA
MANIPUR
TRIPURA
MIZORAM
JHARKHAND
WEST BENGAL
MADHYA PRADESH
GUJARAT
CHHATTISGARH
ORISSA (ODISHA)
MAHARASHTRA
TELANGANA
KARNATAKA
ANDHRA PRADESH
KERALA
TAMIL NADU
0-0.1
0.1-0.4
0.4-1.4
1.4-1.8
1.8-7
7-15
BAY OF BENGAL
ARABIAN SEA
INDIAN OCEAN
Groundnut Shell (Million Tons)
N
0-0.01
0.01-0.04
0.04-0.09
0.09-0.15
0.15-0.25
0.25-0.4
BAY OF BENGAL
ARABIAN SEA
INDIAN OCEAN

(a) (b)

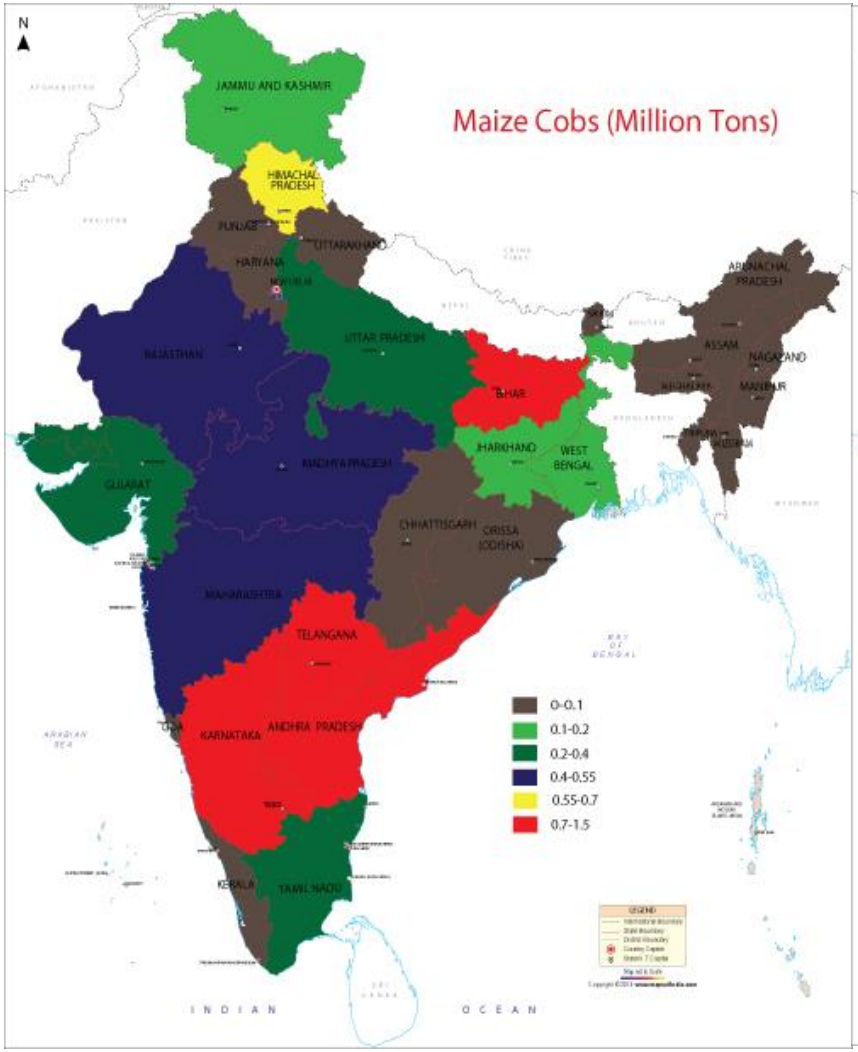
N
Maize Cobs (Million Tons)
JAMMU AND KASHMIR
HIMACHAL PRADESH
PUNJAB
UTTARAKHAND
HARYANA
NEW DELHI
RAJASTHAN
UTTAR PRADESH
BIHAR
ARUNACHAL PRADESH
ASSAM
NAGALAND
MANIPUR
JHARKHAND
WEST BENGAL
SIKKIM
ODISHA
MADHYA PRADESH
GUJARAT
CHHATTISGARH
ORISSA (ODISHA)
MAHARASHTRA
TELANGANA
KARNATAKA
ANDHRA PRADESH
KERALA
TAMIL NADU
0-0.1
0.1-0.2
0.2-0.4
0.4-0.55
0.55-0.7
0.7-1.5
INDIAN
OCEAN

(c)

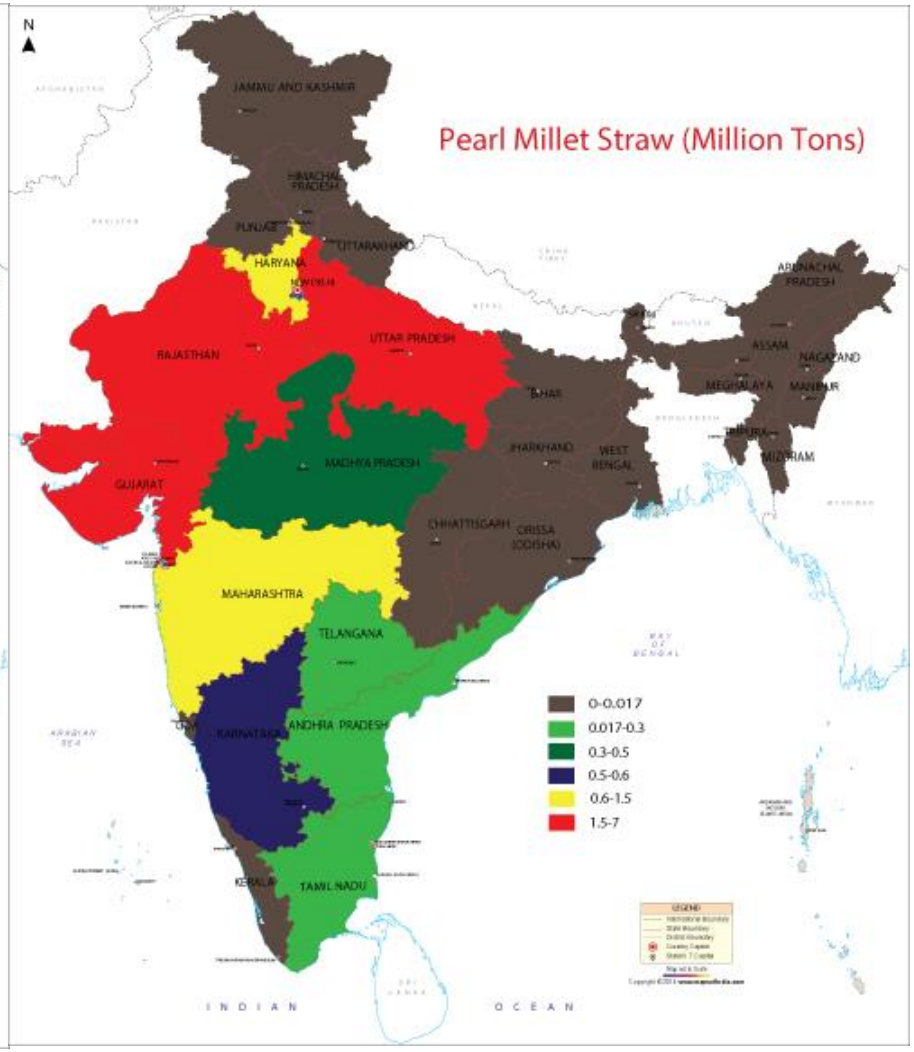
N
Pearl Millet Straw (Million Tons)
JAMMU AND KASHMIR
HIMACHAL PRADESH
PUNJAB
UTTARAKHAND
HARYANA
NEW DELHI
RAJASTHAN
UTTAR PRADESH
BIHAR
ARUNACHAL PRADESH
ASSAM
NAGALAND
MEGHALAYA
MANIPUR
TRIPURA
MIZORAM
JHARKHAND
WEST BENGAL
MADHYA PRADESH
GUJARAT
CHHATTISGARH
ORISSA (ODISHA)
MAHARASHTRA
TELANGANA
KARNATAKA
ANDHRA PRADESH
KERALA
TAMIL NADU
0-0.017
0.017-0.3
0.3-0.5
0.5-0.6
0.6-1.5
1.5-7
INDIAN
OCEAN

(d)

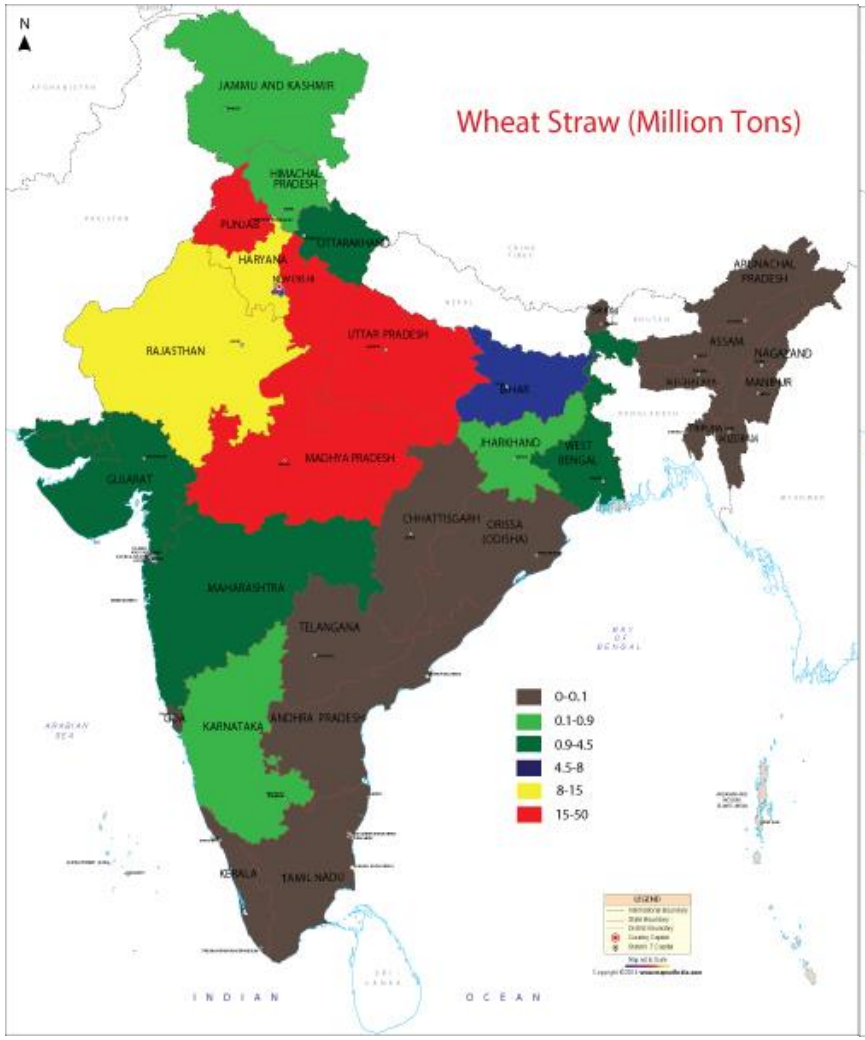
N
Wheat Straw (Million Tons)
JAMMU AND KASHMIR
HIMACHAL PRADESH
PUNJAB
UTTARAKHAND
HARYANA
RAJASTHAN
UTTAR PRADESH
BIHAR
ARUNACHAL PRADESH
ASSAM
NAGALAND
MANIPUR
JHARKHAND
WEST BENGAL
MADHYA PRADESH
GUJARAT
CHHATTISGARH
ORISSA (ODISHA)
MAHARASHTRA
TELANGANA
KARNATAKA
ANDHRA PRADESH
KERALA
TAMIL NADU
0-0.1
0.1-0.9
0.9-4.5
4.5-8
8-15
15-50
INDIAN
OCEAN

(e)

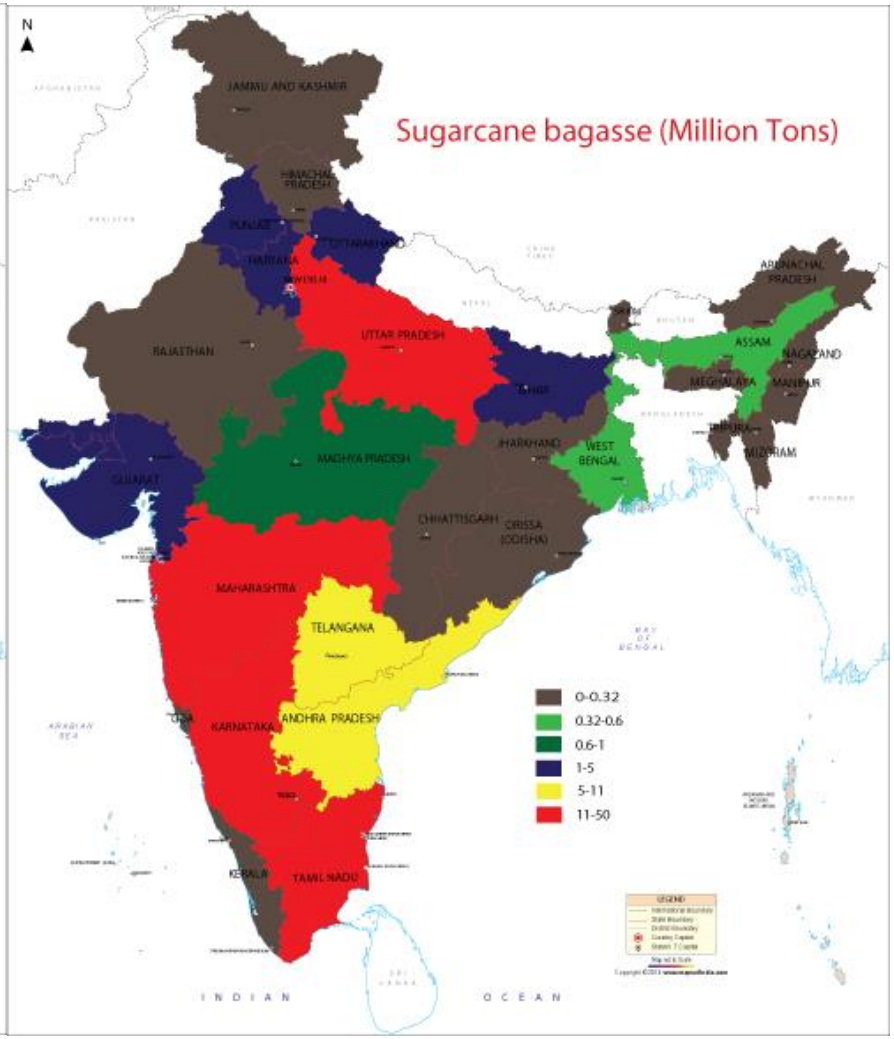
N
Sugarcane bagasse (Million Tons)
JAMMU AND KASHMIR
HIMACHAL PRADESH
PUNJAB
UTTARAKHAND
HARYANA
RAJASTHAN
UTTAR PRADESH
BIHAR
ARUNACHAL PRADESH
ASSAM
NAGALAND
MANIPUR
MEGHALAYA
TRIPURA
MIZORAM
JHARKHAND
WEST BENGAL
MADHYA PRADESH
GUJARAT
CHHATTISGARH
ORISSA (ODISHA)
MAHARASHTRA
TELANGANA
KARNATAKA
ANDHRA PRADESH
KERALA
TAMIL NADU
0-0.32
0.32-0.6
0.6-1
1-5
5-11
11-50
INDIAN
OCEAN

(f)

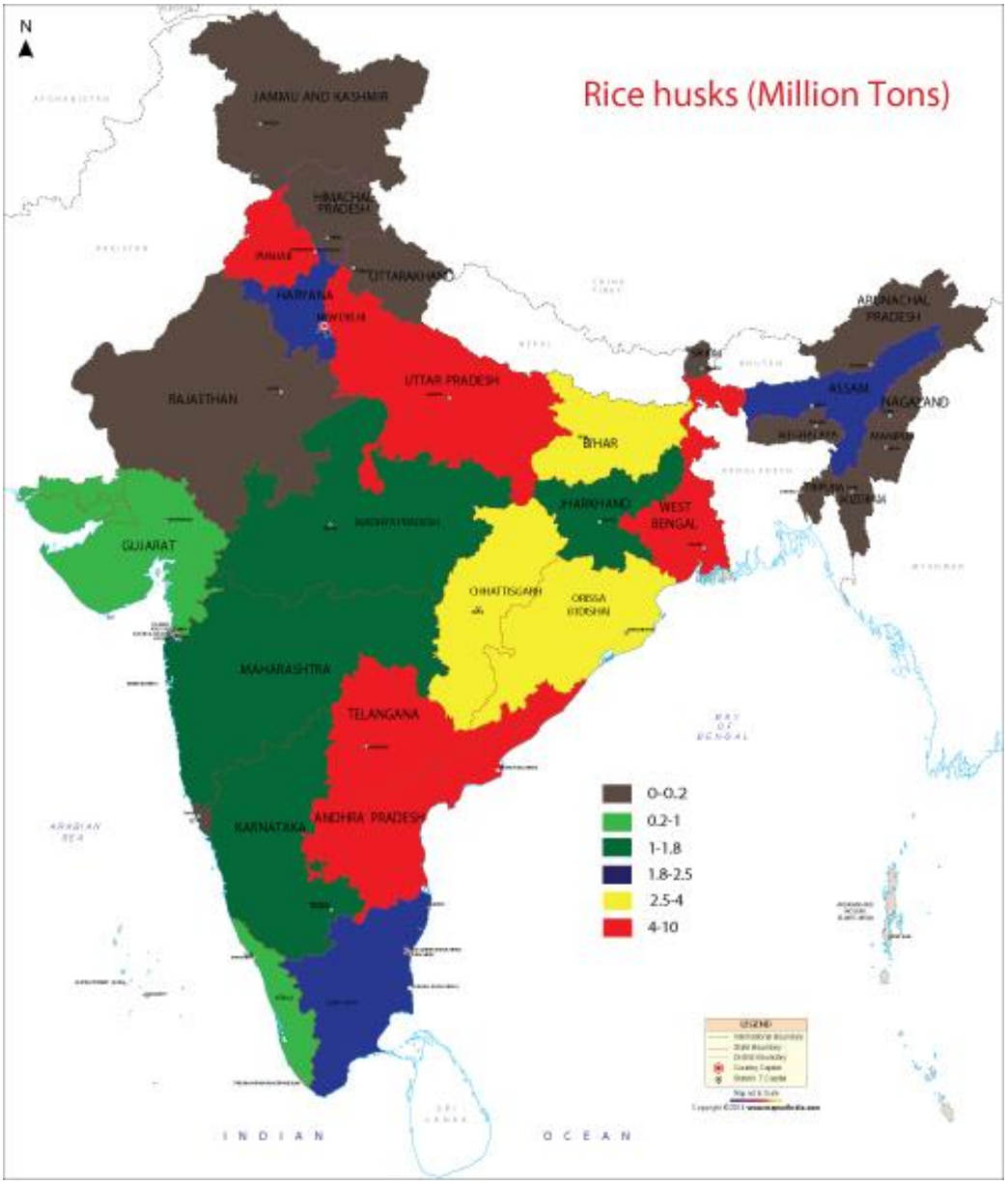

(g)

Figure 6.2 State wise major agricultural based biomass residue potential in India

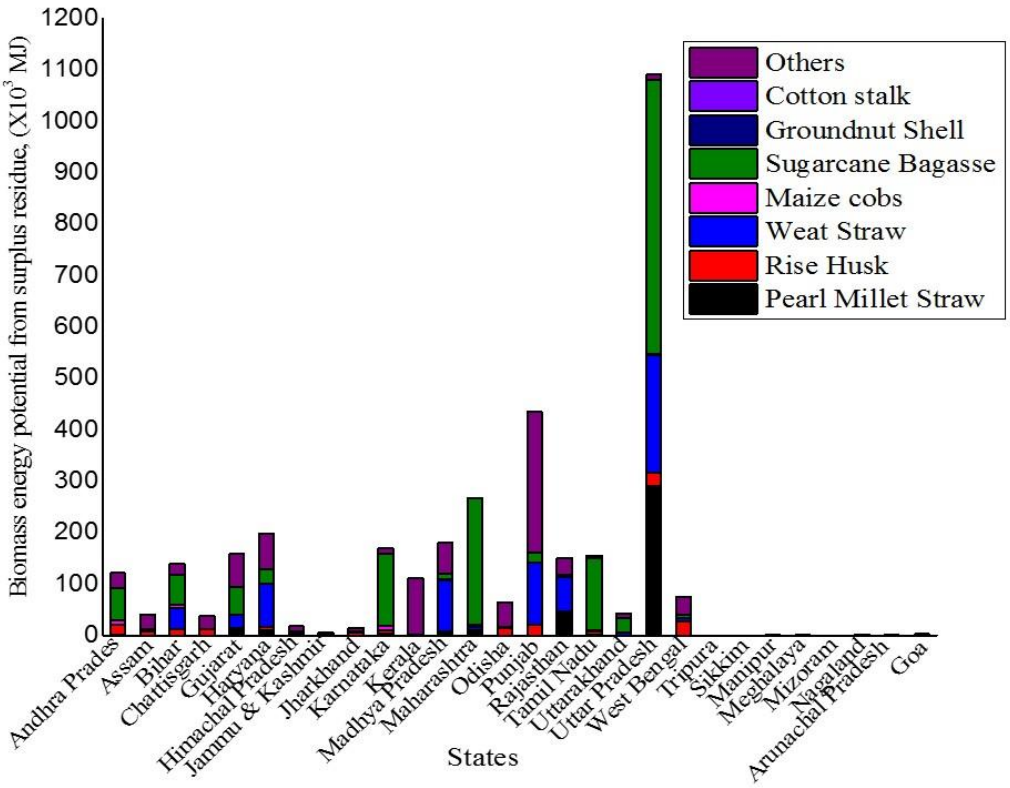

Figure 6.3 State wise biomass energy potential from surplus residue

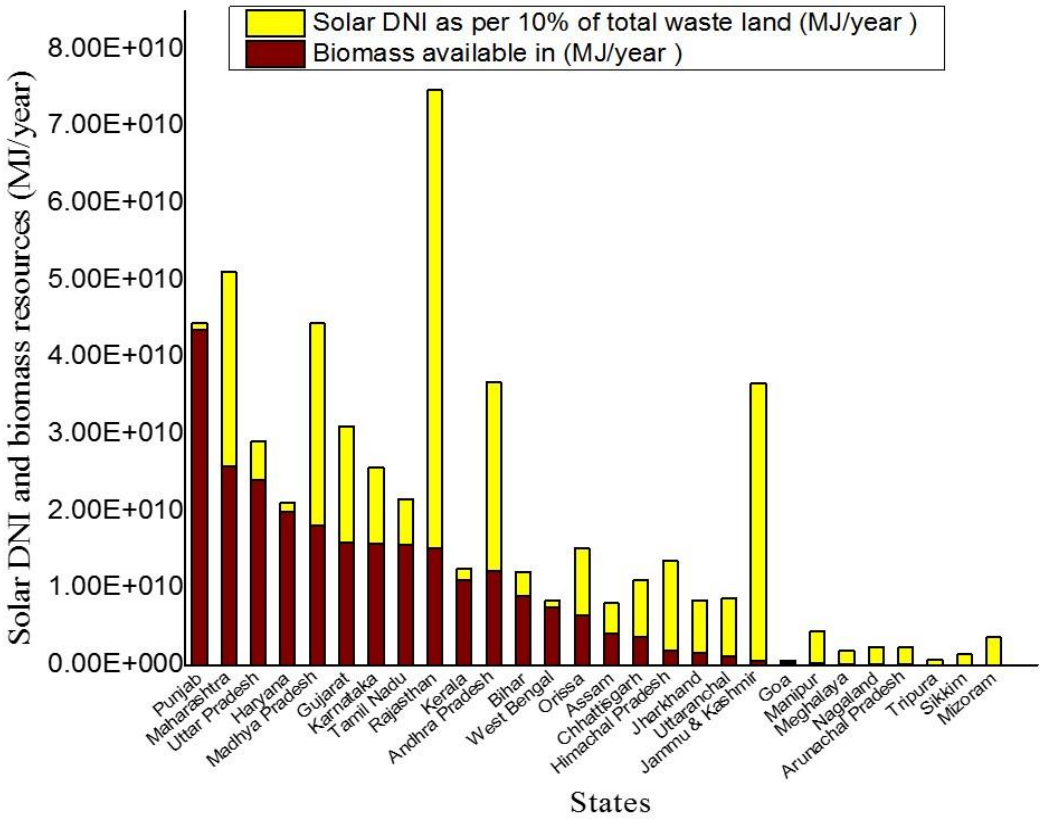

Figure 6.4 State wise solar DNI and biomass resources available in MJ/year

It is seen that (Figure 6.5), in the month of November solar radiation decreases compared to May due to cosine effect and the low level of DNI in the month of December, January, July, August, September is also observed. In this case, remaining heat can be taken to maintain the heated water to superheated condition from the biomass boiler.

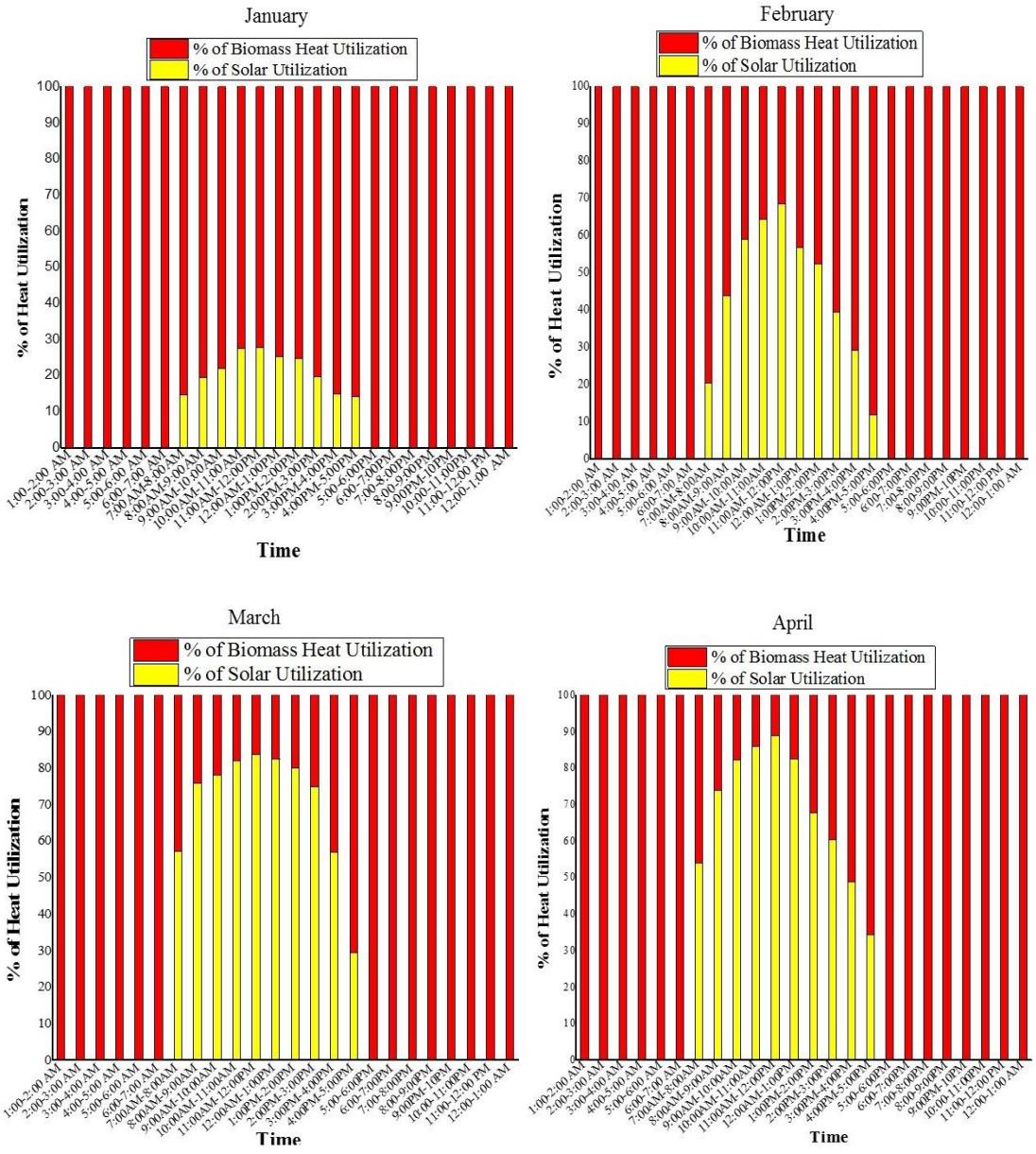

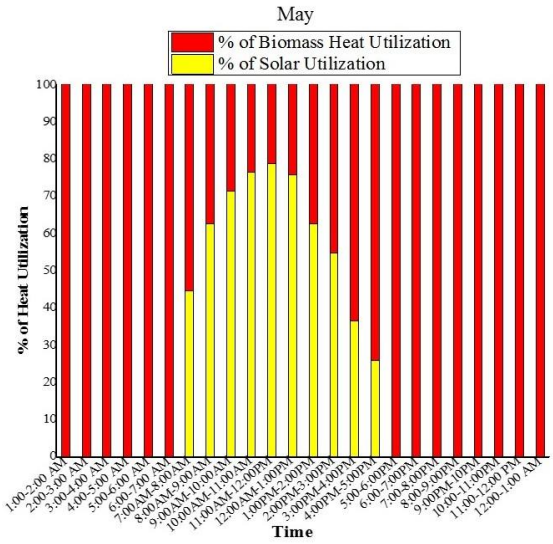
May
% of Biomass Heat Utilization
% of Solar Utilization
% of Heat Utilization
Time

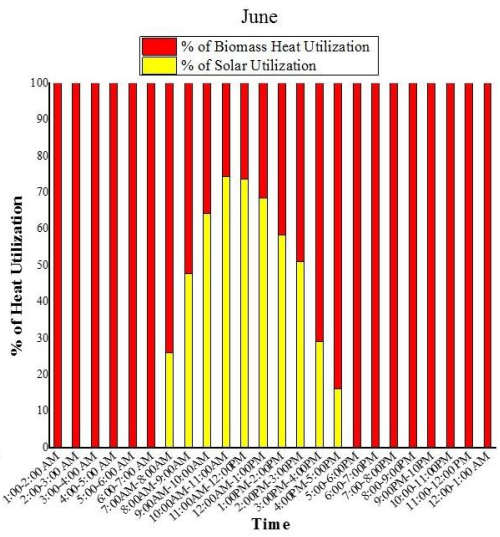
June
% of Biomass Heat Utilization
% of Solar Utilization
% of Heat Utilization
Time

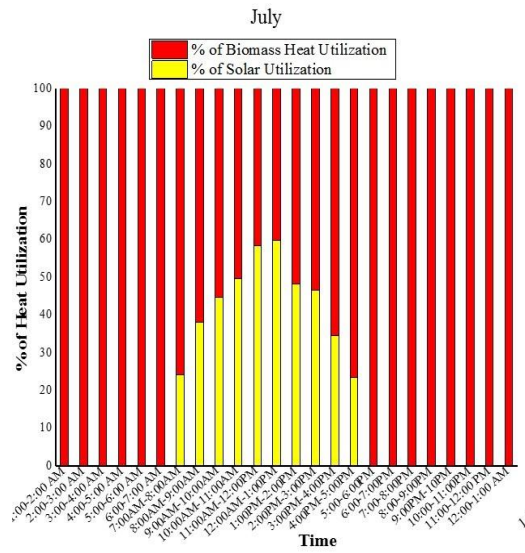
July
% of Biomass Heat Utilization
% of Solar Utilization
% of Heat Utilization
Time

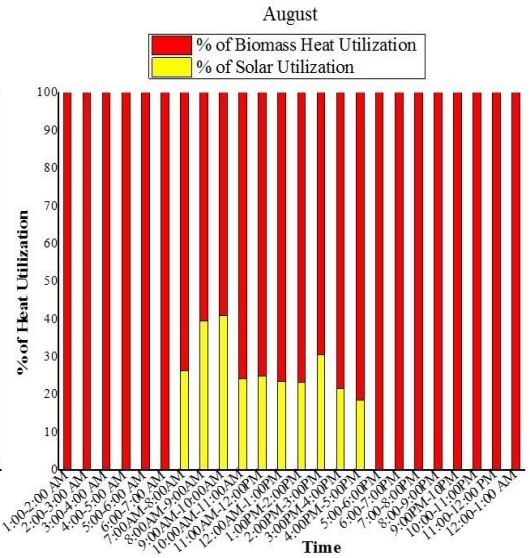
August
% of Biomass Heat Utilization
% of Solar Utilization
% of Heat Utilization
Time

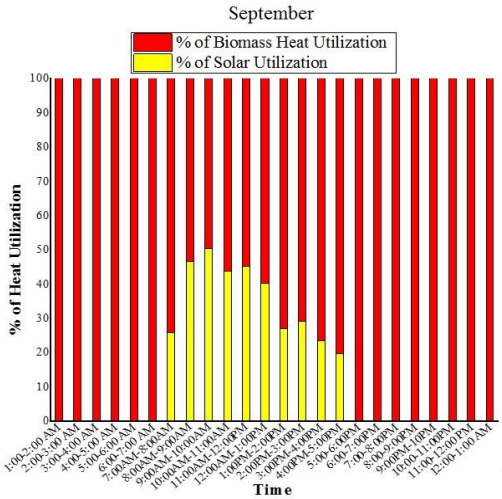
September
% of Biomass Heat Utilization
% of Solar Utilization
% of Heat Utilization
Time

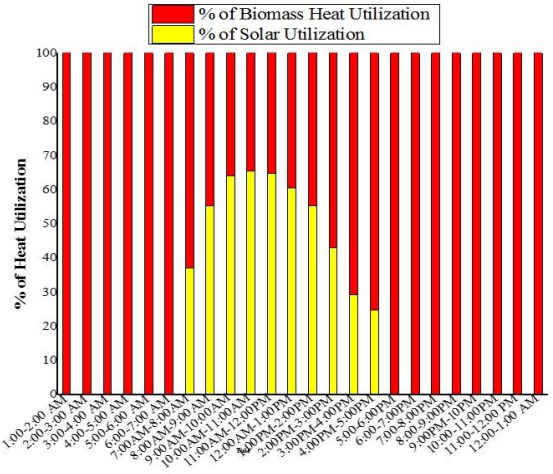
October
% of Biomass Heat Utilization
% of Solar Utilization
% of Heat Utilization

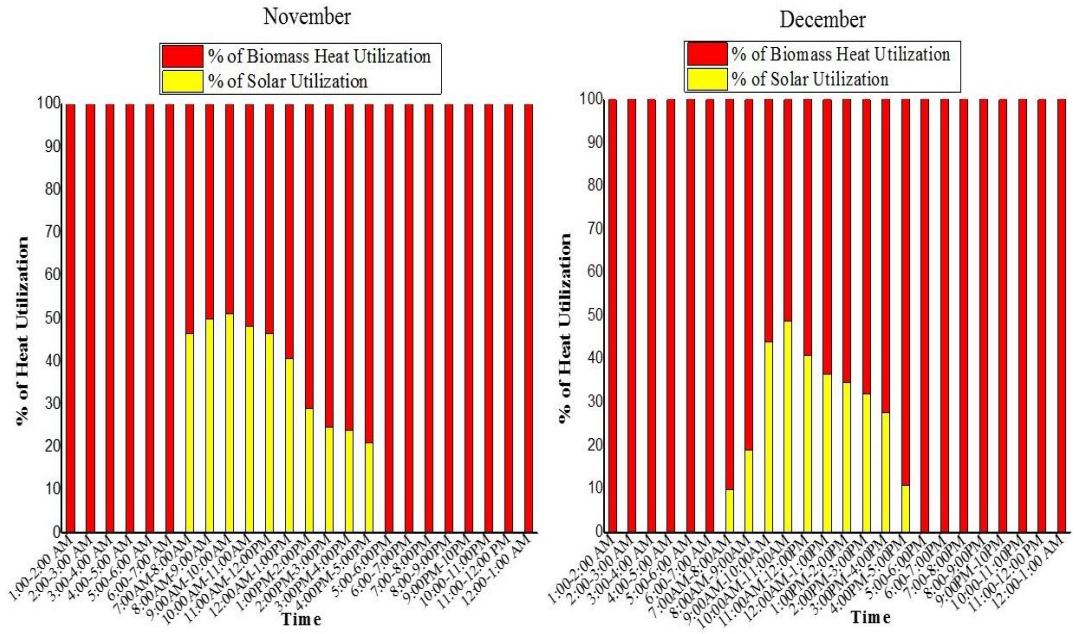

Figure 6.5 Month wise hourly percentage heat utilization from solar and biomass for hybrid system

Figure 6.6 and 6.7 shows the wise percentage heat utilization from solar at mean temperature of 250^{o}C & 310^{o}C respectively and biomass for hybrid system in four regions of India (East: Guwahati, Assam; West: Udaipur, Rajasthan; North: Delhi, South: Madurai, Tamil Nadu). It is seen that, in the eastern region (Guwahati), the contribution of solar heat at the mean temperature of PTC field is 6.5% at 250^{o}C & 5.33% at 310^{o}C respectively, in the month of April. In western region (Udaipur), the contribution of solar heat at the mean temperature of PTC field is maximum up to 12.2% at 250^{o}C & 11% at 310^{o}C respectively, in the month of April. In northern region (Delhi) the contribution of solar heat at the mean temperature of PTC field is 8.55% at 250^{o}C & 7.59% at 310^{o}C respectively, in the month of April. In southern region (Madurai) the contribution of solar heat at the mean temperature of PTC field is 11.6% at 250^{o}C & 10.3% at 310^{o}C respectively, in the month of March.

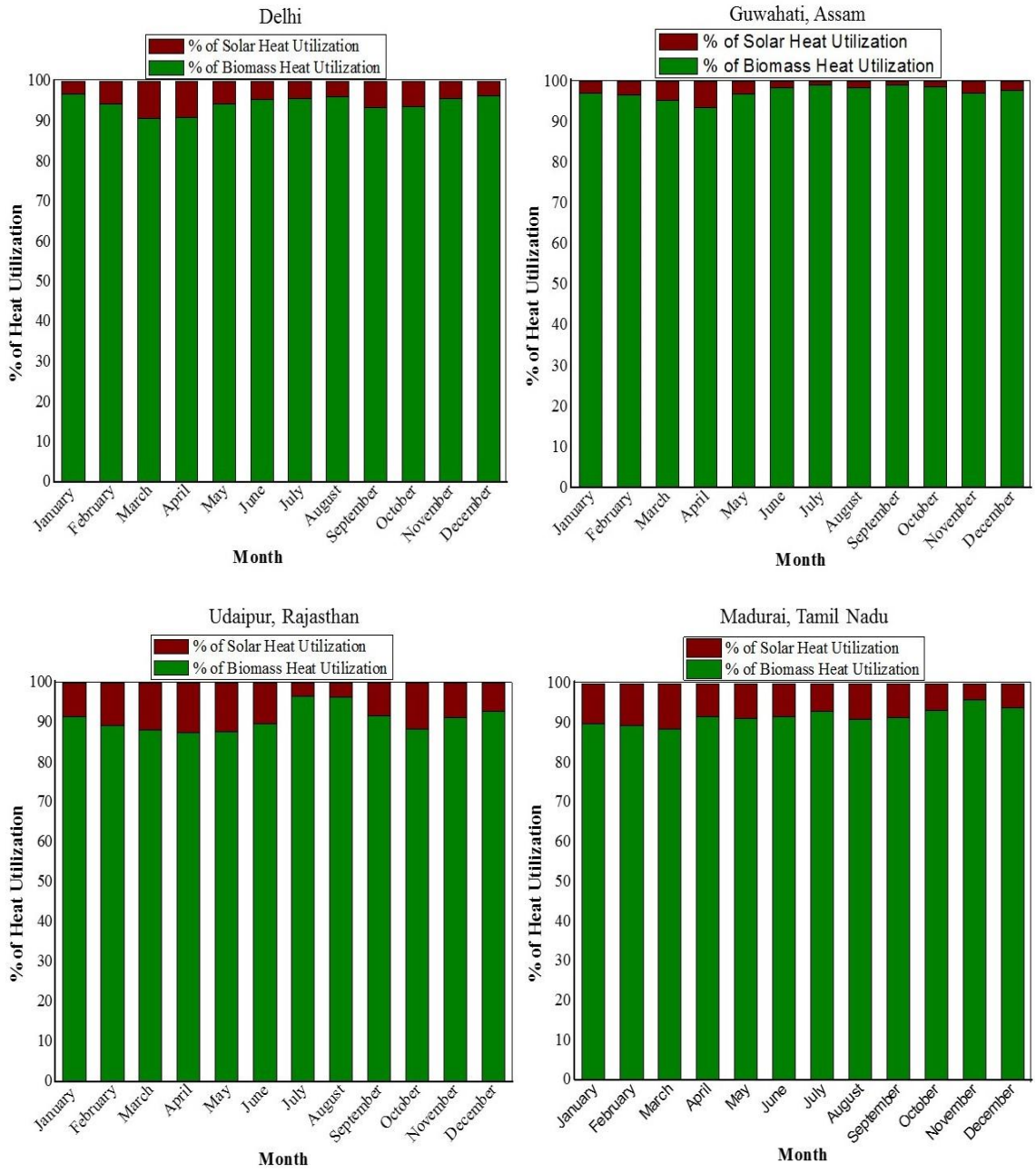

Figure 6.6 Month wise percentage heat utilization from solar at mean temperature of 250 ^{o}C and biomass for hybrid system in four regions of India.

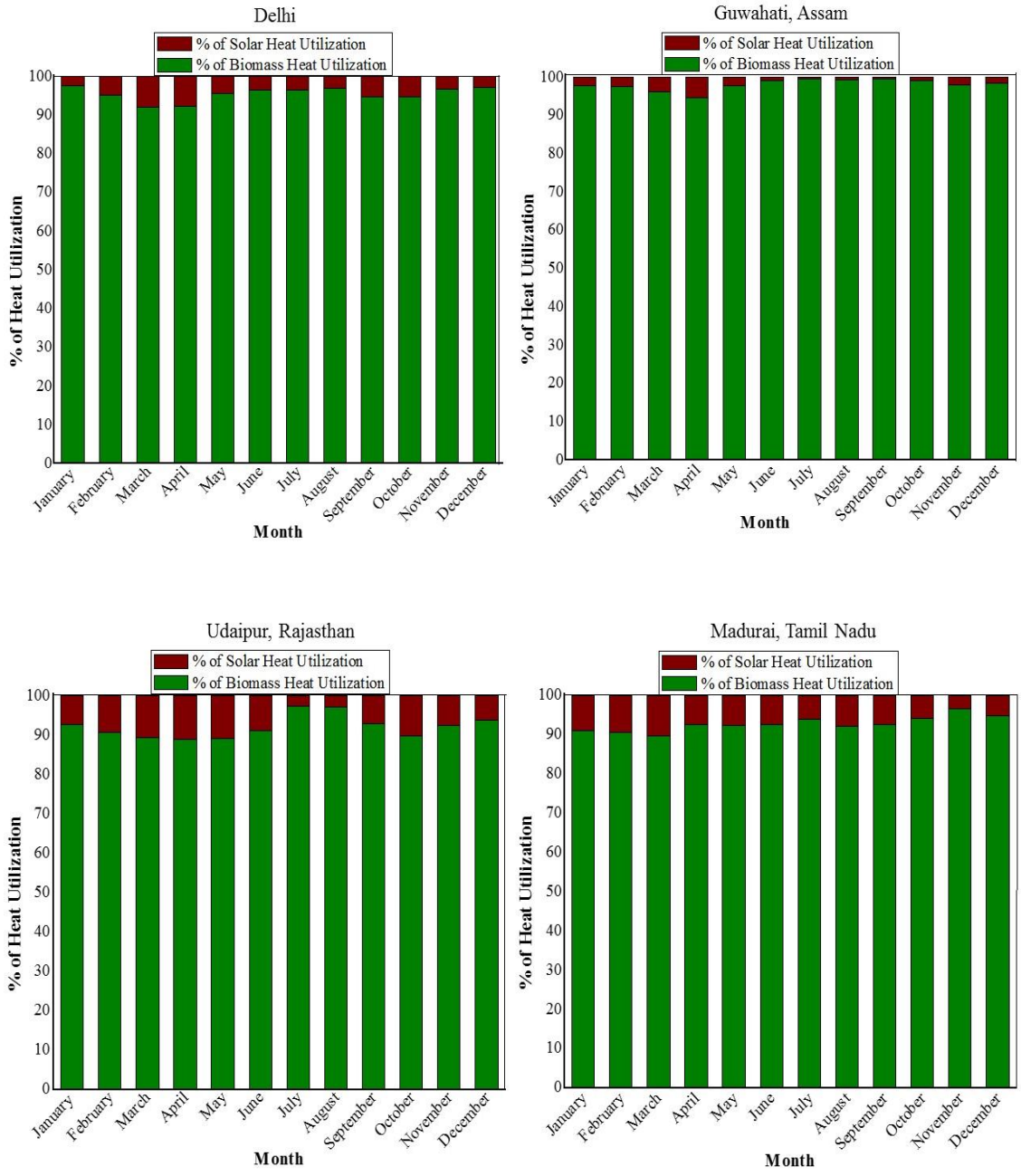

Figure 6.7 Month wise percentage heat utilization from solar at mean temperature of 310 ^{o}C and biomass for hybrid system in four regions of India.

6.2 HYBRID SOLAR AND BIOMASS THERMAL POWER PLANT

The parametric study of the system has been carried out to simulate the network output, energy efficiency, exergy efficiency by varying various input parameters such as beam radiation on tilted surface, condenser pressure, boiler pressure and turbine inlet temperature. Figure 6.8 shows the energy and exergy efficiency of the

PTC field as a function of beam radiation on tilted surface. It is seen that, with increasing of beam radiation on tilted surface the energy efficiency increases from 26.1% to 49.2% and exergy efficiency increases from 30.15% to 36.2%. Figure 6.9 shows that, when condenser pressure is raised from 0.06 bar to 0.15 bar, the energy efficiency decreases from 23.68% to 21.81%, exergy efficiency decreases from 26.66% to 24.43% and turbine work is also decreases from 5.23 MW to 4.82 MW. Turbine inlet temperature variation affects the energy efficiency, exergy efficiency and turbine work of the system as shown in the Figure 6.10. It is seen that as turbine inlet temperature increases from 300^0C to 600^0C, energy efficiency increases linearly from 17.29% to 27.08%, exergy efficiency increases linearly from 24.27% to 26.64% and turbine work increases from 3.83 MW to 5.64 MW. This figure clearly indicates that, the energy & exergy efficiencies are tending to match each towards at 600^0C.

Figure 6.11 shows the energy and exergy efficiency with respect to boiler pressure at various boiler temperatures (400, 450 and 500^0C). The energy efficiency increases slightly from 19.15% (40 bar, 400^0C) to 22.66% (60 bar, 500^0C) with pressure which is not appreciable as the cost of the complete power plant increases due to increase in the boiler pressure. The pressure 60 bar and temperature of 500^0C has been considered as the optimum of the given cycle under the design conditions for HSB thermal power plant. The profile of exergy efficiency follows the same trend as energy efficiency against boiler pressure at these three turbine inlet temperatures.

The energy losses and exergy destruction of the major components of the hybrid system is given in Figure 6.12. It is seen that the heat energy (PTC and biomass boiler) input is highly efficient in energy losses whereas largest losses occur in the solar PTC and biomass boiler in the exergy destruction.

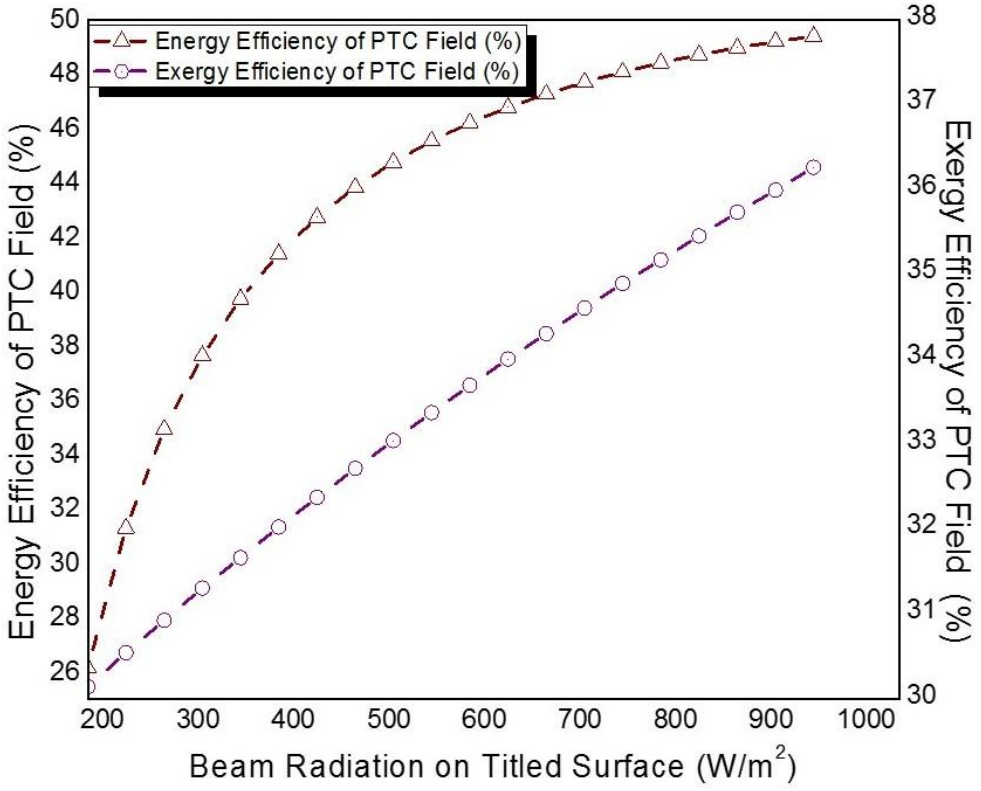

Figure 6.8 Variation of energy efficiency and exergy efficiency of PTC field with change in beam radiation on tilted surface

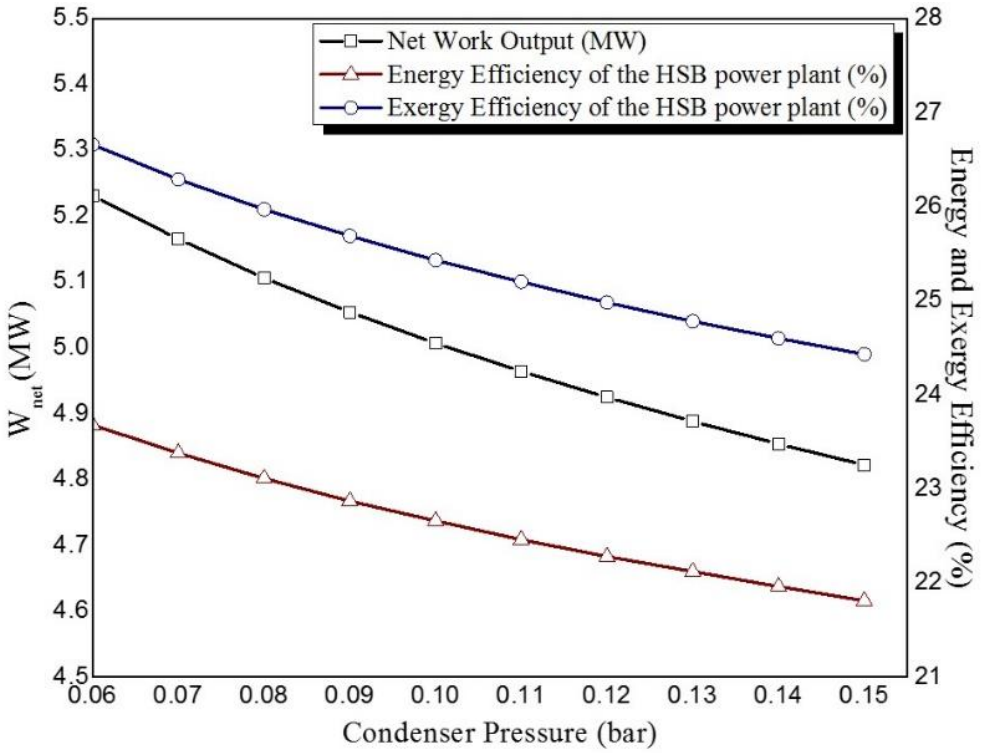

Figure 6.9 Variation of energy efficiency, exergy efficiency and net work output of HSB power plant with change in condenser pressure

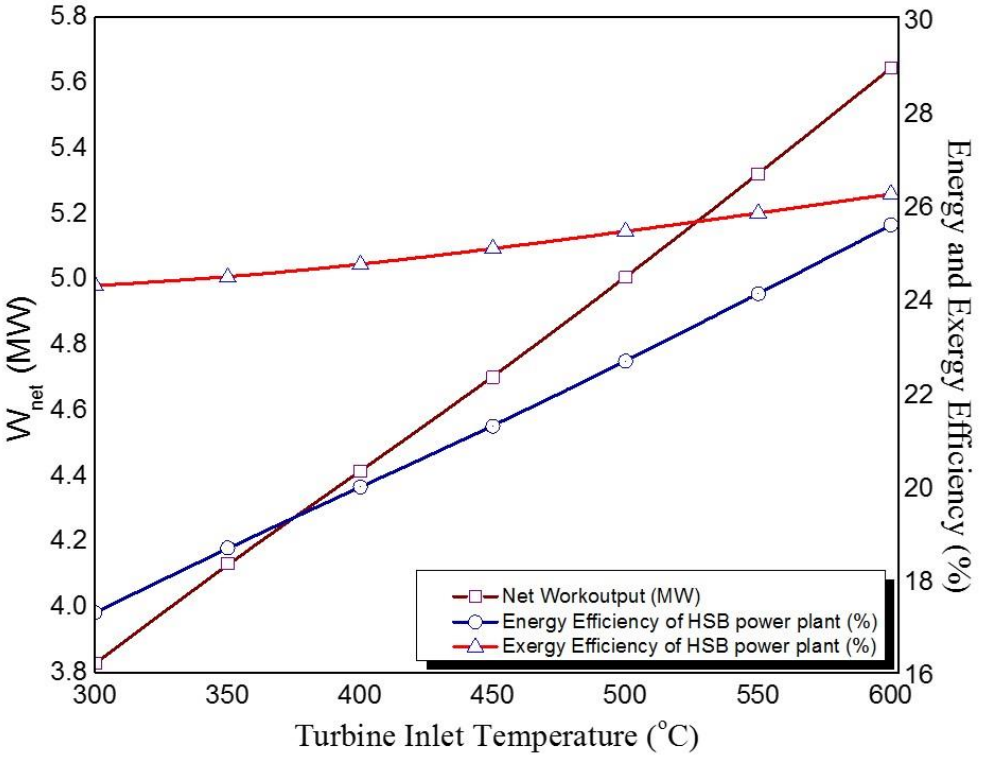

Figure 6.10 Variation of energy efficiencies, exergy efficiencies and network output of HSB power plant with change in turbine inlet temperature

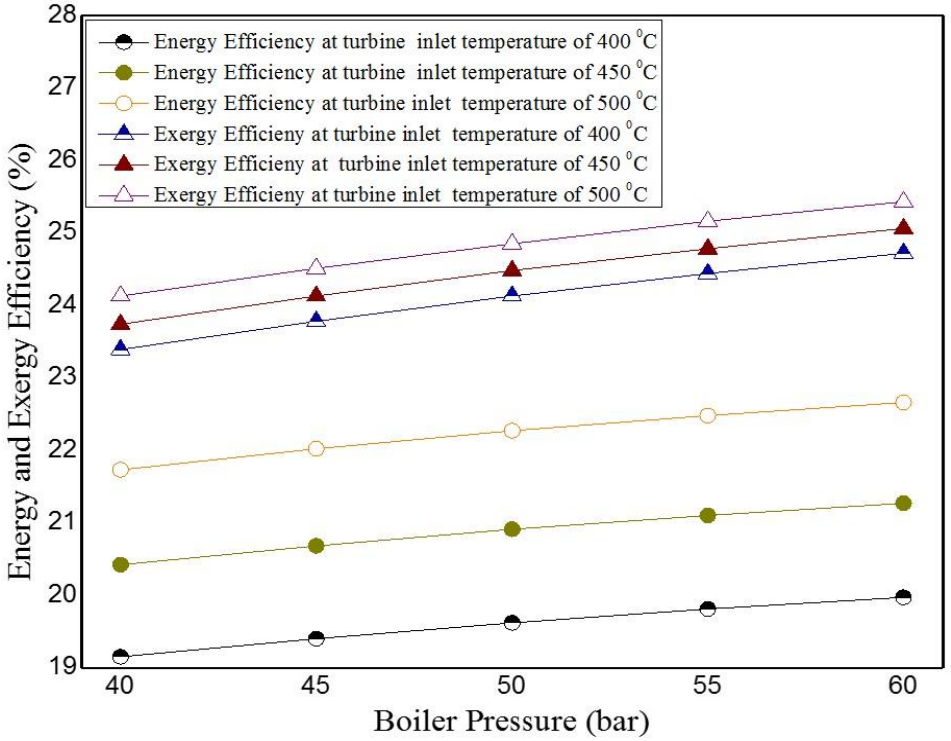

Figure 6.11 Energy efficiencies and exergy efficiencies with change in boiler pressure at three turbine inlet temperature (i.e.400 ºC, 450 ºC & 500 ºC)

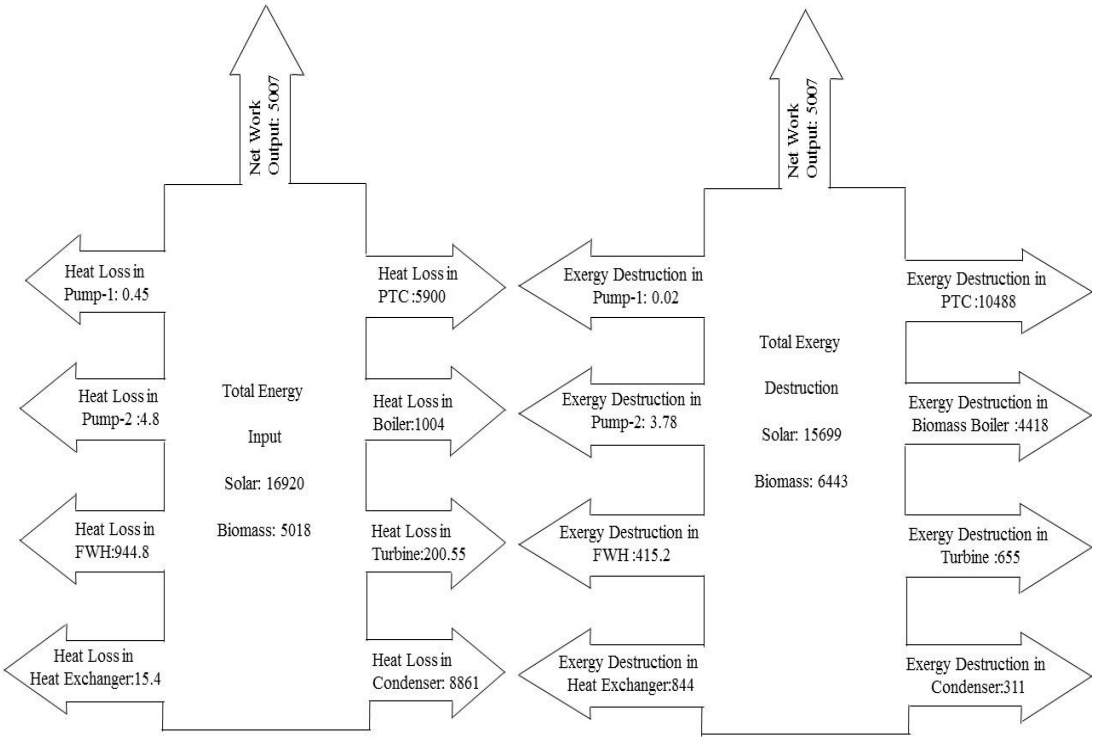

Figure 6.12 Energy losses and exergy destruction (kW) of the major components of the hybrid system

6.3 POLYGENERATION PROCESS IN HSB THERMAL POWER PLANT FOR POWER, COOLING AND DESALINATION

The thermodynamic (energy and exergy) modelling of HSB thermal power plant with cooling and desalination in polygeneration process are presented. The different parametric study is carried out to simulate the results of various useful outputs by varying various input points such as beam radiation on tilted surface and generator heat of VAR system. The various parametric state points of the system are given in Table 6.7. Figures 6.13 and 6.14 show the variation of beam radiation on tilted surface on solar-biomass heat, turbine inlet heat, boiler heat, PTC heat, energy efficiency of PTC field, energy and exergy efficiency of polygeneration in HSB system. It is observed that energy & exergy efficiencies of PTC increases with increase of beam radiation on tilted surface.

Table 6.7 State point properties of the polygeneration process in HSB thermal power plant

State Points	Fluid	Pressure (bar)	Temperature (°C)	Enthalpy (kJ/kg K)	Mass flow rate (kg/sec)
1	Water	0.1	45.8	191.8	5.0
2	Water	5	45.8	192.3	5.0
3	Water	5	98.84	414.5	5.0
4,c	Water	60	99.22	420.2	5.0
5	Water	60	500	3422	5.0
6	Water	5	163	2774	0.85
6’	Water	5	151.9	741.4	0.85
7	Water	0.1	45.8	2243	4.15
8	Water	60	99.22	420.2	5.0
9,a	Water	60	275.6	1221	5.0
X	Therminol VP-1	12	301.6	554.6	25.0
Y	Therminol VP-1	12	240	420.5	25.0
10	LiBr-Water	0.001313	37	81.43	8.308
11	LiBr-Water	0.08453	37	81.43	8.308
12	LiBr-Water	0.08453	126.1	274.8	8.308
13	LiBr	0.08453	142	311.5	7.683
14	LiBr	0.08453	40.1	102.4	7.683
15	LiBr	0.001313	40.1	102.4	7.683
16	Water	0.08453	142	2736	0.6223

17	Water	0.08453	95	398	0.6223
18	Water	0.08453	40	167.6	0.6223
19	Water	0.001313	11	398	0.6223
20	Water	0.001313	11	2521	0.6223
21	Water	0.1	35	192.4	8.937
22	Water	0.1	35	146.7	8.937
23	Water	0.1	37.5	157.1	8.937
24	Water	0.1	50	209.4	8.937
25	Water	0.1	85	355.9	8.937
26	Water	0.1	50.2	210.4	8.641

With the increase of PTC energy efficiency, the PTC heat increases but the overall efficiency of the HSB system in polygeneration decreases due to less efficiency of PTC field compared to biomass boiler. The PTC energy efficiency increases to 51.62 % whereas the biomass boiler efficiency remains constant at 80%. So, the heat taken from solar field is less than the heat taken from the biomass boiler. The biomass heat increases result in increasing the overall efficiency of system when the beam radiation on tilted surface decreases. It is clearly indicated that the heat input sources from solar and biomass is very important for improving the overall efficiency of system and these supplement with each other.

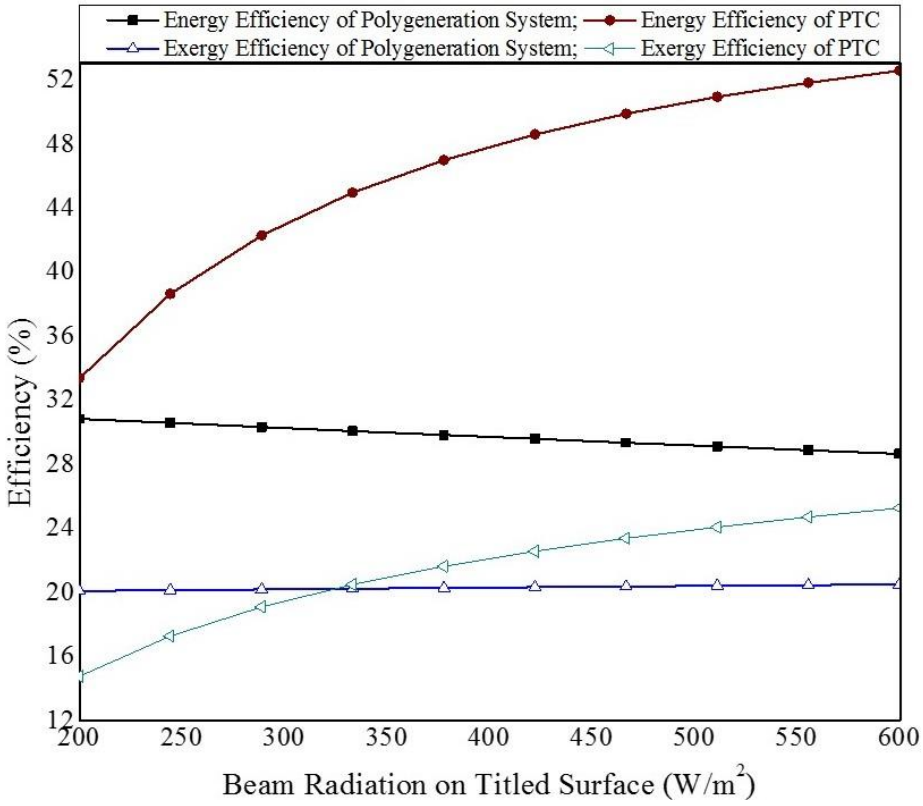

Figure 6.13 Variation of beam radiation on tilted surface on efficiency of PTC and HSB system in polygeneration process

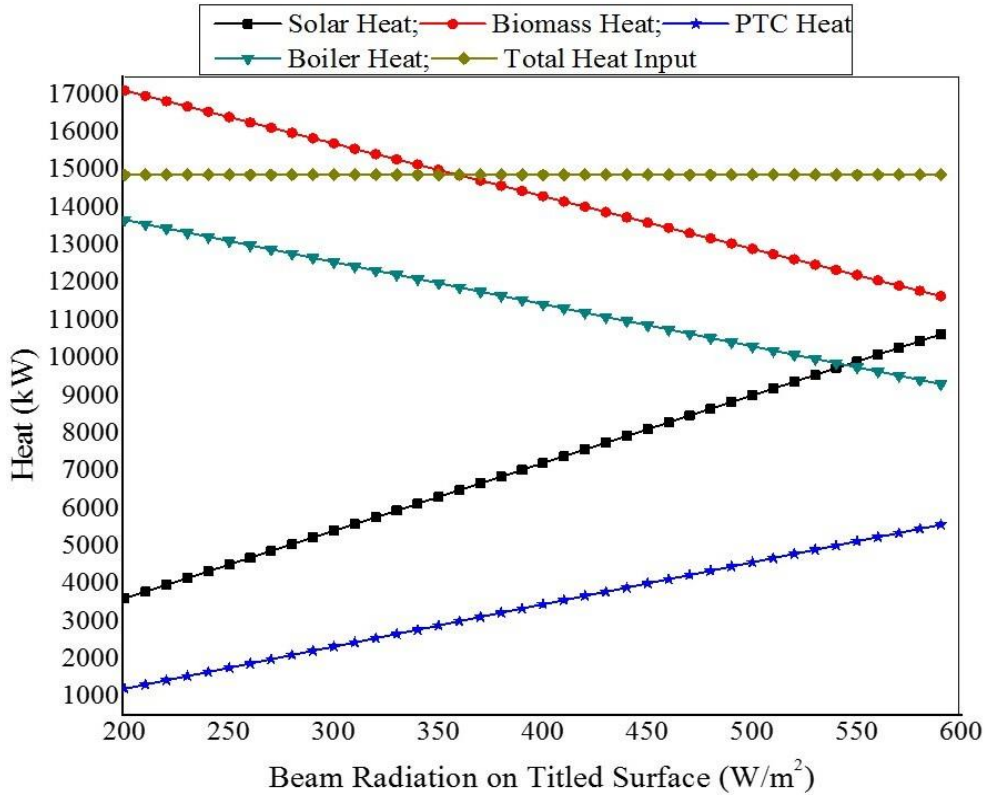

Figure 6.14 Variation of beam radiation on tilted surface on various parameters of HSB system in polygeneration process

From this study it becomes apparent that the heat utilization from solar and biomass is considered as 37.34% (8100 kW) and 62.65% (13588 kW) respectively for modelling of HSB system in polygeneration process. The maximum energy and exergy efficiencies of HSB system in polygeneration process for combined power, cooling & desalination are 30.81% and 20.47% respectively. Figure 6.15 shows the variation of turbine work, evaporator load and output of distilled water of the HSB system in polygeneration process on various generator temperatures. It can be seen that the increase in the generator temperature results in decrease in the turbine work output of HSB power plant.

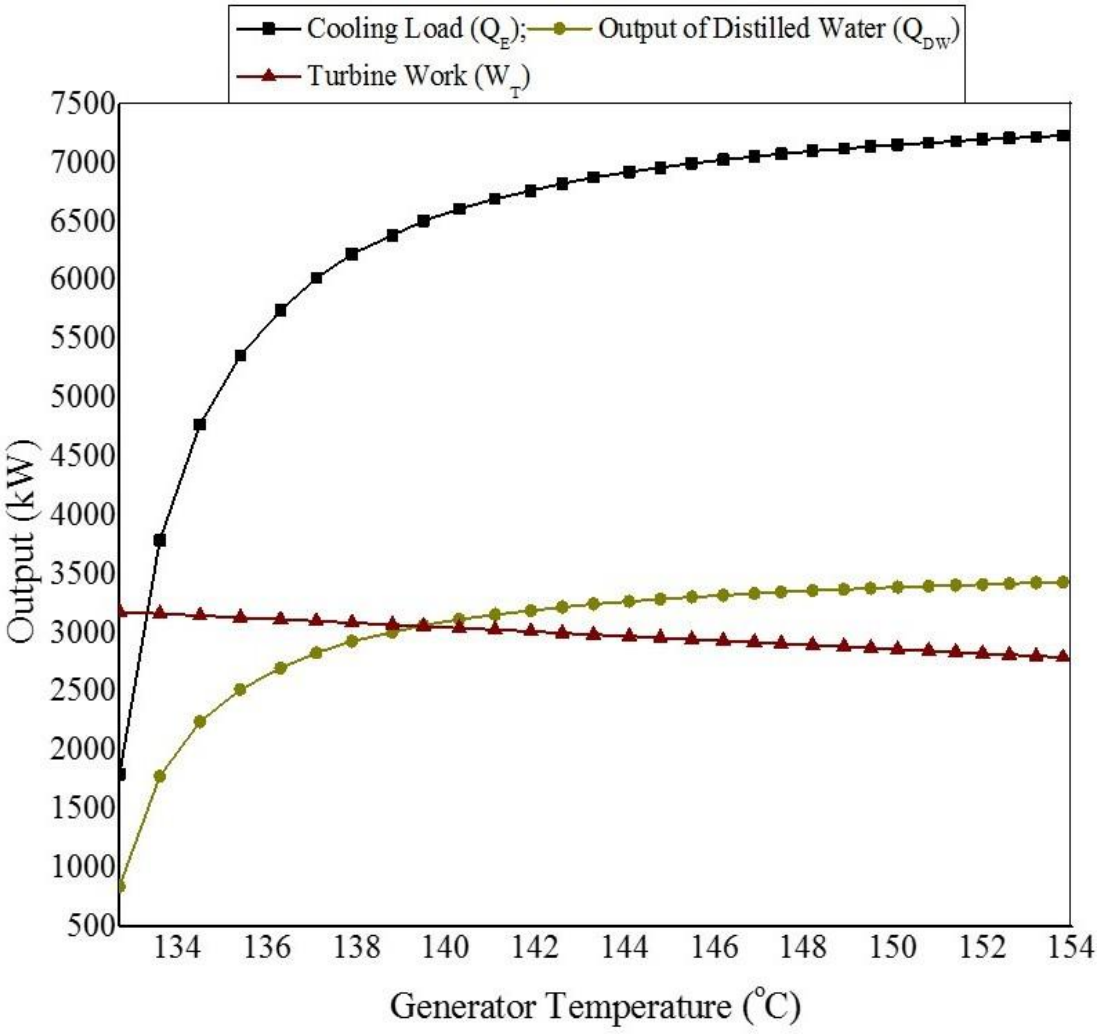

Figure 6.15 Variation of turbine work, cooling load and output of distilled water of the system on various generator temperatures

The evaporator load, output of distilled water continuously increases at a faster rate up to a generator temperature of 142^0C, thereafter the rate of increase in the evaporator load and output distillation declines with increase in generator temperature while keeping other parameters of the system as constant. For better understanding the effect of generator temperature (i.e. generator temperature taken from extracted heat from turbine) on cooling load and desalinated water output, we should concentrate on the effect of temperature on work output, VAR cooling and desalinated water output.

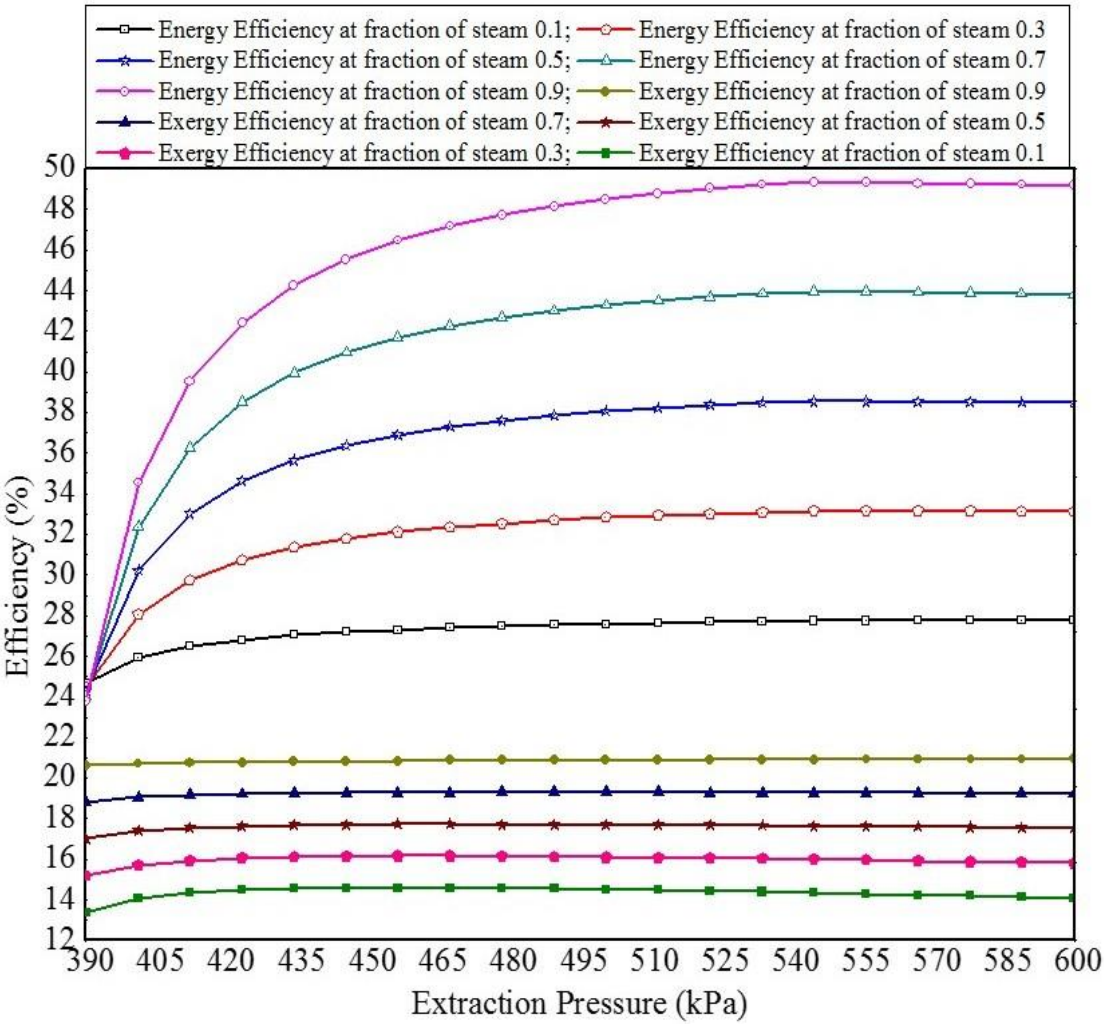

Figure 6.16 Energy and exergy efficiencies with change in extraction pressure from turbine at various fraction of steam (i.e.0.1, 0.3, 0.5, 0.7 & 0.9)

It is clearly indicated from the Figure 6.15 that though the production of electricity decreases due to extraction of heat from turbine for generator heat of VAR cooling system, the complete system meets the energy requirements and its overall efficiency increases.

Figure 6.16 shows the energy and exergy efficiencies with change in extraction pressures in turbine at various fraction of steam (i.e.0.1, 0.3, 0.5, 0.7 & 0.9). The energy efficiency increases slightly from 24.69% to 27.77% at extraction pressure and fraction of steam from 390 to 600 kPa and 0.1 respectively. It is also seen that, the maximum energy efficiency increases to 49.35% at extraction pressure of 555 kPa and fraction of steam of 0.9. The profile of exergy efficiency follows the same trend as energy efficiency against extraction pressure in turbine at these five fractions of steam. Although the energy efficiency increases to 49.35%, but it is not sufficient and to find the best performance (higher energy efficiency, VAR cooling & desalination output) of the HSB system in polygeneration process for combined power, cooling and desalination the optimization utilizing GA is carried out.

6.4 OPTIMIZATION

The optimization using the objective functions, constraints (Table 5.1) and the decision variables are carried out utilizing GA in EES software. In this analysis, the optimization scenarios with the objective functions of energy efficiency, exergy efficiency, VAR cooling system output, desalination output and total output of the polygeneration process in HSB thermal power plant are considered. Figures 6.17 to 6.21 show the corresponding optimization scenarios on energy efficiency, exergy efficiency, VAR cooling system output, desalination output and total output. The energy efficiency, exergy efficiency, VAR cooling system output, desalination output and total output are optimized in 120 numbers of generation. The optimized

energy efficiency is 49.85% at decision variable of extraction pressure, fraction of steam and desalination inlet heated water temperature of 596.5 kPa, 0.89 & 80.08 ^{0}C respectively at 120th number of generation. It is also observed that the optimized value of VAR cooling system is 7278 kW at decision variable of extraction pressure, fraction of steam and desalination inlet heated water temperature of 598.6 kPa, 0.89 & 80.08 ^{0}C respectively. The optimized value of desalination output 4405 kW at closest value of decision variables of total output and energy efficiency of polygeneration process in HSB system as shown in Table 6.8. The optimized exergy efficiency of the system is 20.94% at decision variable of extraction pressure, fraction of steam and desalination inlet heated water temperature of 598 kPa, 0.101 & 89.83 ^{0}C respectively as shown in Figure 6.18.

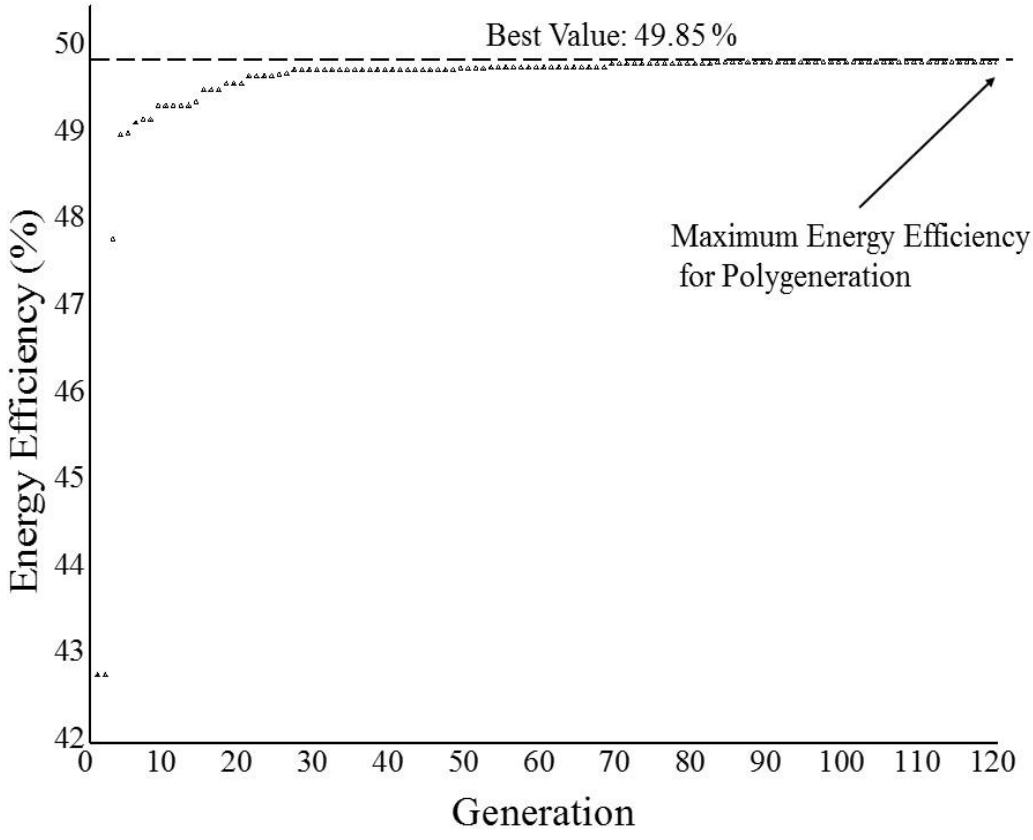

Figure 6.17 Optimization of the system over generations with respect to the energy efficiency of the polygeneration process in HSB system

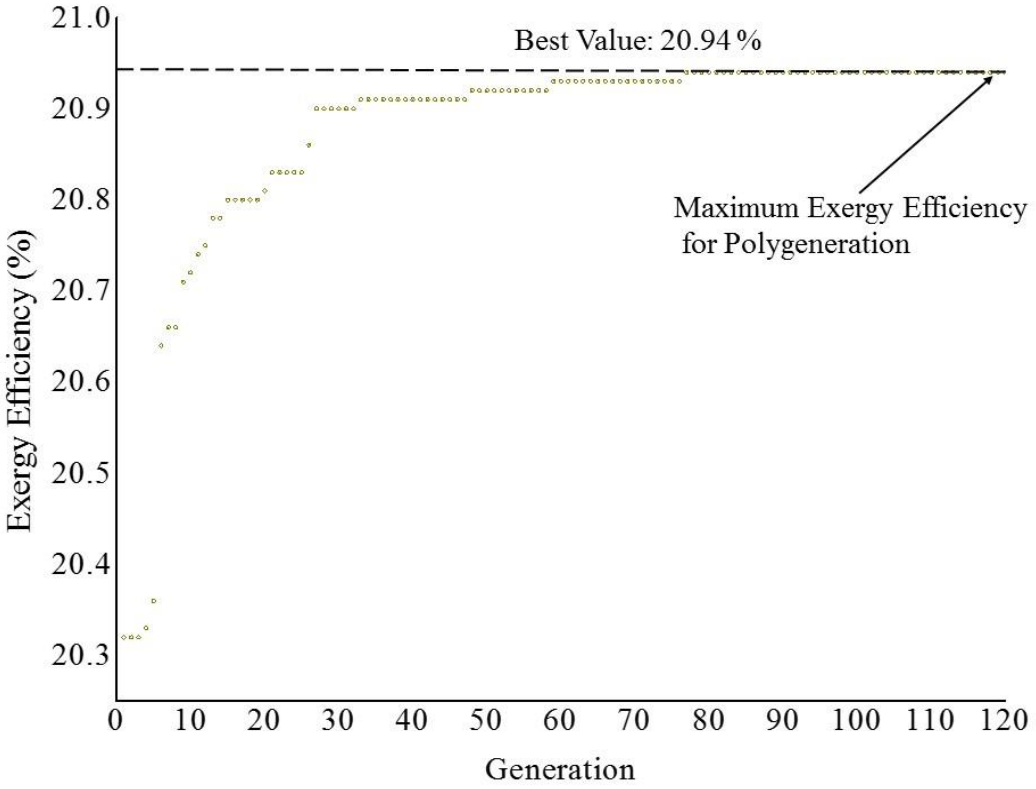

Figure 6.18 Optimization of the system over generations with respect to the exergy efficiency of the polygeneration process in HSB system

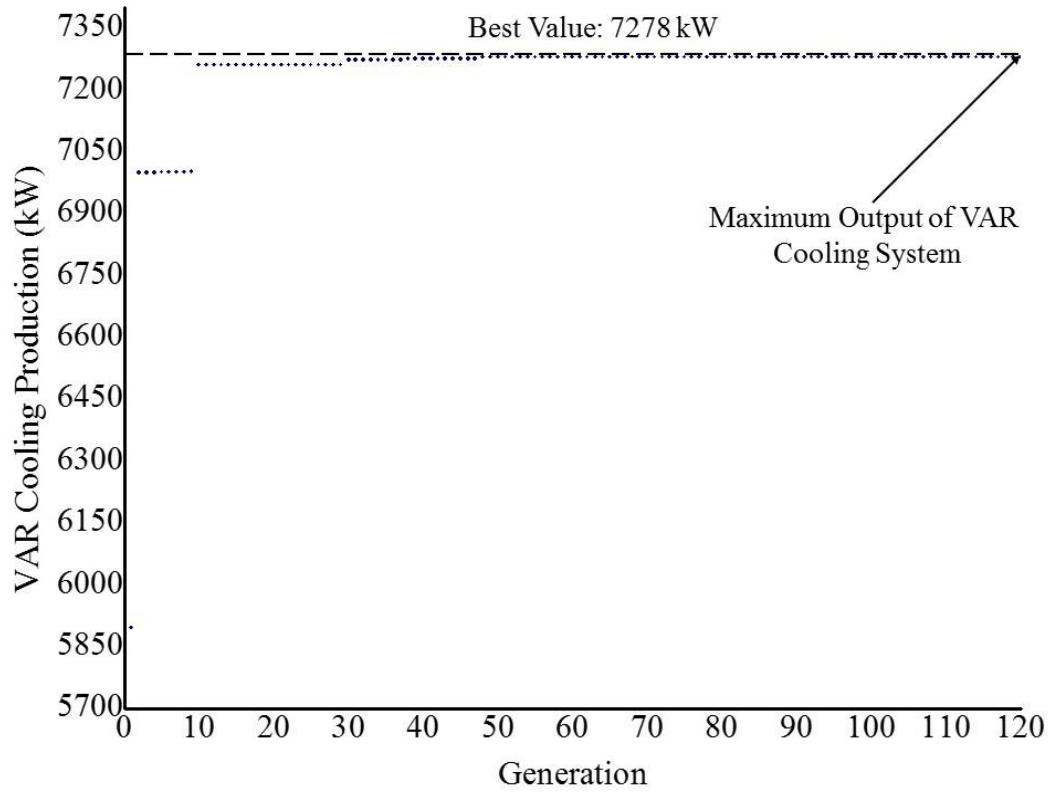

Figure 6.19 Optimization of the system over generations with respect to the VAR cooling production of the polygeneration process in HSB system

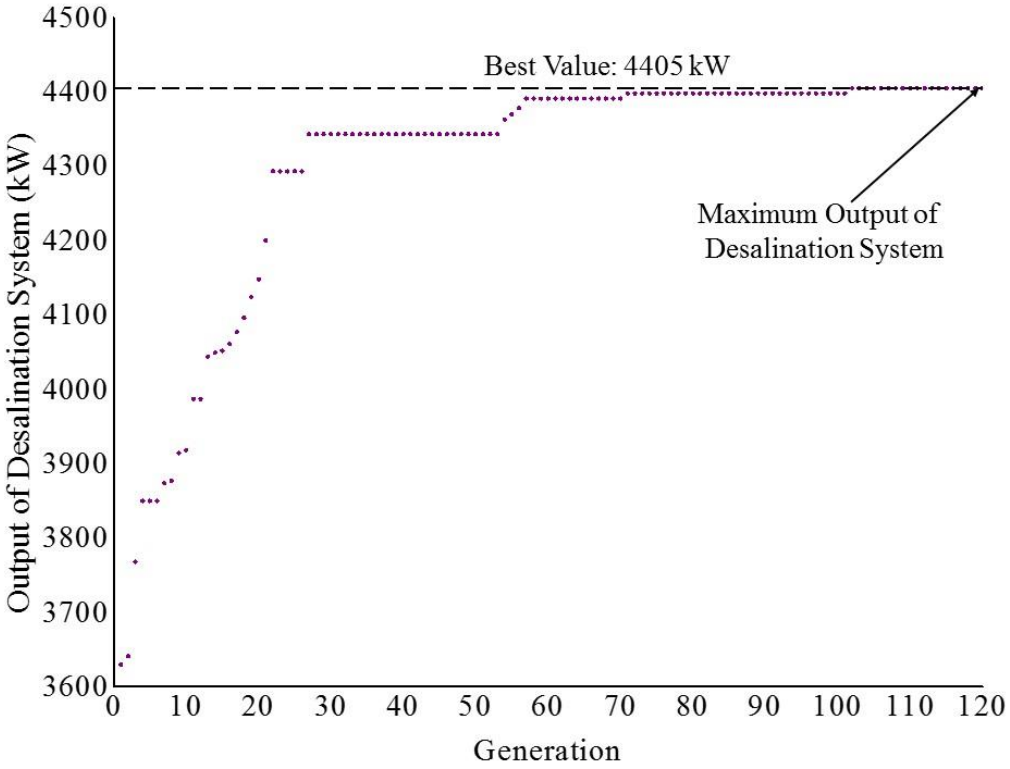

Figure 6.20 Optimization of the system over generations with respect to the output of the desalination system of the polygeneration process in HSB system

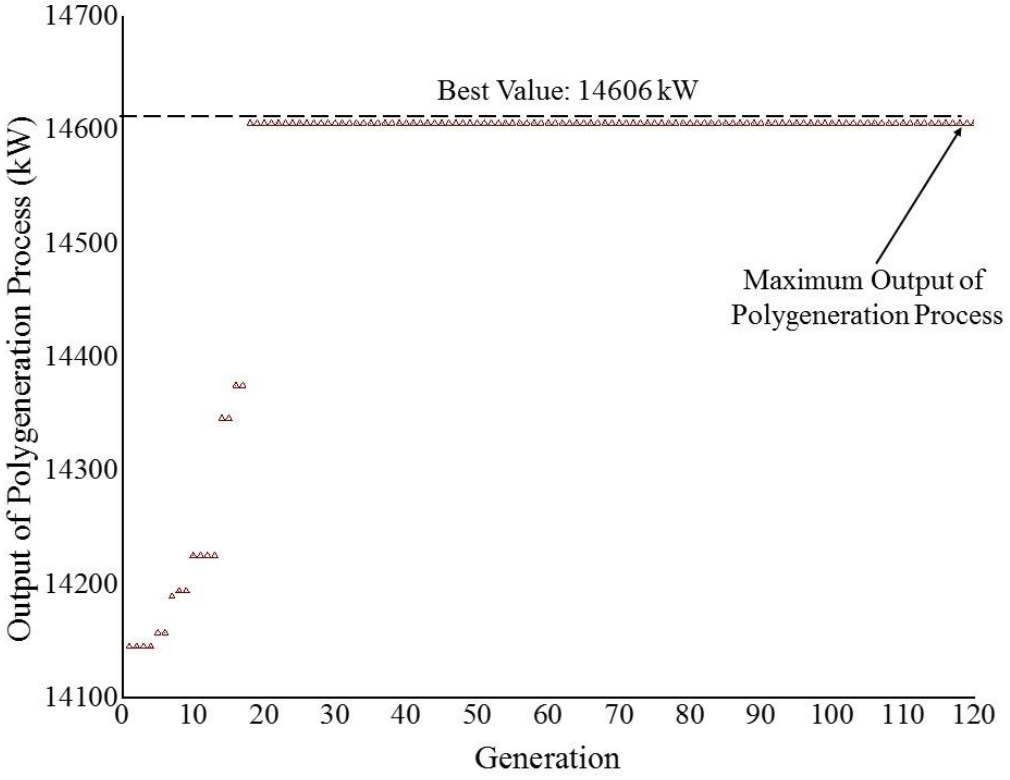

Figure 6.21 Optimization of the system over generations with respect to the output of the polygeneration process in HSB system for power, cooling and desalination

Table 6.8 shows the values of the decision variables in the base case design along with different optimization criteria. In addition, the results of analyses for each optimization criteria are also shown in this table. It is seen that the values for the decision variables are considered (i.e. extraction pressure from turbine, fraction of steam and desalination inlet heated water) to be continuous over the determined constraints for the optimization problem.

Table 6.8 Decision variables for the base case design under various optimization criteria for the polygeneration process in HSB thermal power plant.

Decision Variable	Base Case Design Parameters	Energy Efficiency	Exergy Efficiency	VAR Cooling System	Desalination Output	Total Output
P_6 (kPa)	500	596.5	598	598.6	596.8	597
f	0.17	0.89	0.101	0.89	0.89	0.89
T_{25} $\left({}^{0}C\right)$	82	80.08	89.83	80.08	80.02	80.08

Table 6.9 Optimized various parametric state points properties of the polygeneration process in HSB thermal power plant

State Points	Fluid	Pressure (bar)	Temperature (ºC)	Enthalpy (kJ/kg K)	Mass flow rate (kg/sec)
1	Water	0.1	45.8	191.8	5.0
2	Water	5	45.8	192.3	5.0
3	Water	5	102.3	429.1	5.0
4,c	Water	60	102.7	434.9	5.0
5	Water	60	500	3422	5.0
6	Water	5	182	2810	4.45

6’	Water	5	158.8	670.5	4.45
7	Water	0.1	45.8	2237	0.55
8	Water	60	102.7	434.9	5.0
9,a	Water	60	275.6	1235	5.0
X	Therminol VP-1	12	301.6	554.6	25.0
Y	Therminol VP-1	12	240	420.5	25.0
10	LiBr-Water	0.001313	37	81.43	28.67
11	LiBr-Water	0.08453	37	81.43	28.67
12	LiBr-Water	0.08453	132	288	28.67
13	LiBr	0.08453	148.8	331.4	25.24
14	LiBr	0.08453	30	96.75	25.24
15	LiBr	0.001313	30	96.75	25.24
16	Water	0.08453	148.8	2745	3.429
17	Water	0.08453	95	398	3.429
18	Water	0.08453	40	167.6	3.429
19	Water	0.001313	11	398	3.429
20	Water	0.001313	11	2521	3.429
21	Water	0.1	35	192.4	56.98
22	Water	0.1	35	146.7	56.98
23	Water	0.1	37.5	157.1	56.98
24	Water	0.1	50	209.4	56.98
25	Water	0.1	80.3	336.5	56.98
26	Water	0.1	50.2	210.4	55.09

The various optimization decision variables are closest values in the analysis of energy efficiency, VAR cooling system output, desalination output and total output

of the polygeneration process in the system, which is giving the most optimal results. For the proposed subsystem, the optimized various parametric state points of the system are given in Table 6.9.

Table 6.10 shows the typical values of some important data of a thermal power plant versus polygeneration process in HSB thermal power plant for combined power, cooling and desalination. The coefficient of performance of the conventional air-conditioning system is considered as 2.7 for this analysis.

Table 6.10 Typical values of some important data of a thermal power plant versus polygeneration process in HSB thermal power plant for combined power, cooling and desalination.

Thermal Power Plant	**Polygeneration Process in HSB Thermal Power Plant for Combined Power, Cooling & Desalination System**
T : 500^0C	T :500^0C
P : 60 bar	P :60 bar
W_{SPP} : 5904.25kW	W_{net} : 2923 kW
	Q_e : 7278 kW=2080 Tons of Refrigeration (TR)
	W_{VAR}: 2700 kW (electricity required to produce 2080 TR of cooling)
	Q_{DW} : 4405 kW (6800 liters/hour of drinking water)
	W_{DW} : 4894 kW of electricity required to produce drinking water at an amount of 6800 liter/hour
	Total equivalent electricity load is 10517 kW
Primary Energy Savings (PES): 50.5 %	
The electricity generation from polygeneration process increased to 78.12% as compared to a thermal power plant.	

6.5 COST ANALYSIS

Form the Table 6.11 it is observed that, the payback period of polygeneration in HSB thermal power plant is 1.52 years, while the tariff is Rs.7.45/kWh and the capital cost of Rs. 7460.72 lacs. The payback period for the solar thermal power plant is 18.7 years for the same site, when the tariff is Rs. 12.08/kWh [194] and the capital cost of Rs. 7128/kWh. It is seen that, the Polygeneration in HSB Thermal Power Plant is the most cost effective and efficient as compared to the solar thermal power plant, HSB thermal power plant and cogeneration in HSB Thermal Power Plant.

Table 6.11 Comparison of payback period among solar thermal power plant, HSB thermal power plant, cogeneration in HSB thermal power plant polygeneration in HSB thermal power plant.

	Solar Thermal Power Plant	**HSB Thermal Power Plant**	**Cogeneration in HSB Thermal Power Plant**	**Polygeneration in HSB Thermal Power Plant**
Capital Cost (Rs. in Lacs)	7128	6875.72	7375.72	7460.72
Electricity Tariff (Rs./kWh)	12.08	7.45	7.45	7.45
Payback Period (Years)	18.7	2.55	2.36	1.52

CHAPTER 7: CONCLUSIONS AND RECOMMENDATIONS

In this last chapter of the thesis the overall conclusions of the main findings and results which have been obtained in the above research work and some recommendations are made for future studies to guide researchers for further research works.

7.1 CONCLUSIONS

Polygeneration process in HSB thermal power plant for combined power, cooling and desalination offer an opportunity to increase further efficiency through proper thermodynamic arrangement of different processes or end products as compared to single and cogeneration system. In the system solar and biomass thermal energy is utilized to produce power, cooling and desalinated water. The following concluding remarks are drawn from the thesis work:

- The state wise availability of solar-biomass resources for hybrid thermal power generation and its thermodynamic evaluation (energy and exergy) are analyzed to identify the effects of various parameters. The HSB thermal power plant is an extremely promising energy system and is likely to provide a major share of renewable bulk electricity production. Taking in view, Government of India is making biomass policy to minimize the biomass feed stock in the hybrid power plant for creating the market. Apart from financial benefits to the promoters of these projects, the society will also be benefited due to intangible advantages such as employment generation in rural areas, environmental benefits, distributed power generation, etc. The potential estimated for power generation from the present surplus biomass could be further increased with development of technology and consequent increase in hybrid solar-biomass conversion efficiencies. Further, intensive cultivation of

waste and marginal lands for energy crops, with use of advanced plantation techniques, could enable the country to increase its hybrid power potential even more. In the light of these possibilities that Government of India has been promoting HSB based power generation for enhancing indigenous capability in this area.

- The thermodynamic evaluation (energy and exergy) and optimization of polygeneration process in HSB system for combined power, cooling and desalination system provides the useful information. The system has achieved a maximum energy efficiency of 49.85% at various decision variable of extraction pressure, fraction of steam and desalination inlet heated water temperature of 596.5 kPa, 0.89 & 80.08 ^{o}C of the polygeneration process in HSB thermal power plant. The exergy efficiency of the system is increased to 20.94%. The equivalent electricity generation from polygeneration process in HSB thermal power plant increased to 78.12% as compared to a simple thermal power plant and the PES is 50.5 %.
- The capital cost of the polygeneration process in HSB thermal power plant is Rs. 7460.72 lacs, which is higher than other systems like solar thermal power plant, HSB thermal power plant, Cogeneration in HSB thermal power plant, but the payback period of polygeneration process in HSB thermal power plant decreases to 1.5 years which is 17.2 years less than of solar thermal power plant.
- The system is ideal for industries, office campuses, institutions to fulfill the energy requirements for various applications i.e. electricity, space cooling and drinking water. The major aspect of polygeneration process is especially the developing trends of power generation with cooling & desalination form

HSB thermal power plant. Developments in these regards have taken place over the past two decades are quite encouraging. It is expected that in the near future HSB power plant in polygeneration process will constitute one of the competitive options of electricity generation.

7.2 RECOMMENDATIONS

Further thesis research work is recommended to improve the performance of the scientific characteristics of polygeneration process in HSB thermal power plant and to develop various aspects relating to the implementation of the system. The results obtained from this thesis research work also suggest for future studies as mentioned below;

- Different kind of resources like biogas, municipality solid waste, coal, fossil fuels should be investigated for hybridization with solar thermal power plant to better understanding the overall performance of the system.
- Thermal energy storage in PTC field should be analyzed to provide better understanding and improve the overall performance of the system.
- Additional two such outputs such as cooling with process heat for dairy industry, Ammonia based cooling system for cold storage with desalination can be integrated in place of cooling and desalination as per requirement of demand of the various industry to further increase the overall energy & exergy efficiency, PES and cost analysis with payback period of the system.

LIST OF PUBLICATIONS

PUBLISHED PAPERS

1. U.Sahoo, R.Kumar, P.C.Pant, R. Chaudhary. Development of an innovative polygeneration process in hybrid solar-biomass system for combined power, cooling and desalination. Applied Thermal Engineering 2017;120:560-567.

2. U.Sahoo, R.Kumar, P.C.Pant, R. Chaudhary. Resource assessment for hybrid Solar-Biomass power plant and its thermodynamic evaluation in India. Solar Energy 2016; 139:47-57.

3. U.Sahoo, R.Kumar, P.C.Pant, R. Chaudhary. Scope and sustainability of hybrid solar-biomass power plant with cooling, desalination in polygeneration process in India. Renewable and Sustainable Energy Review, 2015;51:304-316.

4. U. Sahoo, S.K. Singh, R.Kumar, P.C.Pant, I.Barbate. Performance study of an inclined Flat Plate type Solar Water Distillation System. Renewable: wind, water and solar 2016;3:2-5.

5. U.Sahoo, S.K.Singh, R.Kumar, P. Kumar. Mathematical Modelling of Portable Solar Water Heating System. Journal of Technology Innovations in Renewable Energy 2015;4: 91-95.

6. U.Sahoo, S.K.Singh, R.Kumar, P.Kumar, Experimental study of Portable Solar Water heating system. International Journal of Renewable Energy Development 2015;7:107-112.

PUBLISHED CHAPTER

7. U. Sahoo, R. Kumar, S. K. Singh P. C. Pant, and P. Saxena., Evaluation of Solar Thermal Technologies and Applications in India. Advances in Energy Research, 2015; 21:141-189. Hauppauge NY 11788-3619, U.S.A. *(Book Id: 6822 & Chapter Id: 31782).*

REFERENCES

[1] Policy Documents of Jawaharlal Nehru National Solar Mission, Phase-II. Ministry of New and Renewable Energy, India; 2012-13.

[2] C.P. Kumar. Fresh water resources: a perspective. [http://www .angelfire .com /bc/ nihh rrc/documents/fresh.html]; 2012.

[3] Drinking water quality in rural India: Issues and Approach. [www.wateraid.org/~/media/Publications/drinking-water-quality-rural-india. pdf]; 2013.

[4] Solar Heat for Industrial Processes, IEA-ETSAP and IRENA; 2015.

[5] International Energy Agency (IEA), World Energy Outlook, Paris; WEO 2016.

[6] Renewable energy policy network for the 21st century. Global status report on renewables, Paris; 2016.

[7] Central Electricity Authority: monthly all India installed power generation [http://www.cea.nic.in/reports/monthly/installedcapacity/2016/installed_capacity-11.pdf], India; 2016.

[8] Annual Report 2015-16. Ministry of New and Renewable Energy, Government of India; 2016.

[9] State wise installed solar power capacity. Ministry of New and Renewable Energy.[http://mnre.gov.in/file-manager/UserFiles/grid-connected-solar-power-project-installed-capacity.pdf], Govt. of India;2016.

[10] C. Bhushan, A. Kumarankandath and N. Goswami. The State of Concentrated Solar Power in India: A Roadmap to Developing Solar Thermal Technologies in India, Centre for Science and Environment, New Delhi, India;2015.

[11] G.C. Bakos. Design and construction of a two-axis Sun tracking system for parabolic trough collector (PTC) efficiency improvement. Renewable Energy 2006; 31:2411-2421.

[12] H. Mousazadeh, A. Keyhani, A. Javadi, H. Mobli, K. Abrinia, A. Sharifi. A review of principle and sun tracking methods for maximizing solar systems out-put. Renewable and Sustainable Energy Reviews 2009; 13:1800-1818.

[13] S.A. Kalogirou. Parabolic trough collectors for industrial process heat in Cyprus. Energy 2009; 27: 813-830.

[14] Concentrating solar power: Technologies brief, International Renewable Energy Agency; 2013.

[15] Policy Documents of Jawaharlal Nehru National Solar Mission, Phase-I, Ministry of New and Renewable Energy. India; 2012-2013

[16] N.B.Desai, S.Bandyopadhyay, J.K.Nayak, R.Banerjee, S.B.Kedare. Simulation of 1 MW solar thermal power plant. Energy Procedia 2014; 57:507-516.

[17] International energy agency. Technology Roadmap: solar thermal electricity, OECD/IEA, Paris; 2014.

[18] A. Fernandez-Garcıa, E. Zarza, L. Valenzuela, M. Perez. Parabolic-trough solar collectors and their applications. Renewable and Sustainable Energy Reviews 2010; 14:1695-1721.

[19] D. Kruger, A. Heller, K. Hennecke, K. Duer. Parabolic trough collectors for district heating systems at high latitudes? A case study. Proceedings of Eurosun' Copenhagen, Denmark;2000.

[20] V.E. Dudley, L.R. Evans, C.W. Matthews. Test results: industrial solar technology parabolic trough solar collector. Tech. Rep. No. SAND94-1117. Albuquerque: SANDIA; 2014.

[21] T.P. Collins, SA. Parabolic trough solar water heating: renewable technology for reducing water heating costs. Federal technology alert. Washington (United States): produced for the U.S. department of energy (DOE) by the National Renewable Energy Laboratory, a DOE national laboratory; 2000

[22] W.J Platzer. Status quo and new developments in medium temperature collectors. 2nd annual conference of the European technology plat form on renewable heating and cooling. Budapest, Hungary; 2011.

[23] Thermax private limited. [http://www.thermaxindia.com]; 2012.

[24] Solar process heat is becoming sexy. Sun & wind energy 2011; 9: 70–77.

[25] Smirro GmbH.[http://www.smirro.de]; 2012

[26] Koluacik research & development. [http://www.koluacik.com];2012

[27] ECOSTAR. European concentrated solar thermal roadmap document. European commission document No. SES6- CT-2003-502578; 2005

[28] Solar thermal electricity: A global outlook, European solar thermal electricity association, Belgium; 2016.

[29] AREVA Solar. [http://www.areva.com/mediatheque/liblocal/docs/activites/ energrenouvelables/ Reliance Power_Project-2012.pdf]; 2012.

[30] AREVA Solar. [http://www.areva.com/EN/news-753/press-releases-from-the-leader-in-nuclear-energy- and-renewable-energies.html]; 2012.

[31] A.F. Hildebrand and L.L. Vant-Hull. Power with heliostats. Science 1977;198 :1139-1146.

[32] L.L. Vant-Hull. Central tower concentrating solar power (CSP) systems: Concentrating Solar Power Technology Principles, Developments and Applications. Woodhead Publishing Series in Energy 2012:240-283.

[33] N. Goel, J.G. Aguilar, M. Romero, A. Steinfeld, E. Stefanakos, D.Y. Goswami. CRISP Tower-A Solar Power Tower R&D Initiative in India. Energy Procedia 2014; 57:301-310.

[34] S.Y. Wu, L. Xiao, Y. Cao, Y.R. Li. A parabolic dish/AMTEC solar thermal power system and its performance evaluation. Applied Energy 2010; 87:452-462.

[35] J. Kleih. Dish-stirling test facility. Solar Energy Material 1991; 24:231-237.

[36] F. Nepveu, A. Ferriere, F. Bataille. Thermal model of a dish/Stirling systems. Solar Energy 2009; 83:81-89.

[37] S. Snidvongs. The structure and foundation design for small solar thermal dish stirling10 kW power plant for Thailand soft land and poor isolation nature. In ASME 2005 international solar energy conference. American Society of Mechanical Engineers 2005: 729-735.

[38] C.H.Cheng, Y.J. Yu. Numerical model for predicting thermodynamic cycle and thermal efficiency of a beta-type sterling engine with rhombic-drive mechanism. Renewable Energy 2010; 35:2590-2601.

[39] A. Giostri, E. Macchi. An advanced solution to boost sun-to-electricity efficiency of parabolic dish. Solar Energy 2016; 139:337-354.

[40] Concentrating Solar Power Projects. NREL. [http://www.nrel.gov/csp/solarpaces/ projectdetail.cfm/]; 2014.

[41] Megawatt Solutions Pvt. Ltd. [http://megawattsolutions.in/solutions.html]; 2014.

[42] K. Lovegrove., G. Burgess, J. Pye. A new 500 m^2 paraboloid dish solar concentrator. Solar Energy 2011; 85:620-626.

[43] W. Schiel and T. Keck. Parabolic dish concentrating solar power systems; Concentrating solar power technology principles. Developments and applications. Woodhead Publishing Series in Energy 2012:284-322.

[44] India one solar thermal power project. Brahma kumaris.[http://www. india-one.net/images/India-One150dpi.pdf]; 2015.

[45] India One Solar Thermal Power Project. Brahma Kumaris.[http://www. Indiaone.net/images/News%20Letter1%20%20May14.pdf]; 2014.

[46] P. Dimityr. An option for solar thermal repowering of fossil fuel fired power plants. Solar Energy 2011; 85:344-349.

[47] J.H. Peterseima, A. Tadros, S. White, U. Hellwig, J. Landler, K. Galang. Solar tower-biomass hybrid plants maximizing plant performance. Energy Procedia 2014;49:1197-1206.

[48] J.H. Peterseim, U. Hellwig, A. Tadros, S. White. Hybridization optimization of concentrating solar thermal and biomass power generation facilities. Solar Energy 2014; 99:203-214.

[49] J.H. Peterseim, A. Herr, S. Miller, S. White, D.A. O'Connell. Concentrating solar power/alternative fuel hybrid plants: Annual electricity potential and ideal areas in Australia. Energy 2014; 68:698-711.

[50] R. Soria, J. Portugal-Pereira, A. Szklo, R. Milani, R. Schaeffer. Hybrid concentrated solar power-biomass plants in a semiarid region: A strategy for CSP deployment in Brazil. Energy Policy 2015; 86:57-72.

[51] J.D. Nixon, P.K. Dey, P.A. Davies. The feasibility of hybrid solar-biomass power plants in India. Energy 2012; 46:541-554.

[52] J.H. Peterseim, S. White, A. Tadros, U. Hellwig. Concentrating solar power hybrid plants: Enabling cost effective synergies. Renewable Energy 2014; 67:178-185.

[53] D. Morell. CSP Borges. The World's first CSP plant hybridized with biomass. In: CSP Today USA 2012-6th Concentrated Solar Thermal Power Conference; 2012.

[54] U. Sahoo, R. Kumar, P.C. Pant, R. Chaudhary. Resource assessment for hybrid solar-biomass power plant and its thermodynamic evaluation in India. Solar Energy 2016; 139:47-57.

[55] Y. Tanaka, S. Mesfun, K. Umeki, A. Toffolo, Y. Tamaura, K. Yoshikawa. Thermodynamic performance of a hybrid power generation system using biomass gasification and concentrated solar thermal processes. Applied Energy 2015; 160:664-672.

[56] Protermosolar. Abantia and Comsa Emte set up the first facility in the world that combines solar thermal and biomass energy. [http://www.Protermosolar .com/saladeprensa/?q¼en/content/abantia-and-comsaemte-set-first-facility world-combines solar-thermal-and-biomass-energy]; 2012.

[57] N. Kaushika, A. Mishra, M. Chakravarty. Thermal analysis of solar biomass hybrid co-generation plants. International Journal of Sustainable Energy 2005; 24:175-186.

[58] E.D. Gordillo, A. Belghit. A downdraft high temperature steam-only solar gasifier of biomass char: a modelling study. Biomass Bioenergy 2011; 35:2034-2043.

[59] Z. R. Ardebili, F. Manenti, M. Corbetta, C. Pirola, E. Ranzi. Biomass gasification using low temperature solar-driven steam supply. Renewable Energy 2015; 74:671-680.

[60] J. Spelling, B. Laumert, T. Fransson. Advanced hybrid solar tower combined cycle power plants. Energy Procedia 2013; 49:1207-1217.

[61] J. Kotowicz, A. Sobolewski, T. lluk, Energetic analysis of a system integrated with biomass gasification. Energy 2013; 52:265-278.

[62] J.H. Peterseim, A. Tadros, S. White, U. Hellwig, J. Landler, K. Galang. Solar tower biomass hybrid plants-maximizing plant performance. Energy Procedia 2013; 49:1197-1206.

[63] M. Safarik, L. Richter, F. Mockel, S. Kretschmar. Performance data of a small capacity absorption chiller. In: Proceedings of the International Conference on Solar Air-conditioning, Bad Staffelstein. Germany 2005:106-110.

[64] A. Syed, M. Izquierdo, P. Rodriguez, G. Maidment, J. Missended, A. Lecuona. A novel Experimental investigation of a solar cooling system in Madrid. International Journal of Refrigeration 2005; 28:859-871.

[65] U. Desideri, S. Proietti, P. Sdringola. Solar-powered cooling systems: technical and economic analysis on industrial refrigeration and air-conditioning applications. Applied Energy 2009; 86:1376-1386.

[66] M. Ortiz, H. Barsun, H. He, P. Vorobieff, A. Mammoli. Modelling of a solar assisted HVAC system with thermal storage. Energy and Buildings 2010; 42:500-609.

[67] G. Florides, S. Kalogirous, L. Wrobel. Modelling simulation and warning impact assessment of a domestic-size absorption solar cooling system. Applied Thermal Engineering 2002;22:1313-1325.

[68] F. Storkenmaier, M. Harm, C. Schweigler, F. Ziegler, J. Albers, P. Kohlenbach, T. Sengewald. Small-capacity water/LiBr absorption chiller for solar cooling and waste-heat driven cooling. International Congress of Refrigeration. Washington, DC. USA; 2003.

[69] Annual report. Solar Energy Centre, MNRE, India; 2012-13.

[70] W.S. Duff, R. Winston, J.J. O'Gallagher, J. Bergquam, T. Henkel. Performance of the Sacramento demonstration ICPC collector and double effect chiller. Solar Energy 2004; 76:175-180.

[71] Q. Ming, Y. Hongxi, H.A. David. A solar thermal cooling and heating system for a building: Experimental and model based performance analysis and design. Solar Energy 2010; 84:166-182.

[72] A. Lokurlu, G. Müller. Experience with the worldwide first solar cooling system based on parabolic trough collector (Solitem PTC 1800) combined with double effect absorption chiller. In proceeding of the 1st International conference solar sir-conditioning 2005:298-302.

[73] A.M. El- Nashar. Optimizing the operation parameters of a solar desalination plant. Solar Energy 1992;48:207-213.

[74] K. Schwarzer, M. Eugenia, C. Faber, C. Muller. Solar thermal desalination system with heat recovery, Desalination 2001;137:23-29.

[75] H. Müller-Holst, M. Engel hardt, W. Scholkopf. Small-scale thermal seawater desalination simulation and optimization of system design, Desalination 1999;122:255-262.

[76] M. Rasool Qtaishat, F. Banat. Desalination by solar powered membrane distillation systems. Desalination 2013; 308:186-97.

[77] J. Hong Jin, Y.K. Hee. Performance evaluation of multi-effect distiller for optimized solar thermal desalination. Applied thermal engineering 2013; 61:491-499.

[78] C. Rubio, J. Uche, N. Dejo. Optimization of desalted water production in a polygeneration scheme for the tourist sector. Desalination 2008; 223:464-475.

[79] M. Daniel, U. Javier, R. Javier. Assessment of high temperature organic Rankine cycle engine for polygeneration with MED desalination: A

preliminary approach. Energy Conversion and Management 2012; 53:108-117.

[80] G. Angrisani, C. Roselli, M. Sasso. Distributed micro trigeneration systems. Program Energy Combust Science 2012; 38:502–521.

[81] F.A. Al-Sulaiman, F. Hamdullahpur, I.Dincer. Performance comparison of three trigeneration systems using organic rankine cycles. Energy 2011; 36: 5741-5754.

[82] L. Hongquiang, G. Lio, H. Hui, J. Hongguang. Performance analysis of new biomass based power based polygeneration system for power & methanol. International for Green Energy 2008; 5:297-312.

[83] G. Angrisani , K. Bizon, R. Chirone , G. Continillo , G. Fusco , S. Lombardi., Development of a new concept solar-biomass cogeneration system. Energy Conversion and Management 2013; 75:552-550.

[84] C. Francesco, P. Adolfo, V. Laura. Design and dynamic simulation of a novel polygeneration system fed by vegetable oil and by solar energy. Energy Conversion and Management 2012:204-213.

[85] M. Dennticed'Accacia, M. Sasso, S. Sibilio. Micro-combines heat and power in residential and light commercial application. Applied Thermal Engineering 2003; 23:1247-1259.

[86] P.M. Heteu, L. Bolle. Economied'energie en trigeneration. International Journal Thermal Science 2002; 41:1151-1159.

[87] M. Carlos Rubio, M. J. Uche, M.G. Amaya, A. Angel. B. Rújula. Design optimization of a polygeneration plant fueled by natural gas and renewable energy sources. Applied Energy 2011; 88: 449-457.

[88] G. Chicco, P. Mancarella. Distributed multi-generation: a comprehensive view. Renewable and Sustain Energy Review 2009; 13:535-551.

[89] L.M. Serra, M.A. Lozano, J. Ramos, A.V. Ensinas, S.A. Nebra. Polygeneration and efficient use of natural resources. Energy 2009;34:575-586.

[90] J. H. Santoyo, A. S. Cifuentes. Trigeneration: an alternative for energy savings. Applied Energy 2003; 76:219-227.

[91] N. Fumo, P.J. Mago, L.M. Chamra. Analysis of cooling, heating, and power system based on site energy consumption. Applied Energy 2009; 86:2344-2350.

[92] S. Han, S. Fredrik, D. Lilia, Y. Jinyue. Influence of drying process on the biomass-based polygeneration system of bioethanol, power and heat. Applied Energy 2012; 90:32-37.

[93] A. Narvaez D. Chadwick, L. Kershenbaum. Small-medium scale polygeneration systems: methanol and power production. Applied Energy 2014; 113:1109-1117.

[94] C. Francesco, F. Gabriele, V. Laura. Transient simulation of polygeneration systems based on PEM fuel cells and solar heating and cooling technologies. Energy 2012; 41:18-30.

[95] L. Sheng, G. Lin, Z. Xiaosong, L. Hu, J. Hongguang. Evaluation of cost reduction potential for a coal based polygeneration system with CO_2 capture. Energy 2012; 45:101-106.

[96] F. Calise. Design of a hybrid polygeneration system with solar collectors and a Solid Fuel Cell: Dynamic simulation and economic assessment. International Journal of Hydrogen Energy 2011; 36: 6128-6150.

[97] F.A. Al-Sulaiman, F. Hamdullahpur, I. Dincer. Performance assessment of a novel system using parabolic trough solar collectors for combined cooling, heating, and power production. Renewable Energy 2012; 48:161-172.

[98] M. Zhongqing, Z. Yimeng, Z. Qisheng, Q. Yongbiao, Z. Jianbin, Q. Hengfei. Design and experimental investigation of a 190 kWe biomass fixed bed gasification and polygeneration pilot plant using a double air stage downdraft approach. Energy 2012; 46:140-147.

[99] L. Pei, I.G. Dimitrios, N.P. Efstratios. Modelling and optimization of polygeneration energy systems. Catalysis Today 2007;127:347-359.

[100] L. Pei, N.P. Efstratios, L. Zheng. A mixed-integer optimization approach for polygeneration energy systems design. Computers and Chemical Engineering 2009;33:759-768.

[101] R. Buck, S. Friedmann. Solar assisted small solar tower trigeneration systems. Journal of Solar Energy Engineering 2007; 129:349-354.

[102] U. Sahoo, R. Kumar, P.C. Pant, R. Chaudhury. Scope and sustainability of hybrid solar–biomass power plant with cooling, desalination in polygeneration process in India. Renewable and Sustainable Energy Reviews 2015; 51:304-316.

[103] E.D. Larson. A review of biomass integrated gasifier/gasturbine combined cycle technology and its application in sugarcane industries, with an analysis for Cuba. Energy Sustainable Development 2001; 5:54-76.

[104] E. Casati, F. Casella, P. Colonna. Design of CSP plants with optimally operated thermal storage, Solar Energy 2015; 11:371-387.

[105] M. Wittmann,, M. Eck, R. Pitz-Paal., H.M. Steinhagen,. Methodology for optimized operation strategies of solar thermal power plants with integrated heat storage. Solar Energy 2011; 85:653-659.

[106] M.J. Montes, A. Abánades, J.M.M. Val. Performance of a direct steam generation solar thermal power plant for electricity production as a function of the solar multiple. Solar Energy 2009; 83:679-689.

[107] A. Hoshi, D.R. Mills, A. Bittar, T.S. Saitoh. Screening of high melting point phase change materials (PCM) in solar thermal concentrating technology based on CLFR. Solar Energy 2005; 79:332-339.

[108] J.W. Spencer. Fourier series representation of the position of the sun 1971:172-173.

[109] J. Michalsky. The astronomical almanac's algorithm for approximate solar position 1950-2050. Solar Energy 1988; 40:227-235.

[110] M. Blanco-Muriel, D.C.Alarcon Padilla,T.L.Moratalla, M.L.Coira. Computing the solar vector. Solar Energy 2001; 70:431-441.

[111] I. Read, A. Andreas. Solar position algorithm for solar radiation applications. Solar Energy 2004; 76:577-589.

[112] C.Y. Lee, P.C. Chou, C.M. Chiang, C.F. Lin. Sun tracking systems: a review. Sensors 2009; 9:3875-3890.

[113] R. Grena. An algorithm for the computation of the solar position. Solar Energy 2008; 82:462-470.

[114] H.P. Garg. Treatise on solar energy: Fundamental of solar energy research. John wiley & sons, New York, vol.1; 1982.

[115] ASHRAE. Handbook of HVAC Applications. ASHRAE, Atlanta; 2007

[116] Solar energy vocabulary, International Organization for Standardization ISO; EN ISO 9488: 1999.

[117] F. Kreith, J.F. Kreider. Principle of Solar Engineering. McGraw-Hill. New York; 1978.

[118] R. Perez., P. Ineichen, K. Moore, M. Kmiecik, C. Chain, R. George and F. Vignola. A New Operational Satellite to Irradiance Model. Solar Energy 2002;73: 207-317.

[119] Solar Resource Assessments. [http://mnre.gov.in/sec/solar-assmnt.htm]; 2013.

[120] S. Lohmann., B. Mayer, R. Meyer. Long-term variability of global and direct solar irradiance for solar energy applications. Solar Energy 2006; 80:1390-1401.

[121] Anthony Lopez, Billy Roberts. India Solar Resource (DNI). [http://www.nrel.gov/international/ra_india.html]; 2016.

[122] A. Solar Radiation Energy over India. Indian Meteorological Department and Ministry of New and Renewable Energy. Govt. of India; 2008.

[123] Directorate of Economics and Statistics, Department of Agriculture & Cooperation [http://agricoop.nic.in]; 2012-13.

[124] Indian Biomass Power Association [http://www.indbiopower.com/pdf/Biomass-Crop-Residue-Details.pdf]; 2016.

[125] National Biomass Resource Atlas of India. A Project of MNRE Executed by CGPL, IISc. Bangalore. [http://lab.cgpl.iisc.ernet.in/Atlas];2015.

[126] M. Hiloidhari, D.C. Baruah. Rice straw residue biomass potential for decentralized electricity generation:a GIS based study in Lakhimpur district of Assam, India. Energy Sustain Development 2011; 15:214-22.

[127] J. Singh, B.S. Panesar, S.K. Sharma. Energy potential through crop biomass using geographical information system-a case study of Punjab. Biomass Bioenergy 2008; 32: 301-307.

[128] A. Friedl, E. Padouvas, H. Rotter, K. Varmuza. Prediction of heating values of biomass fuel from elemental composition. Anal Chim Acta 2005; 544:191-198.

[129] T. Minowa, T.Kondo, S.T. Sudirjo. Thermochemical liquefaction of Indonesian biomass residues. Biomass Bioenergy1998;14:517-524.

[130] G. Pilon. Utilization of Arecanut (Areca catechu) husk for gasification. [MSc. thesis]. Department of Bio resource Engineering, Mc Gill University, Montreal;2007. [http://webpages.mcgill.ca/staff/deptshare/FAES/066-Bioresource/Theses/theses/353Guillaume/Pilon2007/353GuillaumePilon2007.pdf].

[131] S.O. Jekayinfa, V. Scholz. Potential availability of energetically usable crop residues in Nigeria .Energy Sources, Part A: Recovery, Utilization Environ Effects 2009; 31:687-697.

[132] Biomass and biofuels calorific values-Biofuels B2B. [http://www. Biofuels b2b.com/useful_info. Php/page=TYPIC].

[133] A. Zabaniotou, O. Ioannidou, E. Antonakou, A. Lappas. Experimental study of pyrolysis for potential energy, hydrogen and carbon material production from lignocellulose biomass. International Journal of Hydrogen Energy 2008; 33:2433-2444.

[134] M. Asadullah, M.A. Rahman, et al. Jute stick pyrolysis for bio-oil production in fluidized bed reactor. Bio resource Technology 2008; 99:44-50.

[135] Jawaharlal Nehru National Solar Mission phase-I. Ministry of New and Renewable Energy, India; 2011-12.

[136] D. Frier, R.G. Cable, Jerusalem. An overview and operation optimization of the Kramer Junction Solar Electric Generating System. ISES World Congress 1999; 1:241-246.

[137] Road Map for Biomass Energy Report: Scaling up Biomass Based Power Generation. MNRE, 2011;3-37.

[138] Renewable Energy Investment. 1st renewable energy global investors meet and expo India. [http://www.re-invest.in]; 2015.

[139] State of Indian Agriculture 2012-2013.

[140] A.K.Tripathi, P.V.R.lyer, T.C.Kandpal, K.K.Singh, Assessment of availability and cost of some agricultural residues used feedstock for biomass gasification and briquetting in India. Energy Conversion and Management 1998; 39:1611-1618.

[141] Hybrid solar-biomass thermal power plant. MNRE. [http://mnre.gov.in/file manager/advertisement/RFP-Biomass-Solar-Hybrid-Technology-for-Power Generation.pdf]; 2014.

[142] MJ. Montes, A. Abánades, JM. Martínez-Val. Performance of a direct steam generation solar thermal power plant for electricity production as a function of the solar multiple. Solar Energy 2009; 83:679-689.

[143] S. Beerbaum, G. Weinrebe. Solar thermal power generation in India techno economic analysis. Renewable Energy 2000; 21:153-174.

[144] T. Kosugi, P.S. Pak. Economic evaluation of solar thermal hybrid H_2O turbine power generation systems. Energy 2003; 28:185-198.

[145] N. Singh, S.C. Kaushik, R.D. Misra. Exergetic analysis of a solar thermal power system. Renewable Energy 2000; 19:135-43.

[146] S.C. Kaushik, Y.P. Abhyankar, S. Bose, S. Mohan. Exergoeconomic evaluation of a solar thermal power plant. International Journal of Solar Energy 2001; 21:293-314.

[147] G. Morin, J. Dersch, W. Platzer, M. Eck, A. Häberle. Comparison of linear Fresnel and parabolic trough collector power plants. Solar Energy 2012; 86:1-12.

[148] A. Kalogirou Soteris. Solar Energy Engineering: Process and Systems. Elsevier; 2009.

[149] S.A. Kalogirou. Solar thermal collectors and applications. Progress in Energy and Combustion Science 2004; 30:231-295.

[150] Y. D. Goswami, F. Kreith, J. F. Kreider, and F. Kreith. Principles of Solar Engineering. Second edition, Taylor & Francis, Philadelphia, PA; 2000.

[151] C. Tzivanidis, E. Bellos, D. Korres, K.A. Antonopoulos, G. Mitsopoulos. Thermal and optical efficiency investigation of a parabolic trough collector. Case Studies in Thermal Engineering 2015; 6:226-237

[152] J. A. Duffie., W.A. Beckman., Solar Engineering of Thermal Processes. John Wiley & Sons, New York, Brisbane, USA 1991; 2nd edition.

[153] S.P. Sukhatme, J.K. Nayak. Solar Energy: Principles of Thermal Collection and Storage, Tata McGraw-Hill Education, New Delhi 2008; 3rd edition.

[154] S.C. Kaushik, V.S. Reddy, S.K. Tyagi. Energy and Exergy analysis of thermal power plants: A Review. Renewable and Sustainable Energy Review 2011; 15:1857-1872.

[155] P. Basu. Combustion and Gasification in Fluidized Beds. USA: CRC Press; 2006.

[156] P.V.R.Iyer, T.R.Rao, P.D.Grover Biomass: Thermo-Chemical Characterization. IIT Delhi. India 2002; 3rd edition.

[157] A. K. Asthana. Biomass as a fuel on small boiler. Asian Productivity Organization. Tokyo; 2009.

[158] ASME, steam generating unit. ASME/ANSI Standard PTC 4.1:1974, Reaffirmed New York; 1991.

[159] PN-EN 12953-11. Shell boilers-part 11: acceptance tests; 2006.

[160] PN-EN 12953-10. Shell boilers-part 10: requirements for boiler feed water and boiler water quality; 2006.

[161] BS 845-1:1987. Methods for assessing thermal performance of boilers for steam, hot water and high temperature heat transfer fluids. British Standard Institution.

[162] IS 13979:1994. Reaffirmed. Method of calculation of efficiency of packaged boilers. BIS. New Delhi; 1999.

[163] Acceptance testing of steam generators; DIN 1942.

[164] A. Bejan, D.W. Kearney, F. Kreith. Second law analysis and synthesis of solar collector systems, Journal of Solar Energy Engineering 1981; 103:23-28.

[165] S.C. Kaushik, R.D. Misra, N. Singh, Second law analysis of a solar thermal power system, International Journal of Solar Energy 2000; 20:239-253.

[166] A. Hepbasli, A key review on exergetic analysis and assessment of renewable energy resources for a sustainable future, Renewable and Sustainable Energy Reviews 2008; 12:593-661.

[167] Y.P. Dai, J.F. Wang, L. Gao, Exergy analysis, parametric analysis and optimization for a novel combined power and ejector refrigeration cycle, Applied Thermal Engineering 2009; 29:1983-1990.

[168] J.F. Lu, J. Ding, J.P. Yang, Heat transfer performance and exergetic optimization for solar receiver pipe, Renewable Energy 2010; 35:1477-1483.

[169] I.Dincer, M.A. Rosen. Exergy, energy, environment and sustainable development. Oxford: Elsevier; 2007.

[170] J.F.Lu, J.Ding,J.P.Yang, Heat transfer performance and exergetic optimization for solar receiver pipe. Renewable Energy 2010; 35:1477-1483.

[171] M.K. Gupta, S.C. Kaushik, Exergy analysis and investigation for various feed water heaters of direct steam generation solar-thermal power plant. Renewable Energy 2010; 35:1228-1235.

[172] R. Petela. Exergy analysis of solar radiation, (Chapter 2), in: N. Enteria, A. Akbarzadeh, Solar Thermal Sciences and Engineering Applications, CRC Press, Taylor & Francis Group; 2013.

[173] T.J. Kotas. The exergy method of thermal plant analysis. New York: Krieger Publishing; 1995.

[174] J. Szargut. Exergy method: technical and ecological applications. UK: WIT Press; 2005.

[175] C.P. Jawahar, R. Saravanan, J.C. Bruno, A. Coronas. Simulation studies on GAX based Kalina cycle for both power and cooling applications. Applied Thermal Engg. 2013; 50:1522-1529.

[176] M. Rivarolo, A.Cuneo, A.Traverso, A.F.Massardo. Design optimization of smart poly-generation energy districts through a model based approach. Applied Thermal Engineering 2016; 99:291-301.

[177] P. Bösch, A.Modarresi, A. Friedl. Comparison of combined ethanol and biogas polygeneration facilities using exergy analysis. Applied Thermal Engineering 2012; 37:19-29.

[178] A.Khaliq, R.Kumar. Thermodynamic performance assessment of gas turbine trigeneration system for combined heat cold and power production. Journal of Engineering for Gas Turbines and Power 2008; 130:024501-4.

[179] A.Buonomano, F.Calise, G.Ferruzzi, L.Vanoli. A novel renewable polygeneration system for hospital buildings: Design, simulation and thermo-economic optimization. Applied Thermal Engineering 2014; 67:43-60.

[180] A. Piacentino, F. Cardona. An original multi-objective criterion for the design of small-scale polygeneration systems based on realistic operating conditions. Applied Thermal Engineering 2008; 28:2391-2404.

[181] U.Sahoo, R.Kumar, P.C.Pant, R. Chaudhary. Development of an innovative polygeneration process in hybrid solar-biomass system for combined power, cooling and desalination. Applied Thermal Engineering 2017; 120:560-567.

[182] U.Sahoo, S.K.Singh, R.Kumar, P.C.Pant, P.Saxena. Evaluation of Solar Thermal Technologies and Applications in India. Advances in Energy Research; 21:141-189.

[183] U. Sahoo, R.Kumara, P.C.Pant, R.Chaudhary. Resource assessment for hybrid solar-biomass power plant and its thermodynamic evaluation in India. Solar Energy 2016; 139:47-57.

[184] S.B.Hou, S.Q.Ye, H.F.Zhang. Performance optimization of solar humidification and dehumidification desalination process using Pinch technology. Desalination 2005; 183:143-149.

[185] I. Dincer, A.Z. Sahin, A new model for thermodynamic analysis of a drying process. Heat Mass Transfer 2004; 47:645-652.

[186] The directive 2004/8/EC of the European Parliament and of the council. Official Journal of the European Union 2004:50-60. [http://www.Zoldforrasenergia.hu/docs/2004-08-EC.pdf].

[187] Holland. Adaptation in natural and artificial systems: An introductory analysis with applications to biology, control, and artificial intelligence, Oxford, England: University of Michigan Press; 1975.

[188] D. M. Goldenberg. Future role of radiolabeled monoclonal antibodies in oncological diagnosis and therapy. Seminars in Nuclear Medicine 1989; 19: 332-339.

[189] A. Konak, D. W. Coit, A. E. Smith. Multi-objective optimization using genetic algorithms: a tutorial. Reliability Engineering and System Safety 2006; 9:992-1007.

[190] S. S. Rao, T.S.Pan, V.B.Venkayya. Optimal placement of actuators in actively controlled structures using genetic algorithms. AIAA Journal 1991;29: 942–943.

[191] Central electricity regulatory commission, New Delhi, India. [http://www.cercind .gov.in/2016/orders/SORE.pdf]; 2016.

[192] Thermax private limited. [http://www.thermaxglobal.com/thermax-absorption-cooling-systems/]; December 2016.

[193] Water and waste water treatment. [http://www.ambaenggs.com/]; December 2016.

APPENDIX

EES code written and used for simulation and optimization of polygeneration hybrid solar and biomass system for power, cooling and desalination.

```
Efficiency_PTCfirstlaw=efficiency_0-(a * ((Tm-Ta)/DNI))-(b*((Tm-Ta)^2/DNI))
"Parabolic trough collector field"
efficiency_0=0.67 "The optical efficiency has been taken as per 1 MW Solar Thermal Power Plant installed at NISE"
a=0.1 "First order coefficient of the collector efficiency"
b=0.001 "Second order coefficient of the collector efficiency"
DNI=450 “DNI”
Ta=35"Ambient temperature"
m_oil=25
Area=18000 "Area of parabolic trough collector solar field"
C_p=2600    "Specific heat of therminol VP-1 J/kg.K"
Q_Solar=(DNI/1000)*Area "Heat from Solar"
Q_PTC=(efficiency_PTCfirstlaw*DNI*Area)/1000
Delta_T=(Q_PTC*1000)/(m_oil*C_p) "Generation of heat energy from PTC field"
T_y=240   "Oil temperature inlet to the PTC field"
T_x=T_y+Delta_T "Oil gets heated from PTC field and inlet to heat exchanger"
Tm=(T_x+T_y)/2 "Mean Temperature"
"State Point -1"
P_1=10
T_1=T_sat(R718,P=P_1)
h_1=Enthalpy(R718,P=P_1,x=x_1)
x_1=0
s_1=Entropy(R718,P=P_1,x=x_1)
"State Point -2"
s_1=s_2
P_2=500
T_2=Temperature(R718,P=P_2,s=s_2)
h_2=Enthalpy(R718,T=T_2,P=P_2)
P_2=P_3
"State Point -5"
P_5=6000
T_5=500
h_5=ENTHALPY(R718,T=T_5,P=P_5)
s_5=ENTROPY(R718,T=T_5,P=P_5)
"State Point -6"
P_6=597
s_5=s_6
x_6=Quality(R718,P=P_6,s=s_6)
T_6=Temperature(R718,P=P_6,s=s_6)
h_6=Enthalpy(R718,P=P_6,s=s_6)
"State Point -6' "
x_69=0
T_69=Temperature(R718,P=P_6,x=0)
h_69=Enthalpy(Water,T=T_69,x=0)
```

s_69=Entropy(Water,T=T_69,x=0)
"State Point 61 "
Eff_1= 0.86
h_61=(h_5-(Eff_1*(h_5-h_6)))
x_61=Quality(R718,P=P_6,h=h_61)
T_61=Temperature(R718,P=P_6,h=h_61)
s_61=Entropy(R718,P=P_6,h=h_61)
"State Point -3"
x_3=0
T_3=(T_69+T_1)/2
h_3=Enthalpy(Water,T=T_3,P=P_3)
s_3=Entropy(R718,P=P_3,T=T_3)
v_3=volume(R718,P=P_3,T=T_3)
f=0.89 "Fraction of Steam used in the feed water heater"
"State Point -4"
s_3=s_4
P_4=6000
T_4=Temperature(R718,P=P_4,s=s_4)
h_4=Enthalpy(R718,T=T_4,P=P_4)
"State Point 41 "
Eff_41= 0.86
h_41=(h_3+((h_4-h_3)/(Eff_41)))
T_41=Temperature(R718,P=P_4,h=h_41)
s_41=Entropy(R718,P=P_4,h=h_41)
"State Point 8"
T_8=T_4
P_8=6000
h_8=Enthalpy(Water,T=T_8,P=P_8)
s_8=Entropy(Water,T=T_8,P=P_8)
Effectiveness_HeatExchanger=(T_x-T_y)/(T_x-T_8)"Heat Exchanger Effectiveness"
"State Point 9"
h_9= ((m_oil*C_p*Delta_T)/(m_water*1000))+h_8
m_water=5 "mass flow rate of water"
T_9=Temperature(Water,P=P_8,h=h_9)"Water gets heated from Heat Exchanger"
s_9=Entropy(Water,P=P_8,h=h_9)
"State Point-a"
T_9=T_a
h_9=h_a
"Total Input Energy from PTC and Biomass"
q_in89=h_9-h_8
q_in95=(h_5-h_9)
q_inheatHSB=(q_in89+q_in95)*m
q_in=(Q_solar+Q_biomass) "Input heat energy from solar i.e. state point 8-9 and biomass i.e. state point 5-a resources "
"Ultimate Analysis of Ricehusk Biomass"
C=38.5
H=5.7
N=0.5
O=39.8
S=0

moisture content=10
HHVb=(338.3*C)+(1443*(H-(O/8)))-(94.2*S)
L.H.V=HHVb-(226.04*H)-(25.82*moisture content) "Lower Heating Value of Ricehusk kJ/kg"
m_biomass=Q_biomass/L.H.V "Biomass kg/hour"
"Boiler Losses, Rice husk boiler "
Air_theoritical=((11.43*C)+(34.5*(H-(O/8))+(4.32*S)))/100
Air_Excesssupplied=(O_fluegas/(21-O_fluegas))*100 "percentage of excess air supplied"
m_fg=(1+(Air_Excesssupplied/100))*Air_theoritical "Actual mass of air supplied"
Cp_fg=0.23
Cp_2=0.45 "Specific heat of superheated steam"
T_fg=200
Humidityfactor=0.018
M_ricehusk=0.1
LHV=2996.172249
Moisture_ricehusk=10
Ash_Ricehisk=0.15
GCV_bottomash=900
GCV_flyash=650 "ration_bottomtoflyash=80:20"
O_fluegas=7 "Percentage of oxygen in flue gas"
Humidity_Air=0.018 "kg of water/kg of dry air"
L_b1=(m_fg*Cp_fg*4.18*(T_fg-Ta)*100)/L.H.V "Loss due to dry flue gas (sensible heat)"
L_b2=(9*(H/100)*(584+Cp_2*4.18*(T_fg-Ta))*100)/L.H.V "Loss due to hydrogen in biomass"
L_b3=(M_ricehusk*(584+Cp_2*4.18*(T_fg-Ta))*100)/L.H.V "Loss due to moisture in biomass"
L_b4=(m_fg*humidityfactor*Cp_2*4.18*(T_fg-Ta)*100)/L.H.V "Loss due to moisture in air"
Amountofbottomashperkg=0.8*Ash_Ricehisk
Heatloss_bottomash=Amountofbottomashperkg*GCV_bottomash*4.18 "Kcal/kg of rice husk"
L_b5=Heatloss_bottomash*100/L.H.V "percentage heat loss in bottom ash"
Amountofflyhperkg=0.2*Ash_Ricehisk "kg"
Heatloss_flyash=Amountofflyhperkg*GCV_flyash*4.18"Heat loss in fly ash Kcal/kgofrice husk"
L_b6=Heatloss_flyash*100/L.H.V "percentage heat loss in fly-ash %"
L_b7=2.3 "Unaccounted heatloss as radiation,convection,carbon monoxide and humidity in air %"
Total_Heatlossinboiler=L_b1+L_b2+L_b3+L_b4+L_b5+L_b6+L_b7
Efficiency_boiler=(100-Total_Heatlossinboiler)/100 "Input Energy from Biomass"
Q_boiler=(h_5-h_a)*m "As per variation of sunshine hours, automatically biomass energy Qbiomass will change i.e. may be increase or decrease"
Q_biomass=Q_boiler/Efficiency_boiler
"State Point -7"
p_7=10
s_61=s_7
x_7=Quality(R718,P=P_7,s=s_7)
T_7=Temperature(R718,P=P_7,s=s_7)

h_7=Enthalpy(R718,P=P_7,s=s_7)
"State Point 71 "
Eff_2= 0.86
h_71=(h_61-(Eff_1*(h_61-h_7)))
x_71=Quality(R718,P=P_7,h=h_71)
T_71=Temperature(R718,P=P_7,h=h_71)
s_71=Entropy(R718,P=P_7,h=h_71)
"State Point 21 "
Eff_21= 0.86
h_21=(h_1+((h_2-h_1)/(Eff_21)))
T_21=Temperature(R718,P=P_2,h=h_21)
s_21=Entropy(R718,P=P_2,h=h_21)
f1=f "Fraction of Steam used in the feed water heater as per isentropic"
"Cycle Efficiency"
Effriciency=(((h_5-h_6)+(1-f)*(h_6-h_7)-(1-f)*(h_2-h_1)-(h_4-h_3))*m)/q_in)*100
"The hybrid system run at availability of sunshine hours, so h_a i.e. equivelent to h_9 otherwise in non-availability of sunshine hours h_a is equivalent to h_c"
"Cycle Efficiency1"
Effriciency1=((h_5-h_61)+(1-f1)*(h_61-h_71)-(1-f1)*(h_21-h_1)-(h_41-h_3))*m)/q_in)*100
"Specific work output"
W= ((h_5-h_6)+(1-f)*(h_6-h_7))
"Specific work Output 1"
W1= ((h_5-h_61)+(1-f1)*(h_61-h_71))
"Turbine work"
WT= ((h_5-h_61)+(1-f1)*(h_61-h_71))*m "With Loss Turbine Work"
WT_withloss=0.96*WT "Turbine Loss"
WT_energyloss=WT-WT_withloss "Mass flow rate"
m= 5 "Power Outout"
P=m*W "Power Outout 11"
P11=m*W1
m_b=m_biomass/P11 "Condenser heat rejection"
q_c=(h_7-h_1)*(1-f) "Condenser heat rejection at non-isentropic"
q_c1=(h_71-h_1)*(1-f1)
"Exergy Analysis on each point"
T_o=308
"State Point -1"
e_1=h_1-(T_o*s_1)
"State Point -2"
e_2=h_2-(T_o*s_2)"Pump Work"
W_p1=(1-f)*(h_2-h_1)*m"Pump work 2"
W_p2=(h_4-h_3)*m
W_p21=(h_41-h_3)*m"EWp1 Exergy of Pump Work"
EWp1=(1-f)*(e_2-e_1)
"State Point -21"
e_211=h_21-(T_o*s_21) "EWp11 Exergy of Pump Work non isentropic"
EWp11=(1-f)*(e_211-e_1)
"State Point -5"
e_5=h_5-(T_o*s_5)
"State Point -6"
e_6=h_6-(T_o*s_6)
"State Point 61"

e_611= h_61-(T_o*s_61)
"State Point -7"
e_7= h_7-(T_o*s_7)
"State Point 71"
e_711= h_71-(T_o*s_71) "EWT1Turbine Work"
EWT1=((e_5-e_6)+ (1-f)*(e_6-e_7))*m "EWT11 Turbine Work non-isentropic"
EWT11=((e_5-e_611)+ (1-f1)*(e_611-e_711))*m
"Exergy Difference of Turbine Work"
ED_Turbinework=EWT11-WT
"Exergy Destruction of Turbine"
I_Turbinedestrution=T_o*m*((s_61-s_5)+((1-f1)*(s_71-s_61)))
"State Point -3"
e_3=h_3-(T_o*s_3)
"State Point -4"
e_4=h_4-(T_o*s_4)
"State Point 41 "
e_411= h_41-(T_o*s_41) "EWp2 Exergy of Pump Work isentropic"
EWp2=(e_4-e_3) "EWp21 Exergy of Pump Work non-isentropic"
EWp21=(e_411-e_3)
"State Point 8"
e_8=h_8-(T_o*s_8)
"State Point 9"
e_9= h_9-(T_o*s_9)
"Ex_89"
Ex_89=e_9-e_8
"Total input exergy from biomass"
Ex_biomass=m_biomass*phai*L.H.V "Chemical exergy on biomass"
phai=1.0401+(0.1728*(H/C))+(0.0432*(N/C))+(0.2169*(O/C)*(1-0.2052*(H/C)))
"Exergy on boiler"
Ex_Boiler=m*(e_5-e_9) "Second low efficiency”
SecondlowEff_boiler=Ex_Boiler/Ex_biomass
"State Point -E1"
Ex_1=(h_1-(T_o*s_1))*((1-f)*m)
"State Point -E2"
Ex_2=(h_2-(T_o*s_2))*((1-f)*m)
"State Point -E211"
Ex_211=(h_21-(T_o*s_21))*((1-f1)*m)
"State Point -E3"
Ex_3=(h_3-(T_o*s_3))*m
"State Point -E4"
Ex_4=(h_4-(T_o*s_4))*m
"State Point E411"
Ex_411=(h_41-(T_o*s_41))*m
"State Point -E51"
Ex_5=(h_5-(T_o*s_5))*m
"State Point -E6"
Ex_6=(h_6-(T_o*s_6))*(f*m)
"State Point E611"
Ex_611=(h_61-(T_o*s_61))*(f1*m)

"State Point E8"
Ex_8=(h_8-(T_o*s_8))*m
"State Point -E7"
Ex_7=(h_7-(T_o*s_7))*((1-f)*m)
"State Point E711"
Ex_711=(h_71-(T_o*s_71))*((1-f1)*m) "Exergy destruction on turbine"
E_DWT=(Ex_5-Ex_6-Ex_7)-(W*m)
"State Point E9"
Ex_9=(h_9-(T_o*s_9))*m "Exergy destruction on condenser"
ED_C=(Ex_7-Ex_1) "Exergy destruction on condenser non-isentropic"
ED_C1=(Ex_711-Ex_1) "Exergy destruction on FWH"
ED_FWH=(Ex_6+Ex_2-Ex_3) "Exergy destruction on FWH"
ED_FWH1=(Ex_611+Ex_2-Ex_3) "Exergy destruction on pump1"
ED_PUMP1=W_p1-(Ex_2-Ex_1) "Exergy destruction on pump1 nonisentropic"
ED_PUMP11=W_p1-(Ex_211-Ex_1) "Exergy destruction on pump2"
ED_PUMP2=W_p2-(Ex_4-Ex_3) "Exergy destruction on pump2 nonisentropic"
ED_PUMP21=W_p21-(Ex_411-Ex_3) "Exergy on biomass boiler"
E_BM=Q_boiler*(1-T_o/823.5) "Exergy destruction on biomass boiler"
E_DBM=Ex_biomass-(Ex_5-Ex_9)"Exergy on solar"
Ex_Solar=Q_Solar*(1-(T_o/5600))"Exergy as per patels's equation"
Expatels_Solar=Q_Solar*(1-(4/3)*(T_o/5600)+(1/3)*(T_o/5600)^2)"Exergy on PTC collector"
Ex_PTC=(Q_PTC/((T_x+273)-(T_y+273))*(((T_x+273)-(T_y+273))-((T_o)*ln((T_x+273)/(T_y+273))))) "Exergy efficiency of the PTC collector"
Ex_Collectorefficiency=Ex_PTC/Q_Solar"Exergy Efficiency of the PTC collector"
Ex_patelsCollectorefficiency=Ex_PTC/Expatels_Solar "Exergy destruction PTC collector"
ExD_PTC=(Expatels_Solar)-Ex_PTC "Exergy of heat transfer (kW)"
Ex_HE=(Q_PTC/((T_x+273)-(T_y+273))*(((T_x+273)-(T_y+273))((T_o)*ln((T_x+273)/(T_y+273))))) "Exergy destruction of heat exchanger (kW)"
ED_Heatexchanger=Ex_HE-(Ex_9-Ex_8) "Exergy input of the power plant"
Ex_inputofHSB=Expatels_Solar+E_BM "Exergy Efficiency of the power plant"
Ex_Effriciency=((((e_5-e_6)+(1-f)*(e_6-e_7)-(1-f)*(e_2-e_1)-(e_4-e_3))*m)/(Expatels_Solar+Ex_biomass))*100 "Exergy efficiency of the power plant isentropic"
Ex_Effriciency1=((((e_5-e_611)+(1-f1)*(e_611-e_711)-(1-f1)*(e_211-e_1)-(e_411 e_3))*m)/(Expatels_Solar+Ex_biomass))*100m"Energy balance equation of the power plant"
Energy_Diff= Q_PTC+Q_boiler-P-(q_c*m)+W_p1+W_p2"Percenrtage error on energy balance equation of the power plant"
Energy_Diff1=((Q_PTC+Q_boiler-P11-(q_c1*m)+W_p1+W_p21)/(Q_PTC+Q_boiler))*100
"Percentage error on exergy balance equation analysis of the power plant"
Error=(Ex_Solar+(E_BM/1000)+(W_p1/1000)+(W_p2/1000)-(ExD_PTC+(P+ED_C+ED_Heatexchanger+ED_FWH+E_DBM+EWp1+EWp2)/1000))/(Ex_Solar+(E_BM/1000)+(W_p1/1000)+(W_p2/1000))*100
"Cooling System"
c_10=x_LiBrH2O(T_10,P_10)
h_10=h_LiBrH2O(T_10,c_10)
s_10=s_LiBrH2O(T_10,c_10)
T_10=37
P_10=P_sat(Water,T=T_20)

```
T_20=11
T_g=T_69-10
h_10=h_11
P_11=P_10
T_11=T_10
c_10=c_11
s_11=s_LiBrH2O(T_11,c_11)
Effec_2=0.85
T_12=T_11+Effec_2*(T_g-T_11)
c_11=c_12
P_12=P_sat(Water,T=T_17)
T_17=95
h_12=h_LiBrH2O(T_12,c_12)
s_12=s_LiBrH2O(T_12,c_12)
P_13=P_12
c_13=x_LiBrH2O(T_g,P_13)
h_13=h_LiBrH2O(T_g,c_13)
s_13=s_LiBrH2O(T_g,c_13)
T_13=T_16
f_10=(c_13/(c_13-c_10))
f_11=m_12/m_16
P_16=P_12
T_g=T_16
h_16=Enthalpy(Water,x=1,T=T_16)
s_16=Entropy(Water,x=1,T=T_16)
P_17=P_sat(Water,T=T_17)
h_17=Enthalpy(Water,x=0,T=T_17)
s_17=Entropy(Water,x=0,T=T_17)
h_17=h_19
P_19=P_10
T_19=T_sat(Water,P=P_19)
s_19=Entropy(Water,T=T_19,h=h_19)
T_20=T_e
P_20=P_10
h_20=Enthalpy(Water,T=T_e,x=1)
s_20=Entropy(Water,T=T_e,x=1)
h_14=h_13-(f_10*(h_12-h_11))/(f_10-1)
h_14=h_15
c_14=c_13
P_14=P_12
s_14=s_LiBrH2O(P_14,c_14)
c_14=c_15
h_15=h_LiBrH2O(T_15,c_15)
s_15=s_14+0.00231
T_15=T_14
m_13=m_12-m_16
m_13=m_14
m_13=m_15
m_10=m_16*f_10
m_10=m_11
```

m_10=m_12
Q_G=f*m*(h_6-h_69)
m_16=Q_G/(h_16+((f_10-1)*h_13)-(f_10*h_12))
m_16=m_20
m_16=m_17
m_16=m_19
COP=Q_E/Q_G
T_0=308
E_10=m_10*(h_10-T_0*s_10)
E_11=m_11*(h_11-T_0*s_11)
E_12=m_12*(h_12-T_0*s_12)
E_13=m_13*(h_13-T_0*s_13)
E_14=m_14*(h_14-T_0*s_14)
E_15=m_15*(h_15-T_0*s_15)
E_16=m_16*(h_16-T_0*s_16)
E_17=m_17*(h_17-T_0*s_17)
E_19=m_19*(h_19-T_0*s_19)
E_20=m_20*(h_20-T_0*s_20)
E_G=Q_G*(1-(T_0/(T_g+273)))
E_G1=(h_6-h_69)-(T_0*(s_6-s_69))*f*m
E_dG=E_G-E_16-E_13+E_12
Q_Cond=(m_16*h_16)-(m_17*h_17)
E_dC=(E_16-E_17)
E_dTV2=(E_17-E_19)
Q_E=(m_20*h_20)-(m_19*h_19)
E_E=Q_E*((T_0/(T_e+273))-1)
E_E1=m_20*((h_20-h_19)-(T_0*(s_20-s_19)))
E_dE=(E_19-E_20)
Q_A=(m_15*h_15)+(m_20*h_20)-(m_10*h_10)
E_dA=(E_20+E_15-E_10)
Q_HX1=m_10*(h_12-h_11)
E_dHX1=(E_11+E_13)-(E_12+E_14)
E_dTV1=(E_14-E_15)
ECOP=E_E/E_G1
Q_gain=Q_G+Q_E
Q_reject=Q_Cond+Q_A
Effec_3=0.9
T_23=37.5
P_23=100
h_23=Enthalpy(Water,T=T_23,P=P_23)
s_23=Entropy(Water,T=T_23,P=P_23)
Q_in2=m_17*(h_17-h_18)
T_18=40
P_18=84.6
h_18=Enthalpy(Water,T=T_18,P=P_18)
s_18=Entropy(Water,T=T_18,P=P_18)
Q_out2=m_23*(h_24-h_23)
T_24=50
P_24=100
h_24=Enthalpy(Water,T=T_24,P=P_24)

s_24=Entropy(Water,T=T_24,P=P_24)
0.9*Q_in2=Q_out2
Q_1in=m_20*(h_16-h_17)
T_25=T_17-15
P_25=100
P_26=100
h_25=Enthalpy(Water,T=T_25,P=P_25)
s_25=Entropy(Water,T=T_25,P=P_25)
T_26=50.25
h_26=Enthalpy(Water,T=T_26,P=P_26)
s_26=Entropy(Water,T=T_26,P=P_26)
T_22=35
h_22=Enthalpy(Water,T=35,P=P_26)
s_22=Entropy(Water,T=T_22,P=P_26)
m_24=(0.9*Q_1in)/(h_25-h_24)
Q_1out=m_24*(h_25-h_24) "Input Heat Energy to Distillation System"
Q_Ethdistillation=Q_1out+Q_out2
m_24=m_fw
m_air=0.8*m_fw
P_amb=100
T_27=50
T_n27=240.7263
T_28=65
X=7.591386
A_27=6.11441
Pv_27=(A_27*10^((X*T_27)/(T_27+T_n27)))/10
phi_27=Pv_27/P_amb
w_27=0.622-(phi_27*Pv_27)/(P_amb-(phi_27*Pv_27))
T_n28=229.3975
X_28=7.137936
A_28=6.004918
Pv_28=(A_28*10^((X_28*T_28)/(T_28+T_n28)))/10
phi_28=Pv_28/P_amb
w_28=0.619-(phi_28*Pv_28)/(P_amb-(phi_28*Pv_28))
m_Dw=(w_27-w_28)*m_air
m_Bw=m_fw-((w_27-w_28)*m_air)
h_27=T_27*(1.01+(0.00189*w_27))+(2.5*w_27)
{s_27=Entropy(Water,T=T_27,P=Pv_27)}
h_28=T_28*(1.01+(0.00189*w_28))+(2.5*w_28)
s_28=Entropy(Water,T=T_28,P=Pv_28)
E_25and26=((m_fw*h_25)-(m_Bw*h_26))
E_28and27=m_air*(h_28-h_27)
Efficiency_humidification=(E_28and27/E_25and26)*100 "Energy efficiency of humidification"
E_22and23=m_fw*4.18*(T_23-T_22) "Energy of feed water in dehumidification"
Efficiency_dehumidification=(E_22and23/E_28and27)*100 "Energy efficiency of dehumidification"
"Energy balance equation"
Error_Distillation=(m_fw*h_25)-((m_fw*h_23)+(m_Bw*h_26)+(m_Dw*h_22))
"Exergy analysis of MEHD distillation system"
"Exergy of feed water in humidification process"

```
Ex_25and26=(m_fw*(h_25-(T_o*s_25)))-(m_Bw*(h_26-(T_o*s_26)))
Ex_28and27=m_air*(Ex_28-Ex_27)
Ex_22and23=m_fw*((h_23-T_o*s_23)-((h_22-T_o*s_22)))
"Exergy efficiency of humidification"
Eff_Exhumidification=(Ex_28and27/Ex_25and26)*100
"Exergy efficiency of dehumidification"
Eff_Exdehumidification=(Ex_22and23/Ex_28and27)*100
Error_exdistillation=m_fw*(h_23-(T_o*s_23))+m_Bw*(h_26-
(T_o*s_26))+m_Dw*(h_22-(T_o*s_22))-m_fw*((h_22-(T_o*s_22))-(h_25-
(T_o*s_25)))
Cp_air=1.004 "Specific heat of air"
Cp_vap=1.872 "Specific heat of vapor"
R_air=0.287 "Gas constant of air"
R_vapor=0.461 "Gas constant of vapor"
w_dst=0.4 "Relative humidity at dead state point"
T_28K=T_28+273
T_27K=T_27+273
Ex_28=(Cp_air+(w_28*Cp_vap*(T_28K-T_o)))-
T_o*((Cp_air+(w_28*Cp_vap))*ln(T_28K/T_o)-
(R_air+(w_28*R_vapor))*ln(Pv_28/P_amb))+T_o*((R_air+(w_28*R_vapor))*ln((1
+(1.6078*w_dst))/(1+(1.6078*w_28)))+(1.6078*w_28*R_air*ln(w_28/w_dst)))
Ex_27=(Cp_air+(w_27*Cp_vap*(T_27K-T_o)))-
T_o*((Cp_air+w_27*Cp_vap)*ln(T_27K/T_o)-
(R_air+w_27*R_vapor)*ln(Pv_27/P_amb))+T_o*((R_air+(w_27*R_vapor))*ln((1+(
1.6078*w_dst))/(1+(1.6078*w_27)))+(1.6078*w_27*R_air*ln(w_27/w_dst)))
"Energy efficiency of multi effect humidification and dehumidification distillation
system"
Q_indistillation=m_fw*(h_25-h_23)
h_125=Enthalpy(Water,x=0,T=T_25)
h_1251=Enthalpy(Water,x=1,T=T_25)
h_1252=h_1251-h_125
s_125=Entropy(Water,x=0,T=T_25)
s_1251=Entropy(Water,x=1,T=T_25)
s_1252=s_1251-s_125
Effi_energydistillation=(m_Dw*h_1252/Q_indistillation)*100
Q_distillation=m_Dw*h_1252
Q_exdistillation=m_Dw*(h_1252-(T_o*s_1252)) "Exergy efficiency of multi effect
Humidification and Dehumidification Distillation System"
Q_exindistillation=m_fw*((h_25-T_o*s_25)-(h_23-T_o*s_23))
Effi_exergydistillation=((m_Dw*(h_1252-(T_o*s_1252)))/Q_exindistillation)*100
"Energy analysis of polygeneration  system"
Eff_Energypolygeneration=((WT+Q_E+(m_Dw*h_25))/(Q_solar+Q_biomass))*100
"Total Output of Polygeneration"
W_polygeneration=WT+Q_E+Q_distillation
"Exergy Uutput of polygeneration"
Ex_Polygenerationoutput=WT+E_E+(m_Dw*(h_25-(T_o*s_25)))
"Exergy efficiency of polygeneration system"
Eff_Exergypolygeneration=((WT+E_E+(m_Dw*(h_25-(T_o*s_25))))
                          /(Expatels_Solar+Ex_biomass))*100
```